Delft University of Technology

Investigation of the Impacts of Climate Variability and Land Use Changes on the Hydrology of the Geul River Catchment

A. Tsiokanos

TU Delft

Investigation of the Impacts of Climate Variability and Land Use Changes on the Hydrology of the Geul River Catchment

by

A. Tsiokanos

to obtain the degree of Master of Science
at the Delft University of Technology,
to be defended publicly on Friday July 8, 2022 at 12:30 PM.

Student number:	5294274	
Project duration:	January 1, 2022 – June 29, 2022	
Thesis committee:	Dr. ir. M.M. Rutten,	TU Delft, chair
	Prof. dr. ir. R. Uijlenhoet,	TU Delft
	ir. R. Velner,	Sweco
	ir. K.F. Jansen,	Sweco

This thesis is confidential and cannot be made public until July 8, 2023.

An electronic version of this thesis is available at http://repository.tudelft.nl/.

Cover Image: Erosion at the Geul river (source: https://www.flickr.com/)

TU Delft

SWECO

***”Δὶς ἑς τὸν αὐτὸν ποταμὸν οὐκ ’ὰν ἐμβαὶης” - ”You cannot step twice into the same river”*, Heraclitus of Ephesus (Greek philosopher)**

Preface

This report culminates my graduation thesis; the last piece of work to obtain the Master of Science degree in Civil Engineering (Water Management track) at the Delft University of Technology. The recent floods in Limburg (July 2021) constitute the trigger for the current thesis, as they have done for many other initiatives and studies. This exceptional catastrophe provided a fertile ground for harvesting knowledge, in order to be better prepared for future calamities. I am very happy to contribute to such a fascinating study area and collaborate with eminent researchers.

I was lucky and privileged to conduct my research under the supervision of an inspiring committee. First and foremost, I would like to thank my principal supervisor Dr.ir. Martine Rutten for her continuous support, guidance, and feedback and for her trust in my abilities throughout my thesis. In addition, I would like to express my gratitude to Prof.dr.ir. Remko Uijlenhoet for his insightful and extensive feedback on all my deliverables and for playing a crucial role in the thesis writing and organization. Furthermore, I would like to thank Roel Velner for the discussions, his trust, and the opportunity to combine my thesis with an internship at Sweco. Also, I thank Koen Jansen for his comments and recommendations.

There are no words that can adequately express my gratitude to my family for their unconditional love and sacrifices all these years and for supporting and giving me the opportunity to broaden my horizons abroad.

I find it really moving that this work brings me one step closer to realizing my goals and becoming an engineer that really shapes perspectives and not just objects. The last two years were two strange and intense years, but undoubtedly they form one of the greatest chapters of my life.

Athanasios Tsiokanos
Delft, June 2022

Abstract

The Geul river, a tributary of the Meuse located in the south Netherlands, Belgium, and part of Germany, is vulnerable to extreme hydrological events, such as floods, droughts, and erosion. There is evidence that these conditions are exacerbated by land use and climate changes. This thesis focuses on investigating the temporal variability and trends of hydrometeorological variables, as well as the main land use changes in the Geul river catchment. Accordingly, this thesis aims to improve understanding of the impacts of climate change and human intervention on the hydrological response of the Geul. In the first part of the thesis, temporal changes in (extreme) precipitation regimes for the period 1951-2021 and potential evaporation for the period 1965-2021, are identified by calculating trends for each 30-year moving period within the available time frames. The main land use changes are evaluated using CORINE annual land cover maps for the period 1990-2018. Changes in discharge regimes are investigated using a multi-temporal approach in which trends are evaluated in every possible combination of start and end years. In the second part of the thesis, the effects of climate variability and land use changes on the variability of runoff patterns are assessed. This is achieved by correlating the rates of change between extreme precipitation and maximum discharges all over the moving periods. The work also includes the use of a water balance separation framework to estimate the attribution of alterations in mean stream flows to land use and climate changes. A statistically significant increase in very wet days is reported in the area that mainly derives from the winter period. The extreme summer precipitation shows a relatively strong increase since the 1980s. The trend analysis in the potential evaporation time series suggests a very strong and stable increase. The main land use changes dominated before the 1970s, while there do not appear to be significant changes in the catchment from 1990 to 2018. Extreme annual discharges show an increasing insignificant tendency, while mean stream flows are decreasing. Results suggest that the variability of extreme and mean flows is mainly driven by climate variability, while at the same time the effects of land use changes on runoff patterns are not visible for the period 1970-2021. This study emphasizes that climate change should be incorporated into flood designs and climate adaptation strategies should be provided.

Contents

1 Introduction **1**
1.1 Problem statement and motivation . . . 1
1.1.1 Climate change . . . 1
1.1.2 Land use changes . . . 2
1.1.3 Importance of time series trend analysis . . . 2
1.1.4 Related studies on the Geul catchment . . . 2
1.1.5 Developments in trend time series analysis . . . 3
1.2 Research objective and research questions . . . 3
1.3 Reading guide . . . 4

2 Study Area **5**
2.1 Landscape . . . 5
2.2 Hydro-climatic setting . . . 7
2.3 Land use . . . 8
2.3.1 Historical review . . . 8
2.3.2 Current land use . . . 9

3 Methods and Materials **11**
3.1 Trend analysis of (extreme) rainfall time series . . . 11
3.1.1 Data . . . 11
3.1.2 Methodology . . . 13
3.2 Trend analysis of potential evaporation time series . . . 16
3.2.1 Data . . . 16
3.2.2 Methodology . . . 17
3.3 Land use changes . . . 17
3.4 Trend analysis of discharge time series . . . 18
3.4.1 Data . . . 18
3.4.2 Meta-data . . . 20
3.4.3 Methodology . . . 21
3.5 Attribution and Validation . . . 22
3.5.1 Correlations between maximum discharges and precipitation extremes . . . 22
3.5.2 Separating the effects of land use and climate changes on mean flows . . . 22
3.5.3 Validation . . . 24

4 Results **25**
4.1 Trend analysis of (extreme) rainfall time series . . . 25
4.1.1 General overview of the trends . . . 25
4.1.2 Long-term variability of the trends . . . 28
4.1.3 Trend stabilites . . . 31
4.2 Trend analysis of potential evaporation time series . . . 32
4.2.1 Directions and magnitudes . . . 32
4.2.2 Variability of the trends . . . 33
4.2.3 Change points . . . 34
4.3 Land cover changes . . . 34
4.3.1 Land use changes between 1990 and 2018 . . . 34
4.3.2 Other human interventions . . . 35
4.4 Trend analysis of discharge time series . . . 36
4.4.1 Annual maxima . . . 36
4.4.2 Annual mean . . . 41

4.5 Attribution and Validation . . . 46
4.5.1 Maximum flow variability attribution . . . 46
4.5.2 Mean flow attribution . . . 48
4.5.3 Validation . . . 48

5 Discussion **51**
5.1 Implications . . . 51
5.2 Limitations and uncertainty . . . 53
5.2.1 Precipitation . . . 53
5.2.2 Evaporation . . . 54
5.2.3 Land use . . . 54
5.2.4 Discharge . . . 54
5.2.5 Attribution . . . 55
5.3 Guidance and recommendations . . . 55

6 Conclusions and future directions **57**
6.1 Conclusions . . . 57
6.2 Future research directions . . . 59

References **66**

A Trend analysis of rainfall time series **67**
A.1 Long term variability . . . 67
A.1.1 Winter . . . 67
A.1.2 Spring . . . 70
A.1.3 Summer . . . 72
A.2 Precipitation trend stabilities . . . 74

B Land use changes **79**
B.1 Whole catchment . . . 79
B.2 Subcatchments . . . 79

List of Figures

2.1 Location of the Geul catchment and the countries that share it. 5
2.2 Overview map of the Geul catchment area with its tributaries along the Netherlands (taken from: van Heeringen et al., 2022) 6
2.3 Elevation map of the Geul catchment 7
2.4 Hydrological response of the Geul (lower figure) at Meerssen during an extreme rainfall event (upper figure) on 11 November 2010. Precipitation hourly measurements are based on Maastricht station. Large fluctuation in discharges is visible. 8
2.5 Monthly averages for precipitation, reference evaporation (Maastricht station) and discharge in the Geul catchment 8
2.6 Land cover map for the Geul catchment in 1950 (taken from: Tu, 2006) 9
2.7 Land cover map of the Geul catchment based on CORINE Land Cover (European Environmental Agency, 2018) 10

3.1 Spatial distribution of the precipitation stations 12
3.2 Potential evaporation time series in 2021 as an example of the used dataset. 16
3.3 Land cover data analysis flow chart 18
3.4 Subcatchments and relevant stations. 19
3.5 Framework for seperating the effects of land use and climate change on streamflows based on Tomer and Schilling (2009) and modified by Renner et al. (2014). Points M_1 and M_2 are the fractions of excess energy and excess water for two studying periods. M_1 (E_{ex1}, P_{ex1}) represents the baseline period (before change) and M_2 (E_{ex2}, P_{ex2}) the altered period (post-change). Changes over the constant long-term aridity index are attributed to land use change (LUC), while changes perpendicular to the aridity index are caused by climate change (CC). The length of the vector R shows the magnitude of the combined changes and θ is the angle between the gradient of M_1 - M_2 and the constant long-term aridity index (taken from Marhaento et al., 2017) 23

4.1 Boxplots illustrating total annual precipitation, annual number of wet days and maximum 24-hour rainfall per year for the stations considered in this study. 26
4.2 Time series of the selected (extreme) precipitation indices as an example for full year periods in Valkenburg station. 26
4.3 Percentages of statistically significant trends calculated for each station and each of the 30-year moving periods. (a) summer; (b) spring; (c) winter; (d) autumn, (e) full year . . 27
4.4 Calculated Z-statistic for each moving periods in summer for Vaals and Valkenburg stations. The red horizontal lines represent the 0.20 significance level. The graphs show that trends starting after the 1980s are statistically significant increasing trends in comparison to previous periods. 29
4.5 Distribution of values of extreme precipitation indices before and after 1980 for Vaals in summer. Blue colors represent values before 1980 and orange after 1980. The continuous lines are the linear trend fits using the least squares approach and the shaded areas the uncertainty of the linear regression fits, in each of the two periods. A clear distinction in directions before and after 1980 can be observed. An increase after 1980 is visible. . 30
4.6 Z-statistic values calculated for each moving window for Ubachsberg in spring period. A shift from increasing to decreasing and again back to increasing trends is visible. 31
4.7 Annual evaporation in full year periods. The continuous line represents the linear trend fit using the least squares approach and the shaded area the uncertainty of the linear regression. A strong increase is visible. 32
4.8 Annual evaporation in seasonal periods and the linear trend fits. Increases for summer and spring are visible. 32

4.9 Calculated Z-statistic value for each moving period for annual evaporation time series in full year and seasonal periods. The horizontal lines represent two significance levels. The trends are very strong and increasing all over the studying period for full year, spring, summer and autumn. 33
4.10 Change point results of full year, spring and summer periods in annual evaporation times series. The red vertical line represents the change point in the time series. The gray bold lines show the mean values before and after the change point. The numbers indicate the mean values for the two subsets. The plots show a considerable increase (change point) after the 1990s. 34
4.11 Land use map for the Geul river catchment for 1990 (a) and 2018 (b). Differences between the two periods are hardly distinguishable. 35
4.12 Time series of annual maximum discharge in the Geul and its tributaries. Annual maximum discharges at Hommerich and Meerssen are almost identical. 37
4.13 Multi-temporal trend analysis for the annual maximum discharges at Meerssen, Hommerich and the Gulp - full year period. Each pixel presents a fixed period, and the color indicates the value of the Z statistic. The same definitions apply to the subsequent figures. Mixed insignificant trends are observed. 37
4.14 Seasonal annual maxima time series and linear fits for Meerssen. 38
4.15 : Multi-temporal trend analysis for the annual maximum discharge at Meerssen. (a) summer; (b) spring; (c) winter; (d) autumn. 38
4.16 Seasonal annual maxima time series and linear fits for Hommerich. 39
4.17 : Multi-temporal trend analysis for the annual maximum discharge at Hommerich. (a) summer; (b) spring; (c) winter; (d) autumn. 39
4.18 Seasonal annual maxima time series and linear fits for the Gulp. 40
4.19 : Multi-temporal trend analysis for the annual maximum discharge in the Gulp. (a) summer; (b) spring; (c) winter; (d) autumn. 41
4.20 Time series of annual mean discharge in the Geul and its tributaries. 41
4.21 Multi-temporal trend analysis for the annual mean discharges in Meerssen, Hommerich and the Gulp. 42
4.22 Seasonal annual mean time series and linear fits for Meerssen. 42
4.23 : Multi-temporal trend analysis for the annual mean discharges in Meerssen. (a) summer; (b) spring; (c) winter; (d) autumn. 43
4.24 Change point results for summer and spring periods in annual mean discharge times series. The plots show a considerable decrease (change point) after 1990. 44
4.25 Seasonal annual mean time series and linear fits for Hommerich. 44
4.26 : Multi-temporal trend analysis for the annual mean discharges at Hommerich. (a) summer; (b) spring; (c) winter; (d) autumn. 45
4.27 Seasonal annual mean time series and linear fits for the Gulp. 45
4.28 : Multi-temporal trend analysis for the annual mean discharges for the Gulp. (a) summer; (b) spring; (c) winter; (d) autumn. 46
4.29 Correlation coefficients between extreme precipitation indices and annual maximum discharge at Meerssen, for the calculated slopes in the moving windows. The dots show the exact values per rainfall station. Strong positive correlation values are visible. 47
4.30 Correlation coefficients between extreme precipitation indices and annual maximum discharge at Hommerich, for the calculated slopes in the moving windows. Strong positive correlation values are visible. 48
4.31 Visualization of the changes of the proportions of excess water (P_{ex}) and energy (E_{ex}) relative to the long term aridity index ($\overline{ET_0}$ / $\overline{P}$). The arrow indicates the direction of change between M1, which represents the baseline period 1970-1981, and M2, which represents the altered period 2010-2021. The change away of the constant aridity index indicates that climate change has a larger contribution, in comparison to land use changes, on mean flow alternations. Although, overall, at the scale of the entire graph, the change appears to be small 49

5.1 Percentages of statistically significant trends calculated for each station in spring, with and without including station Epen. Almost identical percentages can be seen. 54

A.1 Calculated extreme precipitation Z statistic for each moving period in winter for Valkenburg station. . . . 67
A.2 Calculated extreme precipitation Z statistic for each moving period in winter for Vaals station. . . . 68
A.3 Calculated extreme precipitation Z statistic for each moving period in winter for Ubachsberg station. . . . 68
A.4 Calculated extreme precipitation Z statistic for each moving period in winter for Noorbeek station. . . . 69
A.5 Calculated extreme precipitation Z statistic for each moving period in winter for Maastricht station. . . . 69
A.6 Calculated extreme precipitation Z statistic for each moving period in spring for Valkenburg station. . . . 70
A.7 Calculated extreme precipitation Z statistic for each moving period in spring for Vaals station. . . . 71
A.8 Calculated extreme precipitation Z statistic for each moving period in spring for Noorbeek station. . . . 71
A.9 Calculated extreme precipitation Z statistic for each moving period in spring for Maastricht station. . . . 72
A.10 Calculated extreme precipitation Z statistic for each moving period in spring for Epen station. . . . 72
A.11 Stability of statistically significant trends in precipitation indices - summer. . . . 74
A.12 Stability of statistically significant trends in precipitation indices - spring. . . . 75
A.13 Stability of statistically significant trends in precipitation indices - winter. . . . 76
A.14 Stability of statistically significant trends in precipitation indices - autumn. . . . 77
A.15 Stability of statistically significant trends in precipitation indices - full year. . . . 78

B.1 Area and percent land cover changes between 1990 and 2018 for the whole catchment. 79
B.2 Area and percent land cover changes between 1990 and 2018 for each subcatchment. 80

List of Tables

2.1 Situated part per country and its area . . . 6
2.2 Land cover area percentages according to CORINE Land Cover (European Environmental Agency, 2018) . . . 10

3.1 Available rainfall stations and their records . . . 13
3.2 Descriptive statistics of the rainfall stations including dry days (24-hour sums) . . . 13
3.3 Descriptive statistics of the rainfall stations excluding zero values (24-hour sums) . . . 13
3.4 ETCCDI selected extreme precipitation indices . . . 14
3.5 Stability criteria (Lupikasza, 2010). T is the percentage of time in which a trend is statistically significant . . . 15
3.6 Descriptive statistics of the reference evaporation time series (monthly sums) for the period 1965-2021. All values are in mm/month expect CV and Skewness that are dimensionless. . . . 16
3.7 Initial and reclassified land cover classes . . . 18
3.8 Subcatchment areas and their corresponding measuring stations. . . . 19
3.9 Missing discharge values and their percentage in parentheses for different resolutions based on the available periods. Values at coarser resolutions are computed from the 15-min data . . . 19
3.10 Statistics of the analysed mean daily discharge time series. The averages derived after resampling the 15-minute measurements to mean daily values. . . . 20
3.11 Statistics of the analysed maximum daily discharge time series.The maximum daily values are derived from the maximum of the 15-minute discharges per day. . . . 20
3.12 Years that are excluded from the analysis . . . 21

4.1 M-K Z-statistic values and calculated slopes per season for annual evaporation trends. Z-statistic values with a (*) are significant at α=0.01. The remaining values are significant at α=0.05. . . . 33
4.2 Land use distribution in the years 1990 and 2018 for the Geul river catchment including its change . . . 35
4.3 Land use distribution in the years 1990 and 2018 for each sub-catchment. Values in parentheses represent the percentage that each land cover class occupies in the subcatchment. . . . 36
4.4 Seasonal Z-statistic values for annual maximum discharges in Eyserbeek and Selzerbeek (** Significant at the 5% level). The only statistically significant trends are decreasing and found in autumn. . . . 40
4.5 Seasonal Z-statistic values for annual mean discharges for the Eyserbeek and Selzerbeek (** Significant at the 5% level, * significant at the 10% level). The only statistically significant trends are found in autumn. . . . 46
4.6 Analytical values calculated for the attribution of changes. P, Q, ET_0 and ET are the mean annual precipitation totals, discharge, potential evaporation totals and evapotranspiration totals in mm, respectively. P_{ex} is the proportion of excess water and E_{ex} the proportion of excess energy. R is the length of the vector between the two periods and θ is the angle (in degrees) of changes relative to the constant long-term aridity index. R_{LUL} and R_{CC} are the relative attribution of changes in stream flows to land use and climate change, respectively (see Section 3.5.2). . . . 48

A.1 Z-statistic values before (Zbef) and after (Zafter) 1980. Bolds show significant values at the 20% level, * Significant at the 10% level, ** Significant at the 5% level . . . 73

A.2 Sen's slope estimator calculated only for statistically significant trends highlighted in Table A.1 73

B.1 Cross-tabulation of land use changes from 1990 to 2018 (values per class in km^2) . . . 79

1 Introduction

1.1. Problem statement and motivation

1.1.1. Climate change

Human activities have resulted in considerable changes in the climate and the water cycle on a global scale (Abbott et al., 2019; Ceola et al., 2014; Oki & Kanae, 2006). Surface air temperature has been continuously rising due to global warming and is likely to continue rising in the coming century (IPCC, 2021). Precipitation patterns are affected to a great extent by warming effects and are expected to change, leading to higher frequencies of rainfall extremes (IPCC, 2021; Lehmann et al., 2015; Moberg & Jones, 2005; Robinson et al., 2021; Trenberth et al., 2015; van den Hurk et al., 2014). Furthermore, considerable alterations are reported in the seasonal patterns of precipitation (Min et al., 2011; Pall et al., 2011). Unpredictable and intense storm events have impacted urban and rural regions all over the world, and have revealed significant failures of water management practices, due to the fact that most of them were designed using past approaches and climate patterns (Cheng et al., 2017; Grandry et al., 2020). Major flood events appear to be more frequent (Blöschl et al., 2015; Blöschl et al., 2017; Hall et al., 2014; Hirabayashi et al., 2013; Rogger et al., 2017). On the other hand, changes are reported in the aridity of many drought indices across numerous geographical regions (Dai, 2013; Sheffield et al., 2012).

Climate change effects have become visible in the Meuse river, as it is almost completely rain-fed and thus sensitive to variability (Bouaziz, 2021; Driessen et al., 2010; Uijlenhoet et al., 2001), and its tributaries i.e. the Geul river. The most recent example is the enormous amount of precipitation that fell in July 2021 across wide sections of Belgium, Luxemburg, Germany, and the Dutch province of Limburg, leading to devastating flooding. Germany and Belgium were the most affected areas where at least 184 people lost their lives (Kreienkamp et al., 2021). During this extreme event, the Geul river catchment received on average 128 mm of precipitation in 48 hours (Asselman et al., 2022). More than 160 mm in 48 hours are recorded locally (Asselman et al., 2022) in the Geul area, for example, station Ubachsberg (the Netherlands) which is located slightly east of the Geul measured an amount of 182 mm of precipitation. This event led to severe flooding of the Geul river that caused considerable damage in the Dutch cities situated along the catchment. The total damages were estimated to be between 100 million euros (Telegraaf, 2021) and 400 million euros (NOS, 2021). According to Kreienkamp et al. (2021), the intensity of this extreme event has been increased by climate change by approximately 3-19% since 1990. In addition, they reported that the probability of occurrence of a similar event today has grown by a rate from 1.2 to 9 times in the larger area (from the northern Alps to the Netherlands) in comparison to the past, due to global warming (Kreienkamp et al., 2021). This extreme precipitation event is considered as rather rare, especially given that the Geul river was subjected to severe drought during the summer just a few years ago (van Dijk, 2022). According to the local water board, extreme precipitation events and floods appear more frequently in the Geul river catchment, and droughts have caused water supply problems to the small tributaries, but these claims have yet to be supported by scientific evidence. The current safety standards of 1/25 years in the Geul river catchment (van Dijk, 2022) are low (also in comparison to the other places in the Netherlands), as there is evidence that the precipitation patterns have been influenced by climate change. This stresses the importance of

analysing the change in precipitation patterns.

1.1.2. Land use changes

Besides climate change, there has been also a global change in land use. People directly change the systems with large interventions (economic or technical) to keep up the standards of living. These interventions include deforestation and reforestation, urbanization and population growth, agriculture and irrigation, loss of wetlands or floodplains, etc. Land use changes can have considerable impacts on river flows and water balances (McMillan et al., 2016; Rogger et al., 2017). For example, the rampant spread of urban areas raises impervious surfaces and reduces infiltration capacities (Grandry et al., 2020). As a consequence, surface runoff during heavy rainfall events is increased, which may lead to flooding in downstream areas, erosion, and polluted streams (Karamage et al., 2017).

Considerable land use changes and human interventions are reported for the Geul river catchment (Dautrebande et al., 2000). The Geul river catchment has a long history of industrial mining activities, that are mainly observed before the early of 20th century (Stam, 2002). Urbanization and intensification of agriculture in the catchment are also reported (Leenaers, 1989; Stam, 2002). These interventions caused significant changes in the landscape of the catchment and probably affected the stream flows.

1.1.3. Importance of time series trend analysis

The identification of changes and trends in the time series of hydrological and climatological data has piqued researchers' interest in the recent literature (e.g., Blöschl et al., 2017; Hannaford et al., 2021; Imfeld et al., 2021; Mangini et al., 2018; Murphy et al., 2020). The effect of climate change and human interventions can be so strong as to produce gradual or abrupt changes in the studied time series (Haddeland et al., 2014; Tu, 2006; Zhou et al., 2020). Making a critical assessment of the past and current states and providing the long-term trends of hydroclimatic variables play a key role in future predictions (Squintu et al., 2021). Investigating the changes that can cause a hazard/problem is an important stepping stone for managing the risks in an efficient way (Yang et al., 2021) and can facilitate the planning of reliable and meaningful interventions.

The Geul river catchment is vulnerable to flooding and erosion (De Moor et al., 2008; van den Munckhof, 2020; van Dijk, 2022) and these conditions are probably exacerbated by land use and climate changes. For this reason, it is considered vital to study the long-term trends of climate change/ variability, runoff patterns, and land-use changes in the Geul river.

1.1.4. Related studies on the Geul catchment

Almost all studies found (in official journals in Scopus) for the Geul deal with ecology (e.g., Lucassen et al., 2010) and geochemistry (e.g., Cappuyns et al., 2006; Swennen et al., 1994), because of the mining activities in the area. In addition, studies that are investigating human and climate interventions are related to geomorphology. Stam (2002) investigated the impacts of human interventions and precipitation variability on floodplain sedimentation. Vandenberghe et al. (2012) studied the effect of human interventions on the evolution of the Geul. De Moor et al. (2008) assessed the effects of humans and climate on the Geul by reconstructing the landscape development during the Holocene epoch. Dautrebande et al. (2000), during an 18-month pilot project, studied the hydrological response of the Geul using different land use change scenarios and suggested environmentally friendly measures to mitigate the flash floods in the area. Their study showed that the flooding problems of the Geul were caused by a combination of climatic events, land use changes, agricultural techniques, human interventions and management practices in the riverbed e.g., straightening. The results revealed that their proposed land-related measures were unable to efficiently reduce high flows (they achieved a maximum reduction of 10%).

Despite the fact that the vulnerability of the catchment to human interventions and climate variability is scientifically recognized, trend analysis studies are missing. Only two old studies are found using statistical approaches. Agor (2003) in his MSc thesis evaluated the long-term runoff-rainfall relation in the Geul river catchment using statistical analyses, without including an extreme precipitation analysis. Agor (2003) concluded that the peak discharges have not changed between 1951 and 2001 and reported that the annual flows were decreased possibly due to losses from the catchment and human interventions. In addition, Tu (2006) in his dissertation on the evaluation of the impacts of climate change and human interventions in the Meuse, included a statistical analysis of hydroclimatic variables in the Geul catchment and quantified the main land use changes. In contrast to Agor (2003), Tu (2006)

reported no changes in annual runoff/rainfall relation in the Geul for the period 1951-2001 and mentioned that the impacts of land use changes and human interventions on annual flows were negligible. Both studies (Tu, 2006 and Agor, 2003) used statistical tests to detect change points (abrupt changes or shifts mainly of the mean) in the time series, without considering trend tests. Tu (2006) argued that the strong variability of the annual time series in the Meuse may suggest the absence of significant linear trends. This statement is quite controversial and vague because i) the significance of a linear trend can be problematic in extreme precipitation indices as their properties are not suitable for least-squares fitting (Moberg & Jones, 2005), and ii) there are non-parametric statistical tests that can detect significant monotonic tendencies instead of just linear (e.g., Mann-Kendall which is recommended by the World Meteorological Organization (WMO) in hydrometeorological time series).

In precipitation time series usually change point tests are used to check the homogeneity of the data before applying trend analysis tests (Buishand et al., 2013; Lupikasza, 2010). In addition, those types of change point tests can be influenced to a great extent by interventions (Zhou et al., 2019). For instance, both Tu (2006) and Agor (2003) found a change point in the discharges in about 1970 that was caused by relocation of the measuring device. Thus, attributing changes to climate variability or human interventions could be biased. In both studies, the spatial and temporal variability is not taken into account as only the outlet of the catchment is used and a fixed record from 1950 to 2001. In general, the statistical trend analysis studies found for the Geul are very old. In the past two decades, extreme climate events and major floods and droughts were observed. In addition, there is a strong potential for improving the trend analyses in the area as in the existing studies i) not all the available time series were analyzed and ii) statistical techniques were not fully utilized including the newest developments.

1.1.5. Developments in trend time series analysis

Trend analysis studies are moving towards more multi-temporal approaches in many climatic and hydrological time series like precipitation, temperature, snow covers, discharges (Hannaford et al., 2021; Murphy et al., 2020; Stähli et al., 2021), drought indices (Vicente-Serrano et al., 2021), groundwater and baseflows (Hellwig & Stahl, 2018) etc. In a multi-temporal approach, trends are evaluated in every possible combination of start and end years. Assessing trends in many combinations of starting and end years (multi-temporal) can facilitate detecting trends over short periods that potentially could not be found over longer ones (Hellwig & Stahl, 2018). Furthermore, with the multi-temporal technique, the trends' persistence and stability can be assessed over the long-term periods (Lupikasza, 2010).

The significance of a trend depends on the studying time frame and time-series length and can be considerably affected. For this reason, trend tests over a fixed time frame may not be representative of the historical variability. The variability in a time series can vary greatly in terms of directions and magnitudes (Hannaford et al., 2013). The multi-temporal approach deals with these limitations and is considered very powerful (Stähli et al., 2021).

1.2. Research objective and research questions

The main objective of this thesis is to investigate the temporal variability and the trends of hydrometeorological variables and the main land-use changes in the Geul river catchment. Thus, this study aims to improve understanding of the impacts of climate change and human interventions on the hydrological response of the Geul, as they play an important role in the area.

The research objective consists of four parts: (1) the temporal variability of the trends of climatic/meteorological variables i.e., precipitation and evaporation, (2) the spatial and temporal variability of the trends of hydrological response i.e., runoff patterns, (3) the main land-use changes and human interventions, and (4) the connection of the spatial and temporal variability of the runoff trends to the climate variability and land-use patterns. The aforementioned four parts lead to the following research questions that this study aims to answer:

1. What are the temporal variability, the stability, and the trend directions of the extreme and total precipitation in the Geul River catchment?

2. What are the temporal variability, the magnitudes, and the trend directions of the potential evaporation in the catchment?

3. What are the most important land-use changes and human interventions in the area?

4. What are the spatial and temporal variability and directions of the extreme and mean discharge trends in the Geul River catchment?

5. To what extent is the variability of the runoff patterns affected by climate variability and human interventions?

1.3. Reading guide

This thesis is structured into six chapters. To start with, Chapter 2 provides a general overview of the Geul river catchment including landscape, hydro-climatic setting, and land use characteristics. The followed methodology and the used materials are described in Chapter 3. Chapter 3 is divided into five sections, including precipitation, evaporation, land use changes, discharge, and attribution analysis. Each section is devoted to each research question and describes the data used and the methodologies followed. The results of the methods presented in Chapter 3 are reported in Chapter 4. Subsequently, Chapter 5 summarizes the key findings of this research describing their implications, discusses the limitations and the uncertainties of the obtained results, and provides suggestions and recommendations. Finally, Chapter 6 closes off this thesis, answering the research questions presented in this chapter and providing future directions for aspects that could be further investigated.

2

Study Area

The Geul river catchment is the area of interest of this thesis as mentioned in the introductory chapter. This chapter provides general characteristics of the catchment area regarding the landscape (Section 2.1), the hydro-climatic setting (Section 2.2), and land use changes (Section 2.3).

2.1. Landscape

The Geul catchment is located in the Netherlands, Belgium, and part of Germany, close to the border triangle (Figure 2.1). The Geul river originates in Belgium, near the town of Lichtenbusch (municipality of Raeren), close to the border with Germany. It leaves Belgium via Sippenaeken and enters the Netherlands at Cottessen, south of Epen. Then it flows northwest along Gulpen, Wijlre, Schin op Geul, Valkenburg, and Meerssen, before flowing into the Meuse (see Figure 2.2). The total area of the Geul

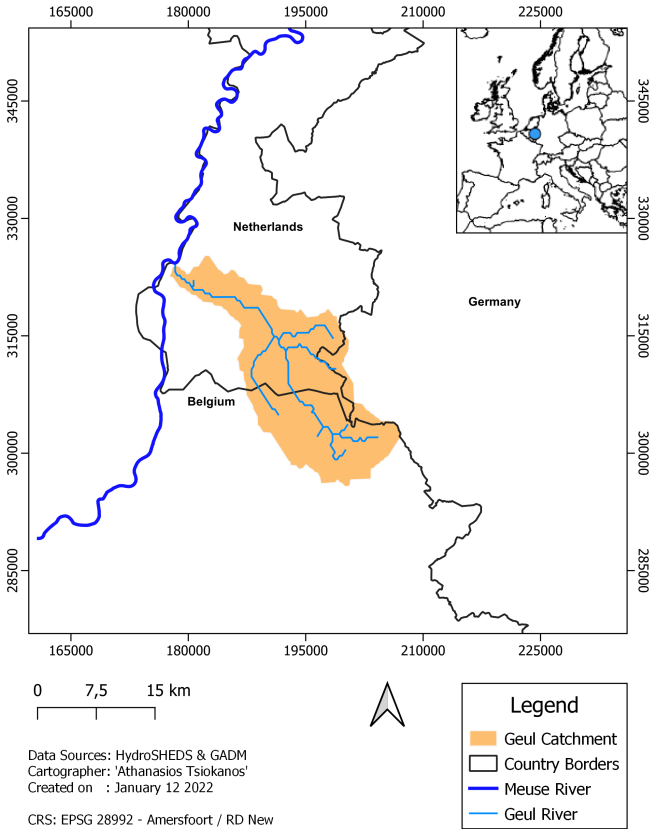

Figure 2.1: Location of the Geul catchment and the countries that share it.

catchment is approximately 344 km^2. Table 2.1 contains the percentages of the total area that belong to each of the countries that share it. The Geul has three main tributaries: i) the Gulp, which originates in

Table 2.1: Situated part per country and its area

Geul River Catchment		
Part	**Area [km^2]**	**Area [%]**
Netherlands	179.7	52.2
Belgium	143.4	41.7
Germany	21.2	6.1
Total	344.3	100

Belgium, enters the Netherlands at Slenaken and flows into the Geul at Gulpen (Azijnfabriek station), ii) the Selzerbeek, which flows into the Geul at Partij and iii) the Eyserbeek. Figure 2.2 shows an overview of the Geul river and its tributaries along the Dutch area.

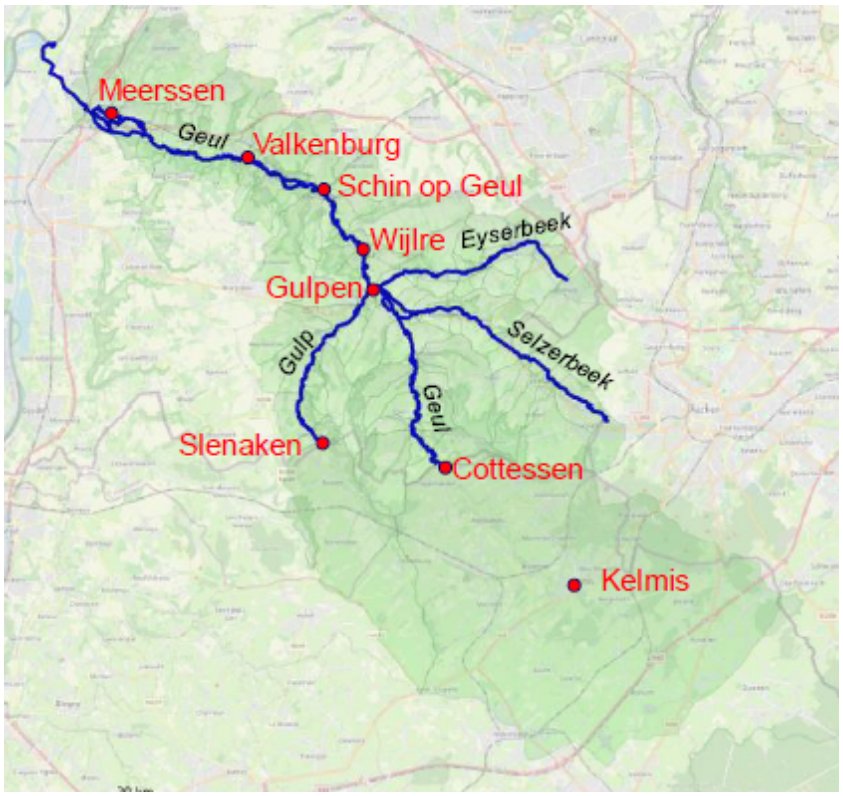

Figure 2.2: Overview map of the Geul catchment area with its tributaries along the Netherlands (taken from: van Heeringen et al., 2022)

The Geul drops about 250 m over approximately 60 km, making it one of the few hilly rivers in the Netherlands. Approximately one third of its total length is in Belgium. The gradient can vary to a great extent all over its length. The gradient drops from 0.2 m/m, at the source, to 0.0015 m/m at the outlet of the catchment (van den Munckhof, 2020). Steep slopes in Belgium contribute to a rapid transport of runoff downstream (van Heeringen et al., 2022). Figure 2.3 depicts the elevation map of the area based on the 30-meter resolution raster downloaded by NASA's Shuttle Radar Topography Mission (SRTM).

In the previous years, the Geul was straightened and its riverbanks protected in order to overcome erosion problems (van den Munckhof, 2020). However, the erosion measures increased the high flows in the Geul (van den Munckhof, 2020). The significant flood events in the Meuse at the end of the 20th century demanded measures for reducing peak discharges. To address this, flood mitigation measures have been implemented in the Geul area during the last years (Tu, 2006). Natural solutions for decelerating the flows and boosting the storage capacities have been carried out, for example

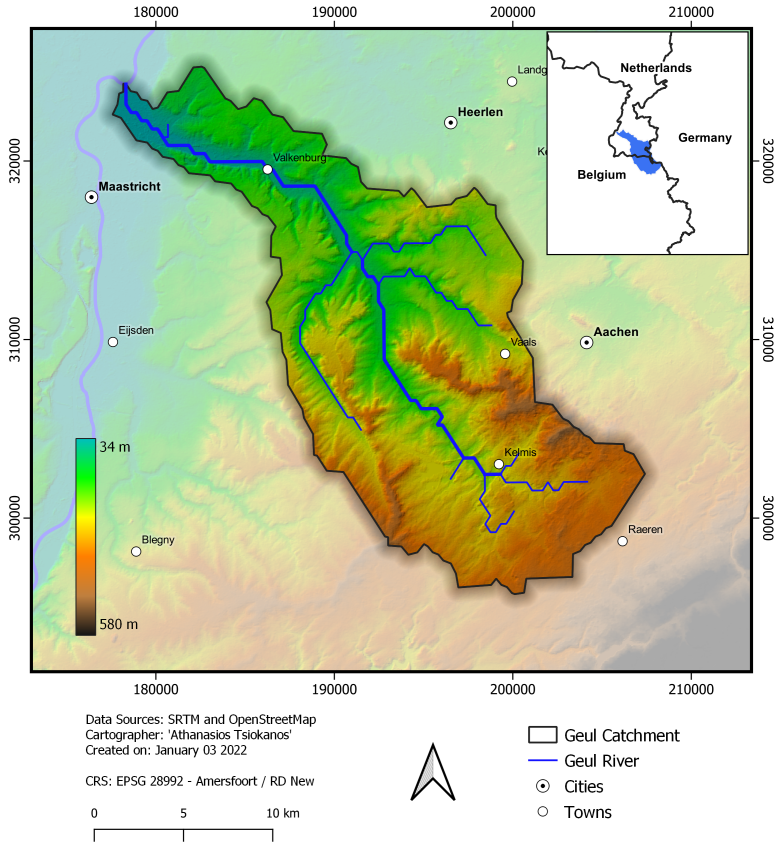

Figure 2.3: Elevation map of the Geul catchment

restoration of meanders (Tu, 2006). No significant artificial interventions influencing the flow have been implemented since 2014 (van Dijk, 2022). Today, the Geul is meandering inside a specific zone (van den Munckhof, 2020) and has little bank protection (van Heeringen et al., 2022).

Quartzites, limestones and sandstones incise the valley of the Geul (van den Munckhof, 2020). A large limestone plateau makes up the middle section of the catchment (Tu, 2006). The main soil type in the Geul is loess (Armstrong, 2013). In addition, Mesozoic and Paleozoic shales are observed (van den Munckhof, 2020). Floodplains are mainly made up of sequences of (fine) sand and loam layers that have a thickness of 2-3 meters approximately (De Moor et al., 2008). Steep sloping banks are observed due to cohesive deposits (van den Munckhof, 2020).

2.2. Hydro-climatic setting

The Geul river has an average discharge of approximately 3.2 m^3/s and is mainly rain-fed (De Moor et al., 2008; van den Munckhof, 2020). As a consequence, its discharge can change dramatically during storm events and droughts. Intense precipitation events can result in overland flow that can cause rapid discharge increases (De Laat & Agor, 2003; De Moor et al., 2008). As an example, the response of the Geul at Meerssen during an extreme precipitation event in November 2010 is presented in Figure 2.4. Large fluctuations in discharges can be observed, ranging from four to more than 40 m^3/s in 30 hours. Local floods are observed mainly in winter season but with no significant damages (De Moor et al., 2008). The annual average precipitation is approximately 870 mm yr^{-1} and is rather uniformly distributed all over the year (see Figure 2.5). Average annual discharge at the outlet of the catchment and potential evaporation are about 307 mm yr^{-1} and 585 mm yr^{-1} respectively, based on time series from 1970 to 2021. The long term evaporative index is approximately 0.67 and the runoff ratio 0.35.

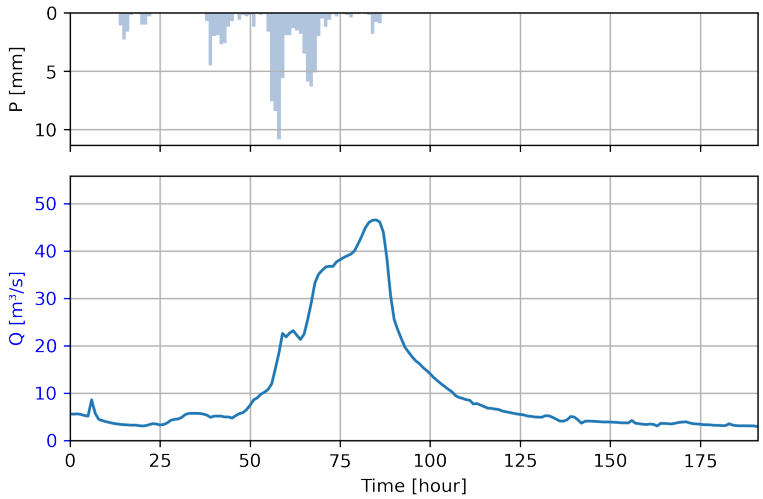

Figure 2.4: Hydrological response of the Geul (lower figure) at Meerssen during an extreme rainfall event (upper figure) on 11 November 2010. Precipitation hourly measurements are based on Maastricht station. Large fluctuation in discharges is visible.

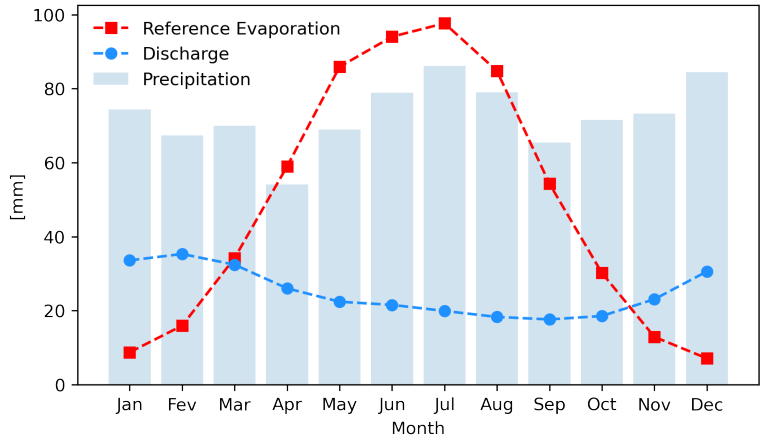

Figure 2.5: Monthly averages for precipitation, reference evaporation (Maastricht station) and discharge in the Geul catchment

2.3. Land use

2.3.1. Historical review

As mentioned in the introduction, the Geul river catchment has a long history of industrial mining activities, mainly before the early 20th century (Stam, 2002). The mining activity during that period caused significant changes in the landscape of the area, resulting in deforestation and channelization of the Geul (Stam, 2002). In addition, a large amount of water was extracted from groundwater due to the mines, causing increased discharges in that period (Dejonghe et al., 1993; Engelen, 1976; Stam, 2002). The industrial mining activity stopped around 1885 (Stam, 2002). This termination caused reforestation of the area which almost coincided with the agricultural crisis of 1878-1895 (Stam, 2002). The agricultural crisis caused changes in the arable lands that altered to pastures and orchards (Stam, 2002). The population expansion in the area started after 1900, according to Dutoo (1994). Dutoo (1994) reported an increase of about 3.45% between 1834 and 1989, and 2.06% between 1989 and 1992, in the total surface of urban areas. It is critical to mention that the agricultural techniques in the area have changed to a great extent since the 1950s, moving towards ”modern agriculture” (Stam, 2002). Grasslands were converted to arable lands, and new crops, like maize and sugar beet, were introduced (Leenaers, 1989; Stam, 2002).

Significant alternations in land use after the 1950s are also reported by Dautrebande et al. (2000). Dautrebande et al. (2000) tried to detect land use changes in the Geul catchment between 1950 and

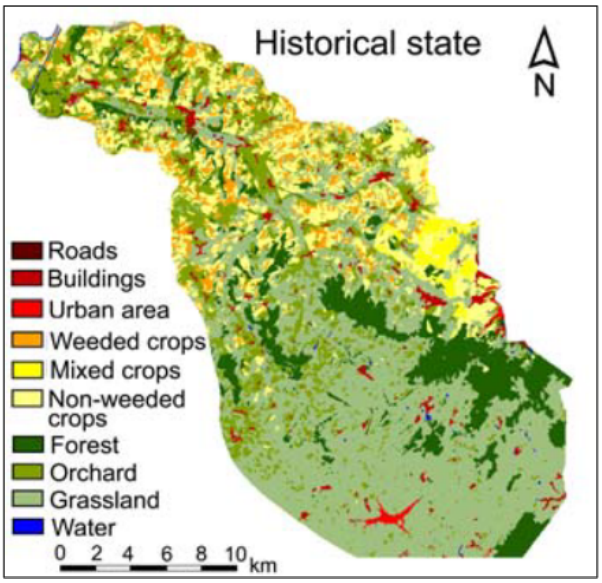

Figure 2.6: Land cover map for the Geul catchment in 1950 (taken from: Tu, 2006)

2000. Figure 2.6 illustrates the historical land use in 1950 according to Dautrebande et al. (2000), as adapted by Tu (2006). According to Dautrebande et al. (2000), grasslands, orchards and forests made up around 73 percent of the land cover in 1950, while they made up about 68 percent in 2000. The urban area increased by almost 5% from 1950 to 2000, while the arable land occupied almost the same area (Dautrebande et al., 2000). Although arable lands remained approximately constant, their composition has changed. More specifically, the proportion of crops like maize, potatoes, beets, vegetables, etc. and mixed crops increased from 29% to 57% (Dautrebande et al., 2000). A small increase in the forest area is also reported (Dautrebande et al., 2000).

2.3.2. Current land use

In order to determine the current land use (Figure 2.7), the CORINE annual land cover map of 2018 is used (European Environmental Agency, 2018), which is considered a reliable source achieving an accuracy of 87% (European Environmental Agency, 2006). Heterogeneous agricultural areas and pastures make up more than half of the catchment area, covering almost 63%. At the same time, urban fabric and forest cover an area of approximately 15% each. The remaining area is made up of arable land, industrial units, mineral extraction sites, sport and leisure facilities, etcetera. Table 2.2 contains detailed values of the percentage of the area that each land use class covers.

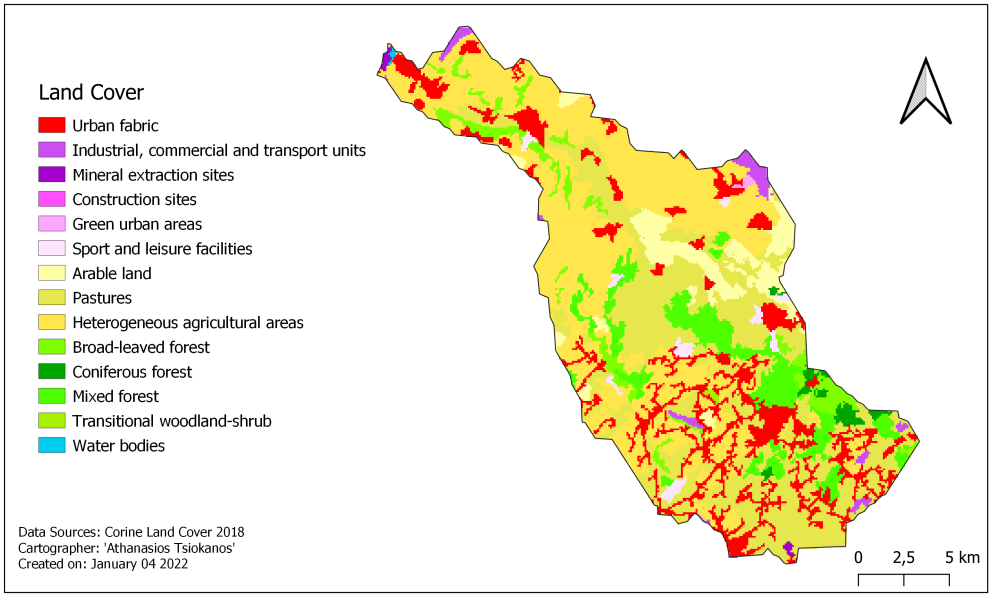

Figure 2.7: Land cover map of the Geul catchment based on CORINE Land Cover (European Environmental Agency, 2018)

Table 2.2: Land cover area percentages according to CORINE Land Cover (European Environmental Agency, 2018)

Land cover	**Geul**
Urban fabric	14.4 %
Industrial, commercial and transport units	1.5 %
Mineral extraction sites	<1 %
Construction sites	<1 %
Green urban areas	<1 %
Sport and leisure facilities	1.2 %
Arable land	5.8 %
Pastures	27.7 %
Heterogeneous agricultural areas	35.5 %
Broad-leaved forest	4.4 %
Coniferous forest	1.0 %
Mixed forest	8.1 %
Transitional woodland-shrub	<1 %
Water bodies	<1 %

3

Methods and Materials

The main goal of this study is to investigate the long-term trends in hydrometeorological variables and the main land use changes in the Geul river catchment, and to understand to what extent the variability of the runoff patterns is affected by climate change and/ or human interventions. This chapter provides information on the methods and materials used in this study. Sections 3.1 and 3.2 describe the data and the methodologies used for the trend analysis in the precipitation and potential evaporation time series (climatic variables), respectively. The data analysis approach used for land cover change detection is elaborated in Section 3.3. Subsequently, Section 3.4 describes the data and the methodologies used for the trend analysis of discharge time series. Finally, an attribution analysis approach and a validation method are presented in Section 3.5.

3.1. Trend analysis of (extreme) rainfall time series

3.1.1. Data

For this study, records of daily precipitation are used from six stations located in the Geul river catchment. The data are downloaded from the online service for meteorological information in the Netherlands [meteobase.nl]. They include precipitation data as produced by the Royal Netherlands Meteorological Institute (KNMI). Specifically, the data used in this study comes from the Netherlands's KNMI manual rain gauge network, which currently includes almost 325 stations. The original network has been in place since 1850. Since 1951, the network size has been nearly constant (Buishand et al., 2013). Observers operate the rain gauges on a voluntary daily basis. Every morning, the quantity of precipitation for the previous 24 hours (from 8 am to 8 am UTC) is monitored and, since 1995, digitally sent to the KNMI. These accumulations do not correspond to calendar days, but this does not affect the goal of the study as the time interval remains constant (shifting the time series 8 hours will provide the same trends). In addition to the volunteer KNMI stations, the Maastricht station is also used, which is an automated station that provides hourly measurements. The hourly data are accumulated to daily data. The rainfall sums for Maastricht do not correspond to the same time interval as for the other stations, but the effect of that is considered negligible for the scope of this study.

The times series are completed without any missing values and are considered to be of high quality. To achieve this, the KNMI performs regular quality tests including but not limited to: 1) separation of multi-day observations to daily records, 2) monthly sum checks, 3) fixing mistakes in date measurements, 4) adding missing values. In addition, station inspectors have been visiting stations on a regular basis since 1951. Reports from those inspections have been preserved at KNMI (Buishand et al., 2013).

For this study, days with significant outliers (values higher than 60 mm in 24 hours) are checked and it is found that all of them occurred during well-known high precipitation or flood events. Another important factor to consider when analysing climate time series is data homogeneity. There are several types of modifications that can occur and can cause significant non-climatic alternations in the data, especially in long time series, such as changes in the location of the measuring station, differences in the manner and the procedures, changes in the instruments/tools, etcetera (Auer et al., 2005; Bhatti et al., 2020; Buishand et al., 2013; Sun et al., 2016; Tian et al., 2017; Wang et al., 2007). For example,

it is known that the Maastricht station has been moved from the town to the airport (near Beek) in 1946, causing a large jump in measured temperatures (Visser, 2005). For this reason measurements for trend analysis at the Maastricht station must be selected after 1946. As a result, it is considered essential to check the homogeneity of the data.

Performing statistical tests for homogeneity on precipitation data measured in daily frequencies is challenging or practically infeasible (Lupikasza, 2010). This can be attributed to the fact that daily time series are substantially noisy. For this reason, the precipitation time series are resampled to monthly sums (as it was also done by Lupikasza (2010) and Tian et al. (2017)) and then tested using two well-known homogeneity tests: the Standard Normalised Homogeneity Test (SNHT) (Alexandersson, 1986; Alexandersson & Moberg, 1997) and Buishand's U test (Buishand, 1984). The SNHT test is widely recognised by the scientific community and has been frequently used in hydrometeorological studies (Ahmad et al., 2015; Bhatti et al., 2020; Kang & Yusof, 2012; Lupikasza, 2010; Ribeiro et al., 2016). The foundation of SNHT is the Test Ratio Method and this approach works best for detecting inhomogeneities towards the start and the end of the time series (Alexandersson, 1986). The U statistics test is a reliable test for detecting change-points in the middle of a series. As for the estimation of the critical values used in the U test, either the tabular form by Buishand (1982) or the Monte Carlo approach can be exploited.

Both tests are applied using the python package "pyHomogeneity" [https://github.com/mmhs013/pyHomogeneity] and using a significance level of 5% (α=0.05). The test results show that the data time series are free of significant errors and no inhomogeneities are detected. However, it should be noted that the spatially changing nature of the precipitation renders the identification of all the inhomogeneities infeasible (Lupikasza, 2010). To deal with this, some allowances need to be made. Buishand et al. (2013) classified most of the relevant stations for this study as homogeneous during the period 1909-2009, using the Menne and Williams Jr (2009) procedure and the untransformed monthly precipitation totals. It is also worth mentioning that no corrections for leakiness were applied by Brandsma et al. (2020) in the manual rain gauge network used in this study, indicating that they work properly.

Belgian stations, in the most upstream part of the catchment, are not used as they contain very short time series. The spatial distribution of the employed precipitation stations is presented in Figure 3.1. Table 3.1 provides an overview of the precipitation stations and the length of the rainfall records.

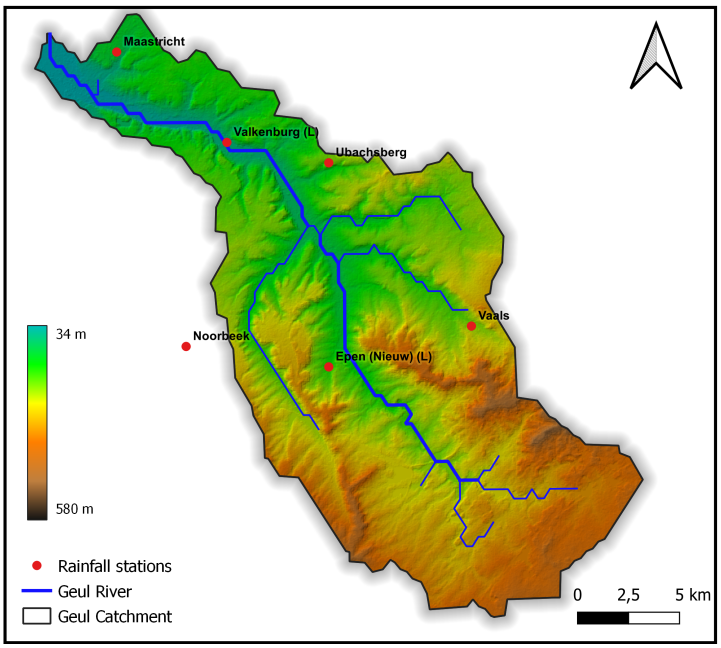

Figure 3.1: Spatial distribution of the precipitation stations

As can be observed, the record periods slightly differ between the selected stations and mainly start in the 1950s, except the new Epen station which has a record from 1981 onward.

Tables 3.2 and 3.3 provide basic descriptive statistics of the rainfall stations. Specifically, Table 3.2 presents statistics including dry days, while Table 3.3 excludes them (statistics without zeros).

Table 3.1: Available rainfall stations and their records

ID	Station	Record Period
963	Valkenburg	1951-2021
968	Vaals	1951-2021
971	Noorbeek	1951-2021
962	Ubachsberg	1956-2021
06380	Maastricht	1958-2021
980	Epen	1981-2021

Table 3.2: Descriptive statistics of the rainfall stations including dry days (24-hour sums)

	Valkenburg	*Vaals*	*Noorbeek*	*Ubachsberg*	*Maastricht*	*Epen*
Fraction of 0s (-)	0.44	0.48	0.49	0.50	0.49	0.49
Mean (mm/d)	2.34	2.55	2.31	2.28	2.08	2.48
Median (mm/d)	0.20	0.10	0.10	0.10	0.10	0.10
Max (mm/d)	80.2	74.0	101.4	98.4	87.4	68.5
STD (mm/d)	4.71	5.04	4.77	4.64	4.38	4.90
CV (-)	2.01	1.98	2.06	2.04	2.10	1.98
Skewness (-)	4.11	3.38	4.63	4.45	4.49	3.79

Table 3.3: Descriptive statistics of the rainfall stations excluding zero values (24-hour sums)

	Valkenburg	*Vaals*	*Noorbeek*	*Ubachsberg*	*Maastricht*	*Epen*
Mean (mm/d)	4.25	4.88	4.55	4.49	4.06	4.84
Median (mm/d)	2.10	2.80	2.60	2.60	2.10	2.90
STD (mm/d)	5.64	6.11	5.88	5.70	5.42	5.95
CV (-)	1.36	1.25	1.29	1.27	1.33	1.23
Skewness (-)	3.30	2.99	3.72	3.57	3.53	2.94

3.1.2. Methodology

Extreme precipitation indices

In this study, the ETCCDI (Expert Team on Climate Change Detection Indices) – recommended climatic extreme indices are used (Ongoma et al., 2018; Peterson & Manton, 2008; Zhang et al., 2011). This type of indices is suitable for precipitation data measured on daily scale and has been frequently used by the scientific community all over the world (Bhatti et al., 2020; Casanueva et al., 2014; Dos Santos et al., 2011; Klein Tank et al., 2002; New et al., 2006; Tian et al., 2017; Tramblay et al., 2013). Considering the crucial climatic conditions that have caused flooding in the past in the study area, as well as what KNMI defines as an ”extreme” precipitation day, six extreme indices are chosen. Trends are examined for full-year periods and over the four climatological seasons: spring, summer, autumn and winter. Table 3.4 shows the definitions of the selected indices. In addition to the ETCCDI extreme precipitation indices, an index representing total annual precipitation, named Rtot, is also taken into account.

Mann-Kendall method

The Mann-Kendall (M-K) test (Kendall, 1955; Mann, 1945) is characterized by the WMO as one of the most useful tests in order to examine the significance of trends in precipitation data time series (Tian et al., 2017). The M-K test is a non-parametric test and has been applied in many hydrometeorological data like temperature, rainfall, and runoff to detect significant trends (Di Baldassarre et al., 2010; Douglas et al., 2000; Gocic & Trajkovic, 2013; Moberg et al., 2006; Murphy et al., 2020; Tabari & Talaee, 2011; Villarini et al., 2011). M-K is a powerful tool as it is simple and robust and can deal with zeros, missing values and outliers, without requiring any data series distribution structures (Šraj et al., 2016; Tian et al., 2017). Furthermore, it outperforms other similar methods for detecting monotonic trends in skewed data like rainfall (Önöz & Bayazit, 2003). The M-K test statistic S is derived from the following equation:

Table 3.4: ETCCDI selected extreme precipitation indices

Name	Index	Units	Definition
Very heavy precipitation days	R30	days	Annual count of days when precipitation >30 mm
Severe precipitation days	R40	days	Annual count of days when precipitation >40 mm
Annual maximum precipitation	RX1D	mm	Annual maximum precipitation of sum for 1 day
Annual maximum precipitation 2 days	RX2D	mm	Annual maximum precipitation of sum for 2 days
Annual maximum precipitation 3 days	RX3D	mm	Annual maximum precipitation of sum for 3 days
Very wet days	R95p	mm	Annual precipitation on wet days >95 percentile
Extremely wet days	R99p	mm	Annual precipitation on wet days >99 percentile

$$S = \sum_{i=1}^{n-1} \sum_{j=i+1}^{n} \mathrm{sgn}(x_j - x_i) \tag{3.1}$$

where n represents the total number of data observations, x_i and x_j denote the data values at time indices i and j (j>i), respectively, and sgn is the signum function which is expressed as follows:

$$\mathrm{sgn}(\gamma) = \begin{cases} 1, & \text{if } \gamma > 0 \\ 0, & \text{if } \gamma = 0 \\ -1, & \text{if } \gamma < 0 \end{cases} \tag{3.2}$$

The variance is determined by the following expression:

$$\mathrm{Var}(S) = \frac{n(n-1)(2n+5) - \sum_{i=1}^{m} t_i(t_i-1)(2t_i+5)}{18} \tag{3.3}$$

where n represents the total number of data observations, m denotes the number of tied groups and t_i is the number of ties of extent i. A collection of sample points with the same values is characterized as a tied group. If the sample size n is larger than 10, the standard normal test statistic Z can be calculated using Equation 3.4:

$$Z = \begin{cases} \frac{S-1}{\sqrt{\mathrm{Var}(S)}}, & \text{if } S > 0 \\ 0, & \text{if } S = 0 \\ \frac{S+1}{\sqrt{\mathrm{Var}(S)}}, & \text{if } S < 0 \end{cases} \tag{3.4}$$

The M-K test is based on the null hypothesis that there is no a trend in the time series. Positive Z values imply rising trends, whereas negative Z values suggest falling trends. Trends are tested at a certain significance level α. If $|Z| > |Z_{1-1/\alpha}|$, the null hypothesis is rejected and a statistically significant trend exists in the time series. $|Z_{1-1/\alpha}|$ is taken from the standard normal distribution table.

Initially, this study exploits the M-K test to detect significant trends and then to assess the stability of a trend. To this end, a python package that contains all the types/modifications of the M-K test, as developed by Hussain and Mahmud (2019), is used. Trends that are significant at α = 0.1 are defined as statistically significant trends and characterized as strong trends, while trends significant at α = 0.2 are also taken into account and characterized as weak trends. Since precipitation is characterized by strong temporal and spatial variation, the statistical significance levels can be lower compared to other climatic variables (Łupikasza et al., 2011; Rapp, 2000). Such significance levels are consistent with existing extreme precipitation trend analysis studies (Lupikasza, 2010; Łupikasza et al., 2011; Tian et al., 2017; Wu et al., 2014).

Considering the fact that the significance of a trend can be influenced to a great extent by the studying time frame (Hannaford et al., 2013; Lupikasza, 2010), a moving 30-year window is applied to the time series. Such a window actually moves 1 year each time over the considered study period.

This technique provides information about the variations of a given index, and its stability in a short-term period. Studying the persistence of a trend all over the 30-year periods provides a clear view about its stability over the whole study period (Łupikasza et al., 2011). This results in 42 periods for stations Valkenburg, Noorbeek, and Vaals (time series from 1951-2021), in 37 periods for Ubachsberg (time series from 1956-2021), in 35 periods for Maastricht (time series from 1958-2021) and in 12 periods for Epen (time series from 1981-2021). The M-K test is applied to each period in each station for all extreme precipitation indices for both seasonal and annual periods.

Trend-strength percentages
The percentages of the statistically significant trends are calculated using the approach proposed by Lupikasza (2010):

$$p_i = \frac{N_{S_i}}{N_T} \times 100 \tag{3.5}$$

where N_T denotes the total number of examined cases (number of stations multiplied with their corresponding total number of 30-year moving periods i.e., 3 stations x 42 periods + 1 x 37 + 1 x 35 + 1 x 12), N_{s_i} the number of trend strength (weak or strong) tested in all cases N_T for a specific extreme precipitation index i, and p_i the final percentage (weak or strong) for this index i. Expressing all strengths from different periods in one index can facilitate understanding the overall image of extreme precipitation in the catchment. Although this study neglects the differences between the periods in the target stations (ideally they should have the same length of time series), except the Epen station, this has no impact on the index relevance as it receives lower values (it counts only for 12 out of 210 studied moving windows). In this thesis, the index p is considered catchment-based rather than station-based. The effect of station Epen on trend-strength results is further discussed in Chapter 5.

Trend stability
The stability of a trend is determined as the percentage of time T in which a trend is statistically significant (weak or strong), where time is the number of 30-year moving periods (Lupikasza, 2010; Tian et al., 2017; Wu et al., 2014). A trend is considered unstable, poorly stable, stable, strongly stable and very strongly stable according to the criteria presented in Table 3.5 (Lupikasza, 2010). Stabilities in the

Table 3.5: Stability criteria (Lupikasza, 2010). T is the percentage of time in which a trend is statistically significant

Criterion	Trend stability type
0% ≤ T <15%	Unstable
15% ≤ T <25%	Poor stability
25% ≤ T <50%	Stable
50% ≤ T <75%	Strongly stable
75% ≤ T <100%	Very strongly stable

Epen station may be biased in comparison to the other stations, as it refers to a more recent period. However, station Epen is needed to identify recent patterns.

Trend magnitude
Sen's slope estimator (Sen, 1968; Theil, 1950), which is a non-parametric test, is used to determine the magnitude of the trends for the following indices: RX1D, RX2D, RX3D, R95p and R99p. A python package as developed by Hussain and Mahmud (2019) is exploited for the calculation of slopes.

Sen's slope test assumes that a monotonic linear trend exists in the times series and its slope in a sample of N pairs of points is expressed by the following equation:

$$\beta_i = \frac{x_j - x_k}{j - k}, i = 1, \dots, N \tag{3.6}$$

where x_j and x_k are the values of measurements at specific time moments j,k. $N = \frac{n(n-1)}{2}$ when only one datum exists in every time period, where n denotes the total number of periods. If there are many measurements in one or more periods then $N < \frac{n(n-1)}{2}$, where n denotes the number of measurements.

The N values of β_i are ranked from smallest to largest and Sen's slope estimator is calculated by the following expressions:

$$\beta = \beta_{[(N+1)/2]}, \text{when } N \text{ is odd} \tag{3.7}$$

$$\beta = \frac{1}{2}\left(\beta_{[N/2]} + \beta_{[(N+2)/2]}\right), \text{when } N \text{ is even} \tag{3.8}$$

Compared to simple linear regression approaches, Sen's slope provides better and more realistic slopes, especially in cases where considerable outliers exist, as it is less influenced by extremes (Caloiero et al., 2020). The sign of the slope indicates the trend direction and it's values the steepness of the trend.

3.2. Trend analysis of potential evaporation time series

3.2.1. Data

For this study, records of daily reference evaporation are used from the meteorological station in Maastricht. The potential evaporation values are computed using the Makkink formula for grass. The Makkink formula has been frequently used in the Netherlands (see De Bruin and Stricker, 2000) instead of the Penman-Monteith equation. The difference between the two equations is that the Makkink value is computed only using temperature and radiation. From 1965 and afterwards measurements of global radiation were used in order to compute the reference evaporation, while from 1952 to 1964, the global radiation was calculated using the relative sunshine duration. For this study, measurements from 1965 to 2021 are used.

The time series were screened in order to detect any suspicious values. The data are complete without any missing values. Table 3.6 contains basic monthly descriptive statistics of the data and Figure 3.2 shows an example of the used data set for year 2021. The values are within the expected ranges, and no unusual values are discovered. The annual average potential evaporation for the time series period (1965-2021) is calculated equal to 582 mm.

Table 3.6: Descriptive statistics of the reference evaporation time series (monthly sums) for the period 1965-2021. All values are in mm/month expect CV and Skewness that are dimensionless.

	Jan	Feb	Mar	Apr	May	Jun	Jul	Aug	Sep	Oct	Nov	Dec
Max	11.8	25.7	49.3	89.1	112	128	139	105	75.6	43.3	18.2	11.0
Min	6.50	10.8	21.5	38.7	56.7	67.9	64.0	62.4	34.7	16.9	9.10	4.70
Mean	8.70	15.9	34.0	58.6	85.6	93.5	97.0	84.0	54.2	30.4	12.9	7.04
Median	8.60	15.5	34.0	58.4	85.1	92.3	96.8	83.4	54.6	29.5	12.7	6.60
STD	1.32	3.09	6.17	11.4	12.9	13.8	16.1	11.1	8.34	4.79	2.09	1.40
CV	0.15	0.19	0.18	0.19	0.15	0.15	0.17	0.13	0.15	0.16	0.16	0.20
Skewness	0.30	0.81	0.35	0.47	0.02	0.17	0.28	-0.07	-0.13	0.06	0.53	0.79

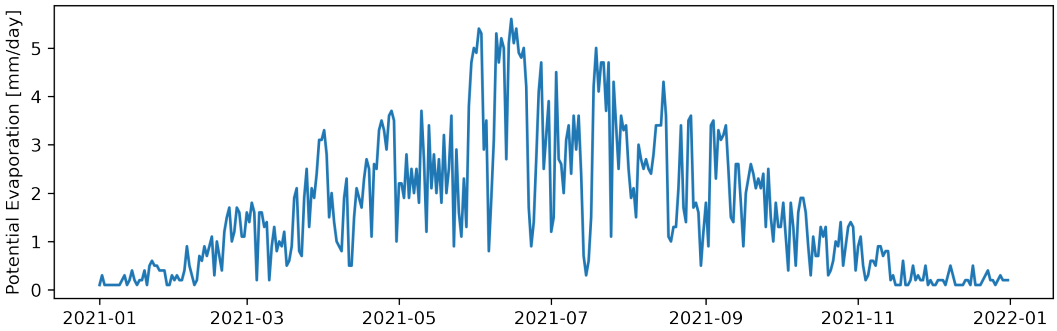

Figure 3.2: Potential evaporation time series in 2021 as an example of the used dataset.

3.2.2. Methodology

Trend detection

The M-K test is used to detect significant trends in the potential evaporation time series in both seasonal and annual periods. The test is applied to the whole time series and the Sen's slope is calculated. In addition, the 30-year moving window approach as described in Section 3.2.1 is also used to the evaporation time series, in order to study the persistence of the trends over the whole study period.

Change points

Change point tests show the time in data where a change e.g. stability of means or variance, is possible. In this thesis the Pettit test (Pettitt, 1979) is used to detect change points (possible breaks in mean values) in the reference evaporation time series.

A random sequence of variables X_1, X_2, ..., X_T is considered to have a change point at a time τ, when X_τ have a common distribution function $F_1(x)$ and X_τ for $t = \tau + 1$,...,T have a distribution $F_2(x)$ and $F_1(x)$ is different than $F_2(x)$. The test is based on the null hypothesis that there is no significant change in the data for $\tau = \mathrm{T}$, while the alternate hypothesis implies the opposite (i.e. a change exists) for $1 < \tau < \mathrm{T}$. The non-parametric statistic K_T tests the null hypothesis and is computed as follows:

$$K_T = max_{1 \le t < T} |U_{t,T}| \tag{3.9}$$

$$U_{t,T} = \sum_{i=1}^{t} \sum_{j=t+1}^{T} \mathrm{sgn}(X_i - X_j) \tag{3.10}$$

where sgn is the signum function as expressed in Equation 3.2. The Pettit test is applied using the python package "pyHomogeneity". A critical probability of 95% is selected for acceptance of a significant change point.

3.3. Land use changes

For this study the CORINE annual Land Cover datasets are used. Figure 3.3 illustrates the data analysis approach used for land cover change detection. Firstly, the data are downloaded using Google Earth Engine (GEE) in tif format. For the sake of this study, two available years are used: 1990 and 2018. The year 1990 is considered as a baseline (oldest available) and the 2018, which is the latest CORINE product, represents the current state. Then using GIS software, the analysis is carried out including geospatial processing, zonal statistics, reclassification and visualization. The final outputs are further processed using python. In addition, the most important human interventions are reported using information provided by the local water board and previous studies.

Based on the CORINE land cover product, 16 classes are found in the study area. The initial land covers are reclassified to 4 main classes with similar runoff coefficients. The reclassification process is based on ESA main land type cover categories (ESA, 2020). The initial and reclassified classes can be seen in Table 3.7. In order to detect changes in land covers, the areal differences for each category are calculated for the two years, for both the whole catchment and per subcatchments.

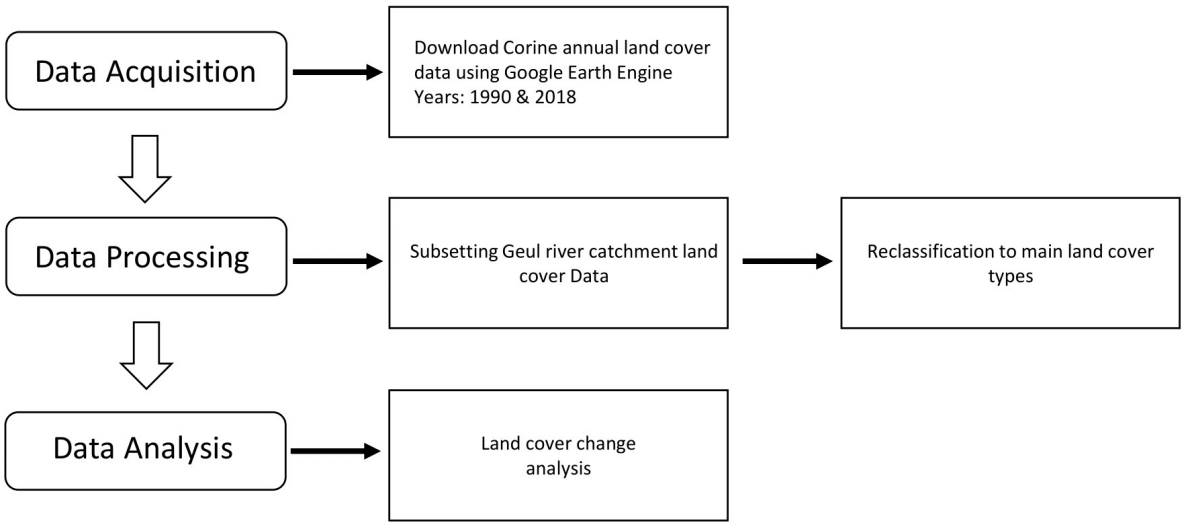

Figure 3.3: Land cover data analysis flow chart

Table 3.7: Initial and reclassified land cover classes

Initial Land Cover Class		Reclassified Cover Class	
Landcover	**Code**	**Landcover**	**Code**
Urban fabric	112	Built-up area	112
Industrial, commercial and transport units	121		
Road and rail networks	122		
Airports	124		
Mineral extraction sites	131		
Construction sites	133		
Green urban areas	141		
Sport and leisure facilities	142		
Pastures	231	Pastures	231
Arable land	211	Agricultural area	211
Agricultural areas (fruits)	222		
Heterogeneous agricultural areas	242, 243		
Broad-leaved forest	311	Forest	312
Coniferous forest	312		
Mixed forest	313		
Transitional woodlands-shrub	324		

3.4. Trend analysis of discharge time series

3.4.1. Data

For this study, discharge time series are used for each station at the outlet of each sub sub-catchment and the outlet of the whole catchment at Meerssen. Each of the tributaries shows a different hydrological response and inundation frequency. For this reason, it is important to investigate the spatial variability within the catchment. Figure 3.4 shows the subcatchments of the Geul and the relevant stations for this study and Table 3.8 includes relevant information.

The data was provided by the local water board and include 15-minute discharge measurements. Water level is monitored in 15-minute time steps and then automatically converted to discharge using rating curves for the station Hommerich. In the Gulp a stage-discharge relation is used in combination with an Acoustic Doppler Current Profiler (ADCP). In the Eyserbeek and the Selzerbeek a trapezoidal flume is used for estimating the discharges since 1992. Currently, at the outlet of the catchment at the

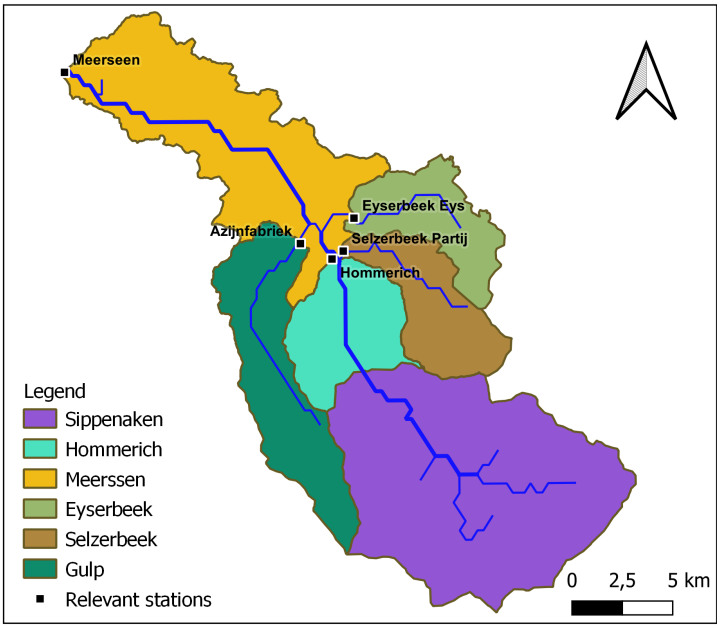

Figure 3.4: Subcatchments and relevant stations.

Table 3.8: Subcatchment areas and their corresponding measuring stations.

Subcatchment	Area [km^2]	Measuring Station	Station Code	Area upstream [km^2]
Meerssen	83.5	Meerssen	10.Q.36	344.3
Hommerich	31	Hommerich	10.Q.30	155
Gulp	47	Azijnfabriek	13.Q.34	47
Selzerbeek	29.6	Partij	12.Q.31	29.6
Eyserbeek	29.2	Eys	11.Q.32	29.2
Sippenaeken	124	Sippenaeken	10.Q.29	124

Meerssen station, the discharges are calculated using ADCP. A historical review about the Hommerich, Gulp and Meerssen stations is presented in Subsection 3.4.2. The time series are incomplete as many values are missing due to malfunctions. In addition, the available time series do not correspond to the same time periods, as the records in Meerssen and Hommerich start from 1970, the records in the Selzerbeek and the Eyserbeek from 1992 and in the Gulp from 1974. In addition, the end periods are not the same. Table 3.9 contains analytical information about the available period in each station and the missing values.

Table 3.9: Missing discharge values and their percentage in parentheses for different resolutions based on the available periods. Values at coarser resolutions are computed from the 15-min data

	Meerssen	**Hommerich**	**Gulp**
Period	1/1/1970 - 10/8/2021	1/1/1970 - 12/11/2021	1/1/1974 - 12/11/2021
Missing (15-minute)	100145 (5.5 %)	164112 (9 %)	239441 (14.2 %)
Missing (hourly)	28692 (6.3 %)	40295 (8.8 %)	54286 (14.1 %)
Missing (daily)	1078 (5.7 %)	1543 (8.1 %)	2183 (12.5 %)
	Selzerbeek	**Eyserbeek**	
Period	1/1/1992 - 14/7/2021	1/1/1992 - 12/11/2021	
Missing (15-minute)	138022 (13.3 %)	3163 (0.30 %)	
Missing (hourly)	34253 (13.2 %)	746 (0.28 %)	
Missing (daily)	1158 (10.7 %)	14 (0.12 %)	

Numerical information about the mean and max daily discharges (of the whole time series period) is presented in Tables 3.10 and 3.11, respectively (statistical moments).

Table 3.10: Statistics of the analysed mean daily discharge time series. The averages derived after resampling the 15-minute measurements to mean daily values.

Station	Mean (average) daily discharge (m^3s^{-1})	Max (average) daily discharge (m^3s^{-1})	Standard deviation (m^3s^{-1})	Coefficient of variation (-)	Coefficient of skewness (-)
Meerssen	3.27	51.1	2.54	0.78	5.00
Hommerich	1.60	36.1	1.81	1.14	5.63
Gulp	0.42	6.85	0.28	0.66	4.47
Eyserbeek	0.12	4.63	0.11	0.94	11.0
Selzerbeek	0.17	2.97	0.15	0.92	5.76

Table 3.11: Statistics of the analysed maximum daily discharge time series.The maximum daily values are derived from the maximum of the 15-minute discharges per day.

Station	Mean (max) daily discharge (m^3s^{-1})	Max (max) daily discharge (m^3s^{-1})	Standard deviation (m^3s^{-1})	Coefficient of variation (-)	Coefficient of skewness (-)
Meerssen	4.34	59.6	3.88	0.89	4.21
Hommerich	2.23	57.8	2.90	1.30	5.83
Gulp	0.56	17.9	0.55	0.98	9.63
Eyserbeek	0.24	11.2	0.38	1.62	8.23
Selzerbeek	0.25	6.28	0.35	1.40	5.64

3.4.2. Meta-data

Meta-data are considered essential in order to interpret the results of the discharge trend analysis correctly. This subsection aims to provide a past and current overview of the studied stations. For this reason, a historical review per station is presented. Based on data provided by the local water board the most important descriptions of measuring station techniques and re-locations are summarized.

Meerssen

From 01-01-1969 to 31-03-1994, water level measurements at Meerssen station were taken, using a measuring weir, from a location downstream of the old paper factory, approximately three kilometers upstream of the confluence with the River Meuse. Until 30-06-1976 the measurements were taken upstream of a threshold (8.30m crest width) at a height of NAP +44.98 m. This threshold was destroyed in 1976, as it was constructed by marl blocks. For this reason, the measurements for the period 01-07-1978 to 31-03-1994 were taken from a location of approximately 100m downstream of the initial threshold, using a crump weir (crest height NAP + 44.96 m, width 9 m, bottom of the river at NAP +44 m). From 01-04-1994 to 01-01-2011 water levels (and subsequently discharges using rating curves) were measured at the Bunde bridge at Meerssen. Since 2011, discharges are measured using Acoustic Doppler Current Profilers (ADCP). The former crump weir at Meerssen was very accurate, while the new techniques with ADCP sensors are less accurate and more sensitive to morphological changes (P. Hulst, personal communication, Jun/2022). For this reason, the measurements were canceled on 14 July 2021 due to morphological changes caused by high water levels.

Hommerich

From 04-09-1969 to 31-12-1977, water level measurements were taken under the bridge at Hommerich and converted to discharges using stage-discharge (Q-H) relations. On 26-09-1978, the measuring station was relocated approximately 200m downstream (at Partij) from the initial place. In February 1984, the station was moved again back to Hommerich, but some meters upstream of the original first location. During the period between September 1978 and February 1984, very large inaccuracies were observed, mainly in the range below 2 m^3/s and above 15 m^3/s.

Gulp (Azijnfabriek)
For the station Azijnfabriek at the Gulp, no specific information is available for the period 1969-1985. Between 01-01-1969 and 31-05-1981 probably a Q-H relation was utilized to derive discharge measurements, while from 01-06-1981 to 31-12-1985 a measuring weir was used. From January 1986 to April 1995, a crump weir was placed. The measuring crump weir was demolished in May 1995 to allow fish migration. After removing the weir, it was not possible to establish a Q-H relation from April 1995 to November 1997, mainly due to large rocks that were placed in 1995. These rocks had major disruptive effects on the Q-H relation and made discharge measurements impossible until about 1998. In November 1997 a new Q-H relation was drawn up again. The new stage-discharge equation was considered unstable and inaccurate. The measuring range of the water level meters could not cope with the low water levels that occur in the Gulp. For this reason, in 2014 an ADCP flow rate meter was placed that is used also today in combination with Q-H equations to estimate discharges.

Eyserbeek (Eys) and Selzerbeek (Partij)
In the Eyserbeek and the Selzerbeek trapezoidal flumes (meetgoot, trapeziumvormig) are used to determine discharges. The Q-H relation in the Selzerbeek has been changed several times in the past.

3.4.3. Methodology

Multi-temporal trend analysis
The Mann-Kendal test is used again in order to detect trends in the discharge time series. Trends are examined over the same periods as precipitation (full-year, summer, spring, autumn and winter) for two main indices: annual maximum and mean flows. It is argued that the results of the M-K trend tests may be affected by the presence of autocorrelation (Renard et al., 2008). For this reason the modified M-K test as proposed by Hamed and Rao (1998) is used for the times series that show strong serial correlation. Hamed and Rao (1998) proposed a variance correction of the M-K test that takes into account the impact of serial correlation.

Most studies use typical trend tests in fixed timeframe periods that may not be representative of the historical variability. The variability of a trend can vary significantly in terms of significance and magnitudes, depending on the selected study period and time lengths (Hannaford et al., 2013; Murphy et al., 2013). To deal with this limitation, this study leverages a “multi-temporal” approach. In this method, the significance of a trend is tested to every possible combination in the time series, with a 30-year minimum window duration. Instead of testing trends for a specific defined significance level, the M-K Z-statistic is calculated for each combination of start and end year periods. This gives a clear indication of the directions and the magnitudes of the trends (Hannaford et al., 2013). A multi-temporal approach was also used in several studies to detect flood variabilities (Hannaford et al., 2013; Hannaford et al., 2021; Petrow & Merz, 2009; Ruiz-Villanueva, Stoffel, et al., 2016; Schmocker-Fackel & Naef, 2010; Stähli et al., 2021), indicating its relevance.

The multi-temporal analysis is applied to the stations in Meerssen, Gulp and Hommerich, as they have a long record from the 1970s. For the remaining stations (in Eyserbeek and Selzerbeek) the typical M-K test is applied to one time interval (whole time series from 1992-2021). Years in which more than 40% of the measured daily values are missing are not included in the analysis. In addition, years in which many seasonal values are missing (e.g. a whole winter) are also excluded. The years mentioned in Table 3.12 are excluded from the multi-temporal trend analysis.

Table 3.12: Years that are excluded from the analysis

Station	Years excluded
Meerssen	-
Hommerich	1970, 1978, 1989
Gulp	1985, 1996, 1997
Selzerbeek	2001, 2010
Eyserbeek	-

The modified M-K test (Hamed & Rao, 1998) is used only for the full-year annual mean discharges that show a relatively strong first-order autocorrelation. For example the full-year annual mean discharge time series in Meerssen has a first order autocorrelation of 0.52 in comparison to the individual

seasons (year by year) where the value does not exceed the 0.25. It can be argued that this step is not so important, as in the discharge analysis only the Z-statistic values are taken into account and not their significance at a certain level, however a relatively small correction improvement is expected. The other time series show insignificant first order serial autocorrelations and the original test is applied.

Change points
The Pettit test is used again to detect change points in the discharge times series (a described in Section 3.2.2). A change point in discharge time series can be caused by several factors, for example land use changes, urbanization, climate change, human interventions, etcetera (Montanari et al., 2013; Zhou et al., 2019). In order to avoid finding a change point in the time series due to relocation or change (at the same location) of a measuring device, only the Meerssen station is used. Meerssen (outlet of the catchment) contains almost complete measurements and its record is considered reliable for periods after the 1970s (Agor, 2003). A critical probability of 95% is selected for acceptance of a significant change point.

3.5. Attribution and Validation

3.5.1. Correlations between maximum discharges and precipitation extremes

In order to investigate to what extent the variability of the maximum discharges is affected by the climate variability, this study proposes a new correlation methodology. In this methodology, the multi-temporal approach used for the annual maximum discharges and extreme precipitation is exploited.

Sen's slopes are calculated for each moving window in the precipitation extreme indices. The same slopes are calculated for each moving window in the discharge time series. Finally, the calculated slopes are correlated, using Pearson's linear correlation method.

With this technique the rate of change between the two variables is evaluated all over the studying time frame. Correlating the rate of change all over the 30-year periods provides a clear view about the connection of the variabilities between the two variables. Both magnitudes and directions can be associated. If the tendencies between two variables are strongly correlated, for example extreme precipitation and extreme discharge are increasing or decreasing in the same periods and with the same rates, then the two variables are also correlated.

The proposed technique provides a clear view of correlation in variabilities and exploits and adds value to the multi-temporal trend analysis instead of the traditional approaches used in the literature that correlate values between two indices (e.g., Hannaford et al., 2013; Ruiz-Villanueva, Stoffel, et al., 2016; Ruiz-Villanueva, Wyżga, et al., 2016; Tramblay et al., 2013).

3.5.2. Separating the effects of land use and climate changes on mean flows

This study exploits the framework developed by Tomer and Schilling (2009) for separating the effects of land cover and climate changes on flows. In their framework, they utilized the variations in the proportions of excess water changes with respect to alternations in the proportions of excess energy. The excess water is determined by the difference between the precipitation (P) and actual evapotranspiration (ET), while the excess energy can be calculated as the amount of potential (ET_0) minus actual evapotranspiration (ET). The ET is taken by closing the long-term annual water balance (precipitation P minus runoff Q). This is based on the assumption that the long-term water storage change ΔS_w becomes zero (see Equation 3.11). The two quantities, excess water and energy, are divided by the available water (P) and energy (ET_0), respectively, resulting in two dimensionless indices: the proportion of excess water P_{ex} and the proportion of excess energy E_{ex}. These two indices can take values between 0 (no excess energy/water) and 1 (maximum excess energy/water) and can be expressed using the Equations 3.12 and 3.13.

$$P = ET + Q + \Delta S_w \tag{3.11}$$

$$P_{ex} = 1 - ET/P \tag{3.12}$$

$$E_{ex} = 1 - ET/ET_0 \tag{3.13}$$

Tomer and Schilling (2009) assume that climate change affects only P and/or E_0, not ET at local scales. This leads to changes to P_{ex} and E_{ex} by the same rate but opposite signs depending on the P/ET_0 ratio. For example, an increasing ratio of P/ET_0 over time leads to an increased P_{ex} and a decreased E_{ex}, while a decreasing ratio leads to a decreased P_{ex} and an increased E_{ex}. A second assumption, is that

the land use changes can affect only ET (and not precipitation P and ET_0), resulting in changes in the same direction for P_{ex} and E_{ex}. This means that land use effects will become visible in simultaneous changes of P_{ex} and E_{ex} in the same direction (increasing or decreasing). Movement of P_{ex} and E_{ex} towards an increase can be caused by a reduction of ET, for example due to deforestation, while decreases in P_{ex} and E_{ex} are caused by increases in ET, for example due to reforestation. A schematic representation of the temporal variation of P_{ex} and E_{ex} and possible potential drivers are presented in Figure 3.5.

Renner et al. (2014) modified the framework of Tomer and Schilling (2009) by considering changes over a constant long-term aridity index ($\overline{ET_0}$ / $\overline{P}$). This modification takes into account the climatic state of the area/catchment, as the initial framework was only applicable in catchments where the precipitation was the same as evaporative demands. According to Renner et al. (2014), changes over the time that are parallel to the constant aridity index $\overline{ET_0}$ / $\overline{P}$, are caused by land use changes (changes in ET). On the other hand, changes perpendicular to the constant aridity index, are attributed to climate as P/ET_0 has changed. To sum up, the movement from a baseline period symbolized as $M_1(P_{ex1}, E_{ex1})$ to an altered period $M_2(P_{ex2}, E_{ex2})$ relative to a constant aridity index, provides the attribution. Changes of P_{ex} and E_{ex} for the same aridity index indicate land uses as driving force, while changes of P_{ex} and E_{ex} away from a constant aridity index indicate climate change as driving force (see Figure 3.5). Marhaento

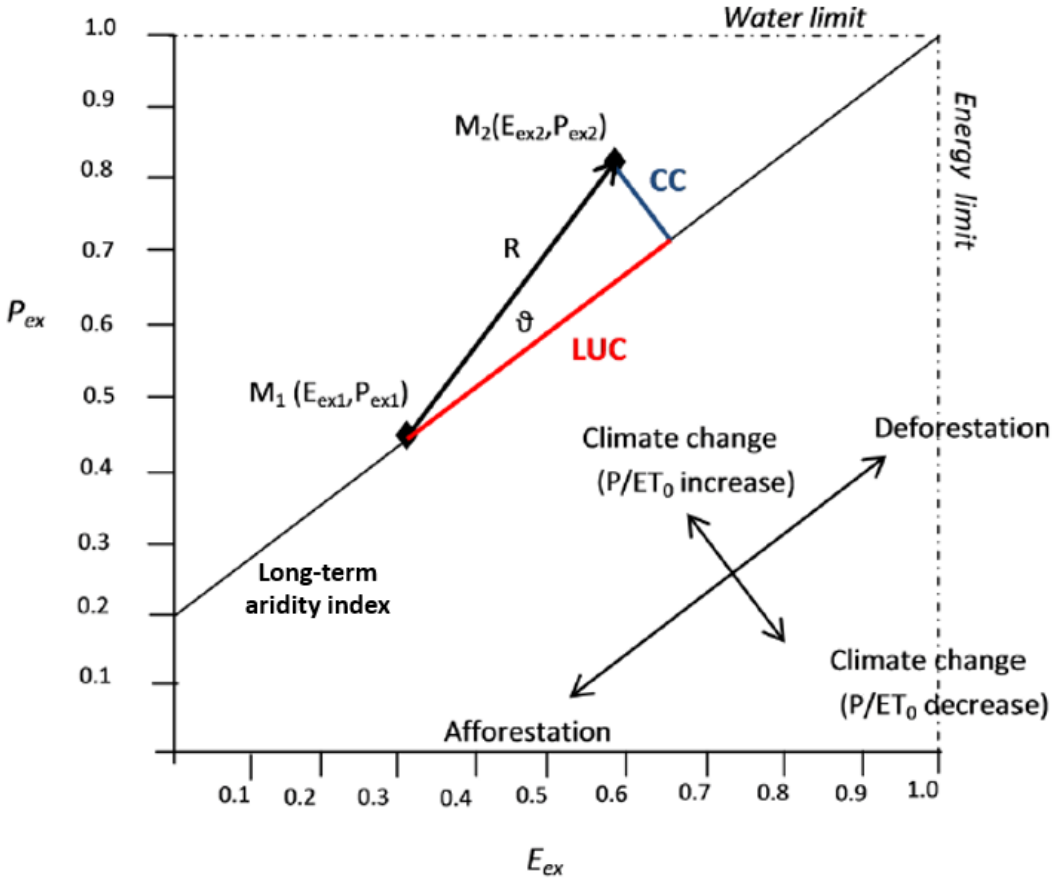

Figure 3.5: Framework for seperating the effects of land use and climate change on streamflows based on Tomer and Schilling (2009) and modified by Renner et al. (2014). Points M_1 and M_2 are the fractions of excess energy and excess water for two studying periods. M_1 (E_{ex1}, P_{ex1}) represents the baseline period (before change) and M_2 (E_{ex2}, P_{ex2}) the altered period (post-change). Changes over the constant long-term aridity index are attributed to land use change (LUC), while changes perpendicular to the aridity index are caused by climate change (CC). The length of the vector R shows the magnitude of the combined changes and θ is the angle between the gradient of M_1 - M_2 and the constant long-term aridity index (taken from Marhaento et al., 2017)

et al. (2017) developed geometric tools in order to calculate the attribution of land use change (LUC) and climate change (CC), as it is shown in Figure 3.5. The magnitude of changes between the baseline period M_1 and M_2 is called R and can be calculated using Pythagoras' theorem. θ is the angle between the gradient of M_1 - M_2 and the constant long-term aridity index and can be calculated based on the

following equations as developed by Marhaento et al. (2017):

$$tan(\theta) = \left| \frac{\frac{\overline{ET_0}}{\overline{P}} - \frac{P_{ex2} - P_{ex1}}{E_{ex2} - E_{ex1}}}{1 + \left(\frac{\overline{ET_0}}{\overline{P}}\right) * \left(\frac{P_{ex2} - P_{ex1}}{E_{ex2} - E_{ex1}}\right)} \right| \tag{3.14}$$

The relative magnitudes of LUC and CC are symbolized as $R_{LUL}(\%)$ and $R_{CC}(\%)$, respectively, and and can be calculated using the following equations:

$$R_{LUL}(\%) = \frac{LUC}{LUC + CC} * 100\% \tag{3.15}$$

$$R_{CC}(\%) = \frac{CC}{LUC + CC} * 100\% \tag{3.16}$$

where $LUC = R\cos\theta$ and $CC = R\sin\theta$.

This study uses the separation framework modified by Renner et al. (2014) and the geometry tools developed by Marhaento et al. (2017) to investigate whether the water balance has been changed and to attribute any changes to CC and/or LUC. The period from 1970 to 2021, during which the hydrometeorological time records are available, is separated into two (12-year) equidistant periods: from 1970 to 1981 and from 2010 to 2021. The period from 1970 to 1981 is considered as the baseline period (M_1 point in Figure 3.5) and the period from 2010 to 2021 as the altered period (M_2 point in Figure 3.5). In the midterm time interval, most of the land use and climate changes are considered to have occurred. Taking adequate long-term averaging periods is considered vital for the assumption that the water storage change ΔS_w becomes zero (see Equation 3.11). For the calculations, the discharge measurements at the outlet of the catchment (Meerssen station), as described in Section 3.4.1, are used. Potential evaporation measurements are used from the meteorological station at Maastricht (see Section 3.2.1). The areal average precipitation in the Geul river catchment is obtained using the Thiessen polygon method. For this calculation, only rainfall stations with records since 1970 are used (see Section 3.1.1). The annual mean precipitation and potential evaporation for each 12-year period are calculated by averaging the yearly totals. The annual mean discharge is calculated by taking the average of the mean annual values. The mean annual discharges are expressed in mm (divided by the catchment area and multiplied by the time).

3.5.3. Validation

The analysis presented above is also used as a validation method for the results obtained in the statistical trend analysis (Sections 3.1, 3.2 and 3.4) and the land use change detection (Section 3.3). For instance, a larger contribution of climate change in stream flows is translated to significant trends of precipitation (P) and potential evaporation (ET_0) in the same direction and of the same magnitudes as trends in mean discharges. In addition, a small contribution of land use changes in stream flow alterations is translated to insignificant alterations in the land use change analysis.

4

Results

In this chapter, the results of the study are presented. To start with, Sections 4.1 and 4.2 present the results related to the trend analysis of the rainfall and potential evaporation time series, respectively. Subsequently, Section 4.3 shows an overview of the land use changes in the catchment area. Afterwards, in Section 4.4 the results of the discharge time series analysis and trend detection are presented. Section 4.4 is divided into two parts. The first part is devoted to maximum discharges and the second one is related to mean flows. Lastly, Section 4.5 provides the results of the attribution analysis for both maximum discharge variabilities and mean flows and includes the findings of the validation method.

4.1. Trend analysis of (extreme) rainfall time series

Figure 4.1 shows boxplots of all stations for the total annual precipitation (Rtot), annual number wet days (a wet day is defined as day with more than one mm precipitation) and maximum 24-hour precipitation per year (RX1D). Figure 4.1 shows that the average annual rainfall ranges from 750 mm to more than 900 mm. Figure 4.2 shows the time series of the selected precipitation indices for full-year periods in Valkenburg station as an indication of the order of magnitude in the area. From Figure 4.2 it can be concluded that R30 and R40 are rare events and their frequency of occurrence ranges from zero to five events per year. In addition, Figure 4.2 indicates the magnitude of the July 2021 event (mentioned in Chapter 1), as it has the largest value from 1950 to 2021 in RX1D, RX2D and RX3D.

4.1.1. General overview of the trends

The moving window approach is used to obtain a broad view of severe precipitation patterns in the catchment. Statistically significant trends, characterized as week and strong, are calculated and expressed as percentages for all studied stations and for different time periods from 1951-2021 as described in Section 3.1.2. This subsection shows the results of the trend-strength percentages.

Figure 4.3 illustrates the percentages of statistically significant trends for all stations in all 30-year moving periods in the studied area for all indices. As mentioned above, weak trends are those that are significant at α=0.2, and strong trends – significant at α=0.1.

Seasons

In summer, trends are moving primarily upwards but also some negative trends (mainly weak) can be detected (Figure 4.3a). However, it should be mentioned that the strong increasing trends far outweigh the decreasing ones and, overall, summers have the largest proportion of strong trends for all the studied periods. The strongest trends are mainly observed in the recent past (from the 1980s-2021) and they cause strong stabilities as explained in the following sections. Index RX1D has strong increasing trends, almost five times more frequent than weak trends (20% strong and 3.8% weak). R99p, RX2D and R30 have strong increasing trends, almost three times more frequent than weak trends, while in R95p, RX3D and R40 the weak upward trends are two times less prominent than the strong trends. On the other hand, decreasing trends in RX1D, R95p, R99p, R30, R40, RX2D and RX3D are found in 18.5 %, 13.8%, 18.5 %, 13.8%, 13.3%, 14.3% and 10.5% of the cases, respectively. The total precipitation (Rtot) shows slightly more upward trends (17.1% increasing and 10.4% decreasing), however this

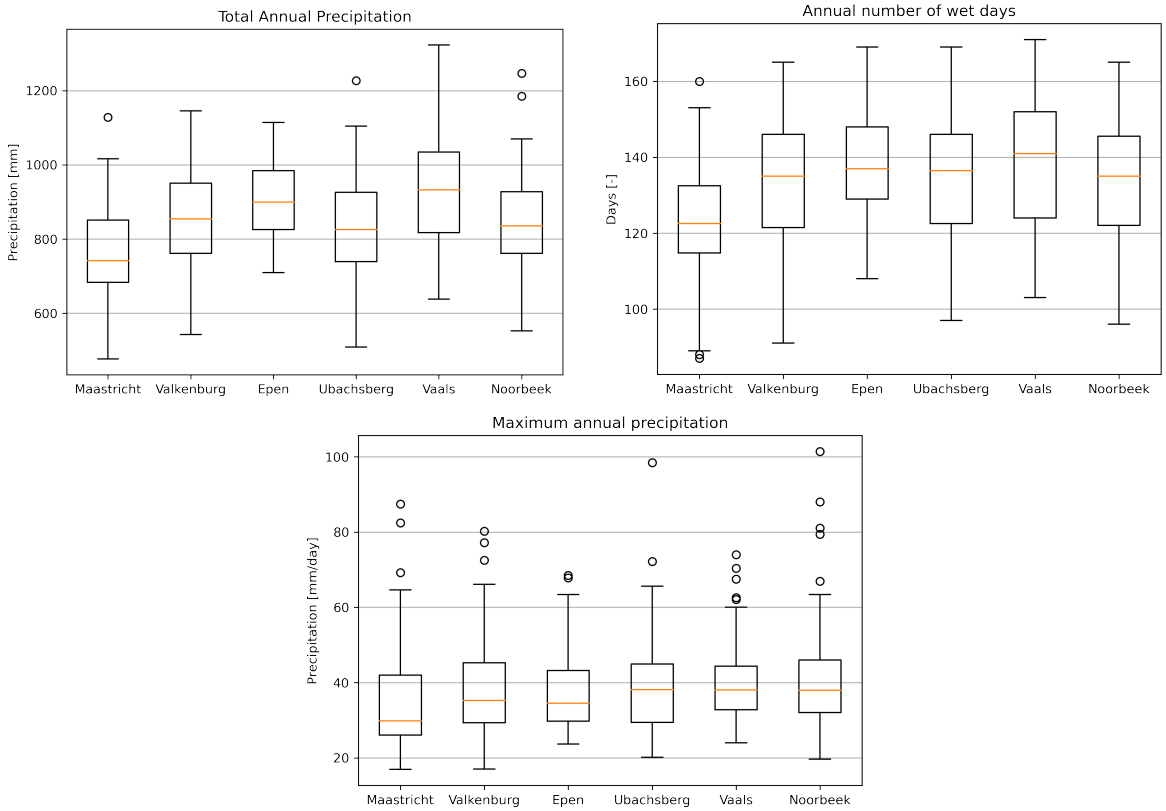

Figure 4.1: Boxplots illustrating total annual precipitation, annual number of wet days and maximum 24-hour rainfall per year for the stations considered in this study.

Figure 4.2: Time series of the selected (extreme) precipitation indices as an example for full year periods in Valkenburg station.

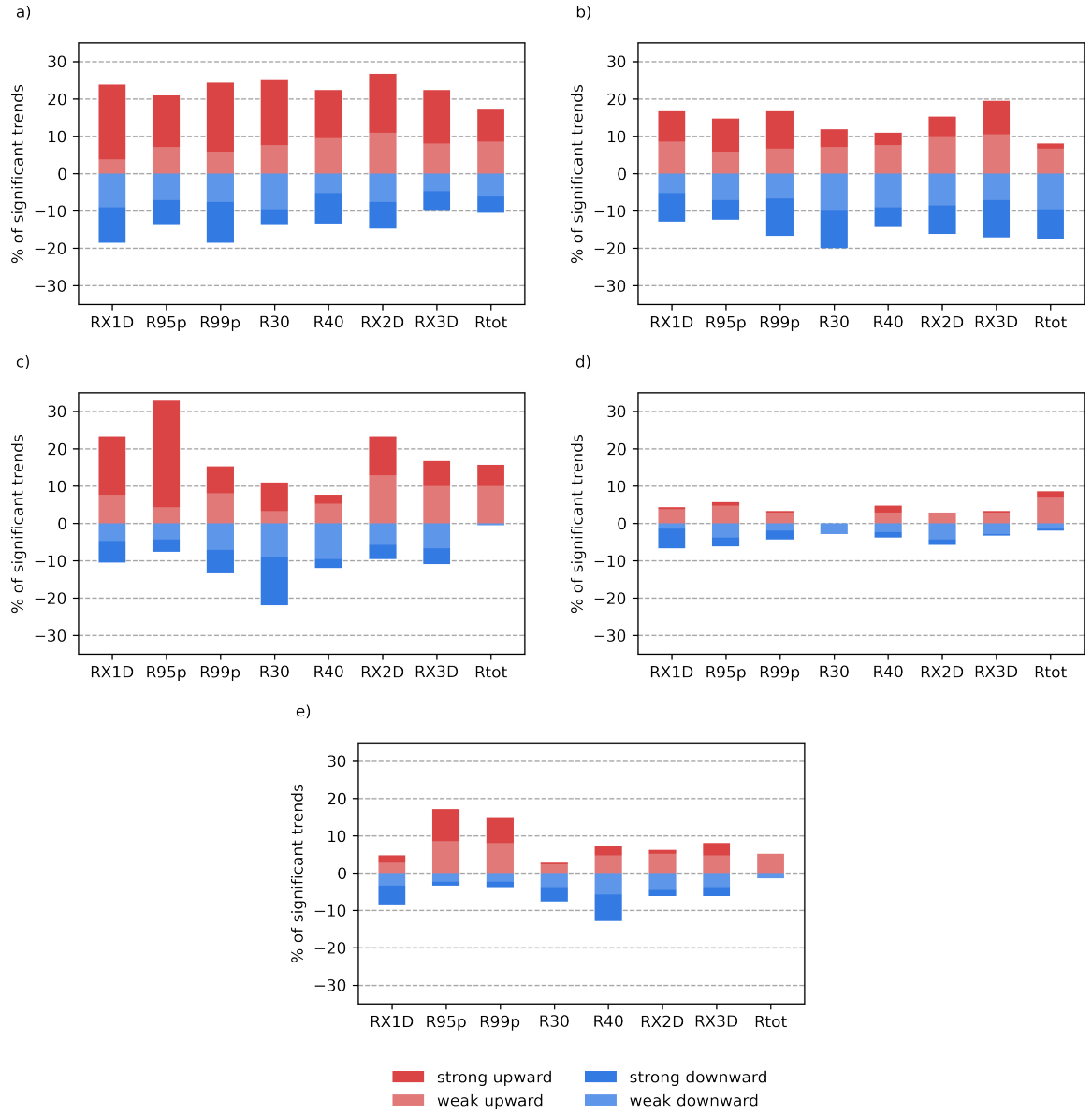

Figure 4.3: Percentages of statistically significant trends calculated for each station and each of the 30-year moving periods. (a) summer; (b) spring; (c) winter; (d) autumn, (e) full year

difference is not considerable. Overall, the difference between increasing and decreasing trends is not clearly disproportionate to the increasing side, however strong trends in the most extreme indices are moving towards an upward direction to a greater extent compared to the downward direction.

In spring (Figure 4.3b), statistically significant downward trends are more prominent than the upward trends, in the indices R30, R40 and Rtot (20%, 14% and 17.6% respectively). In the remaining indices, the fluctuations in percentages among upward and downward trends are not evident (similar percentages in both directions).

During winter (Figure 4.3c), the percentages of statistically increasing trends in indices R95p (32.8%) RX1D (23.3%) and RX2D (23.3%) are much higher than the decreasing trends. It should be noted that the strong upward trends in index R95p represent the 25.8% of the total increasing percentage (i.e. 32.8%), which is the highest percentage of all strong increasing trends. R30 shows a clear decreasing tendency with 21.9% statistically significant trends. The percentage of increasing trends in Rtot is 15%, while the downward trends in the same index are minor. Finally, there is no clear distinction between positive and negative statistically significant trends in R40 and RX3D, as they have almost the same

percentages including mainly weak trends.

In autumn (Figure 4.3d), there is not a clear disproportion between upward and downward trends as the difference is negligible. The percentages of statistically significant trends in all extreme precipitation indices hardly go up to 5% in both directions. It should be noted that R30 shows only decreasing directions (weak trends at almost 2%), while Rtot displays mainly upward trends in approximately 7.5% of the cases, with a small proportion of strong trends.

Full-year

Regarding the full year period (Figure 4.3e), clear directions, with a large proportion of strong trends, are observed in indices R95p, R99p and R40. R95p and R99p move upwards with a percentage of significant trends at 17.1% and 14.8%, respectively. On the other hand, R40 shows downwards trends (12.8%). It is interesting to mention that the percentages of statistically decreasing trends (8.6%) in annual maximum precipitation RX1D are higher compared to the increasing trends (4.7%), however the total percentage and the difference between them are small. In the remaining indices, small tendencies can be observed at low percentages values. These tendencies are mainly weak trends and are considered negligible.

4.1.2. Long-term variability of the trends

This section describes the temporal variability of the statistically significant trends. The variability is expressed as an overall behaviour of the majority of the stations in the catchment and not per station. Thus, small discrepancies may be observed between stations. In general, as the study area is small no considerable differences in patterns of trends are expected.

Summer

A very important factor that needs to be addressed is that the summer's strong trends have started in the recent past and especially the periods starting after the 1980s. After the 1980s, a relatively strong-significant increase is observed in almost all extreme precipitation indices. Figure 4.4 illustrates the results (Z-statistics) from the moving window periods that are used to calculate the trend strengths for summer in two stations: Vaals and Valkenburg. The two stations are selected as an example because in this way the spatial variability of the catchment is considered. The Vaals station is the most upstream station and the station in Valkenburg is in the downstream part (see Figure 3.1). The remaining stations show similar patterns. Each bar in Figure 4.4 represents the Z-statistic value in each 30-year moving window (see Section 3.1.2). The results show a clear reverse of directions. Trends starting mainly before the 1980s are decreasing while a strong increase for trends starting after 1980s in every extreme index is observed. Both increasing directions and magnitudes are significant. This result shows the importance of the moving-window approach in identifying variability and changes in the rainfall time series.

Taking into account the tendency of extreme precipitation indices in summers, two separate periods are examined to test whether changes after the 1980s are significant. The first period is before 1980 and the second after 1980. For those periods, trends and slopes are calculated for every station in summer periods. The results shows a relatively strong increase in all precipitation indices in summer after 1980. The directions and magnitudes are the opposite in the two periods in almost every station. The resulted Z-statistic values and slopes between the two periods can be found in Appendix A.1.3.

Figure 4.5 shows the distribution of the values before and after 1980 (blue color before and orange after) and the fitted linear regression models for the Vaals station in summer. Figure 4.5 reveals the increase in summer after 1980, as there is a clear distinction in directions before and after the aforementioned period in Vaals.

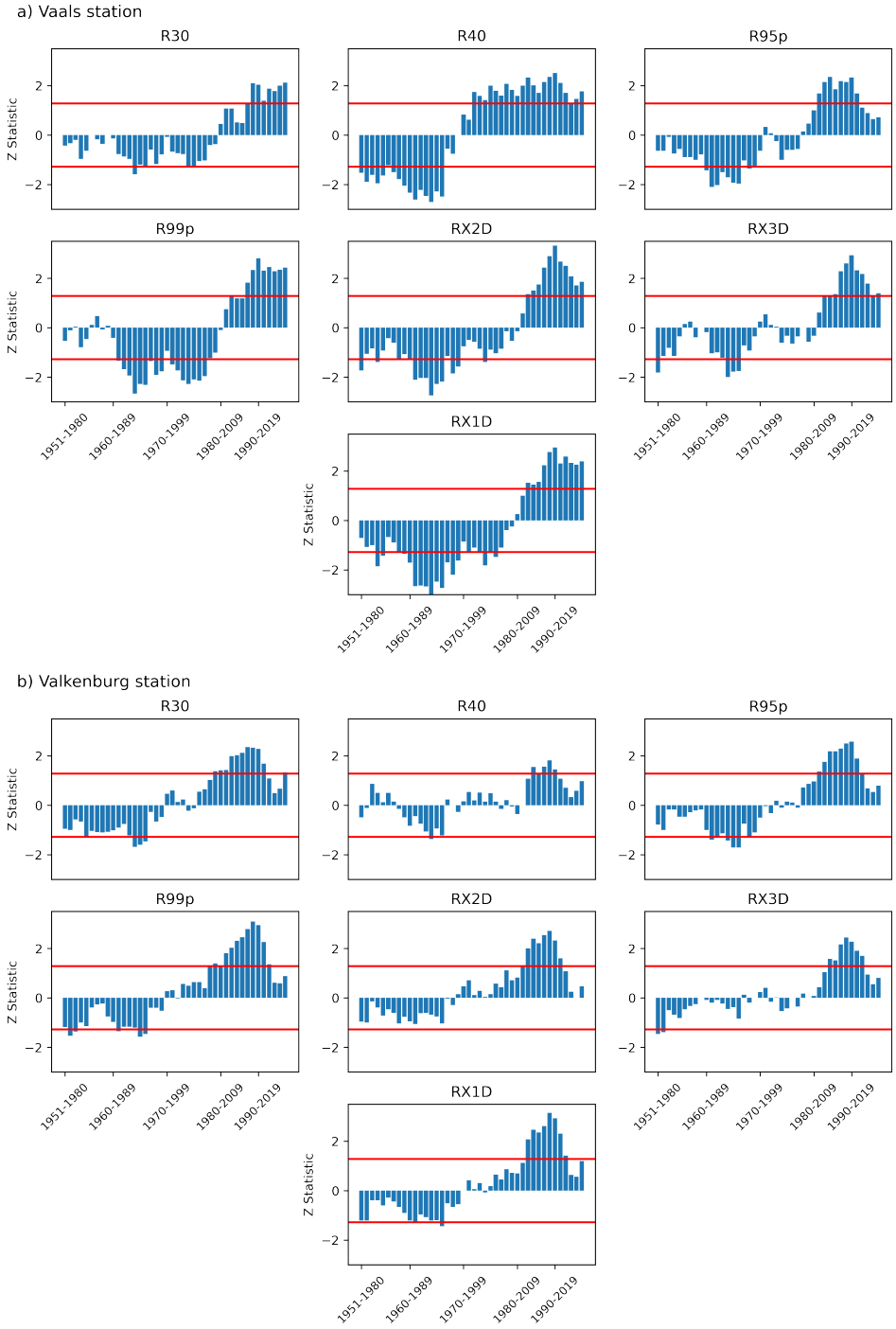

Figure 4.4: Calculated Z-statistic for each moving periods in summer for Vaals and Valkenburg stations. The red horizontal lines represent the 0.20 significance level. The graphs show that trends starting after the 1980s are statistically significant increasing trends in comparison to previous periods.

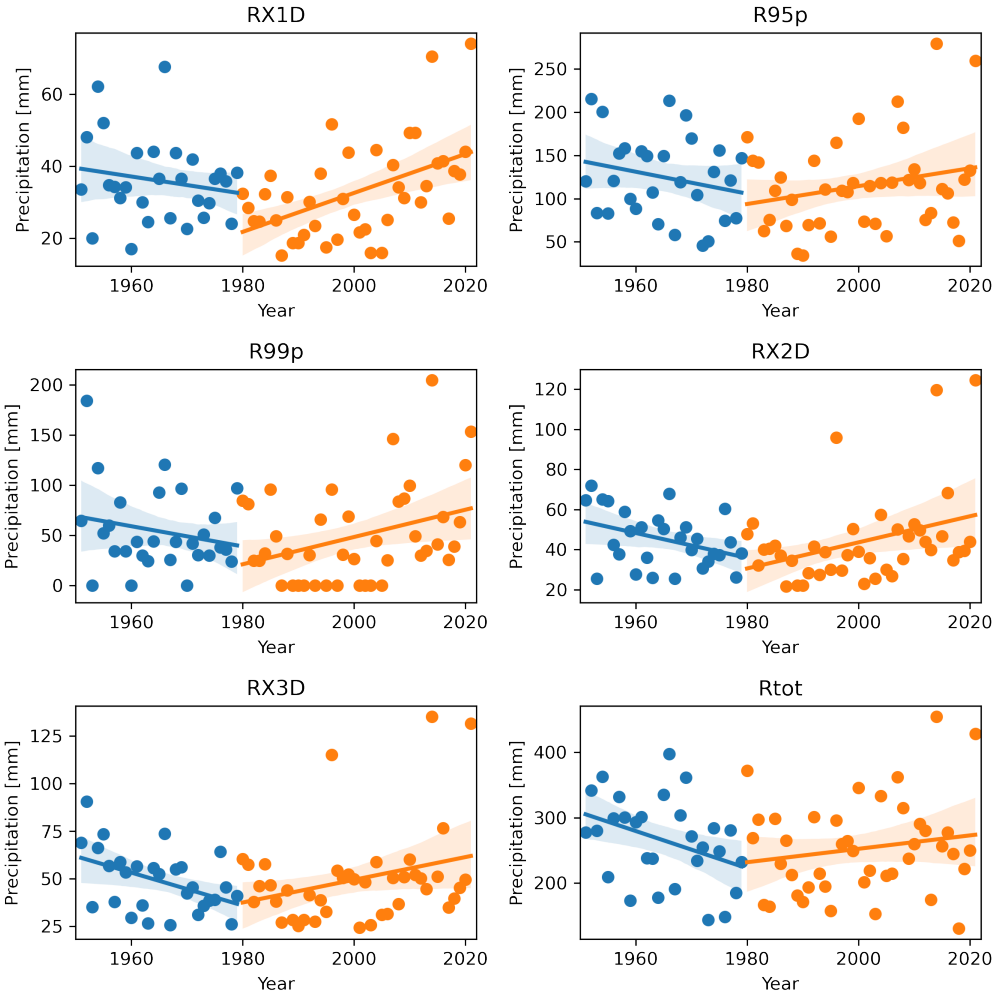

Figure 4.5: Distribution of values of extreme precipitation indices before and after 1980 for Vaals in summer. Blue colors represent values before 1980 and orange after 1980. The continuous lines are the linear trend fits using the least squares approach and the shaded areas the uncertainty of the linear regression fits, in each of the two periods. A clear distinction in directions before and after 1980 can be observed. An increase after 1980 is visible.

Spring

A shift from increasing to decreasing and then back to increasing is observed for the statistically significant trends. In most stations (except station Noorbeek), increasing trends are found for periods starting before the 1970s, while decreasing trends are found in the periods between the 1970s and 1990. In the recent past (last three moving years) the pattern is reversed again to the statistically increasing side. Figure 4.6 shows the results of the moving windows for the Ubachsberg station as example to illustrate the situation described above. The other other stations can be found in Appendix A.1.2.

Winter

The results of the moving windows per station are presented in Appendix A.1.1. Overall, in winter statistically increasing trends are found for the longest periods in indices RX1D, RX2D, RX3D and R95p. However this pattern has changed in the recent past (trends start after the 1980s) to decreasing, mainly insignificant, tendencies. In the indices R30, R40 and R99p in some stations, the decrease after the 1980s is statistically significant.

For autumn and full year periods, the variability is not investigated as the number of statistically significant trends is negligible (see trend strength percentages, Figure 4.3)

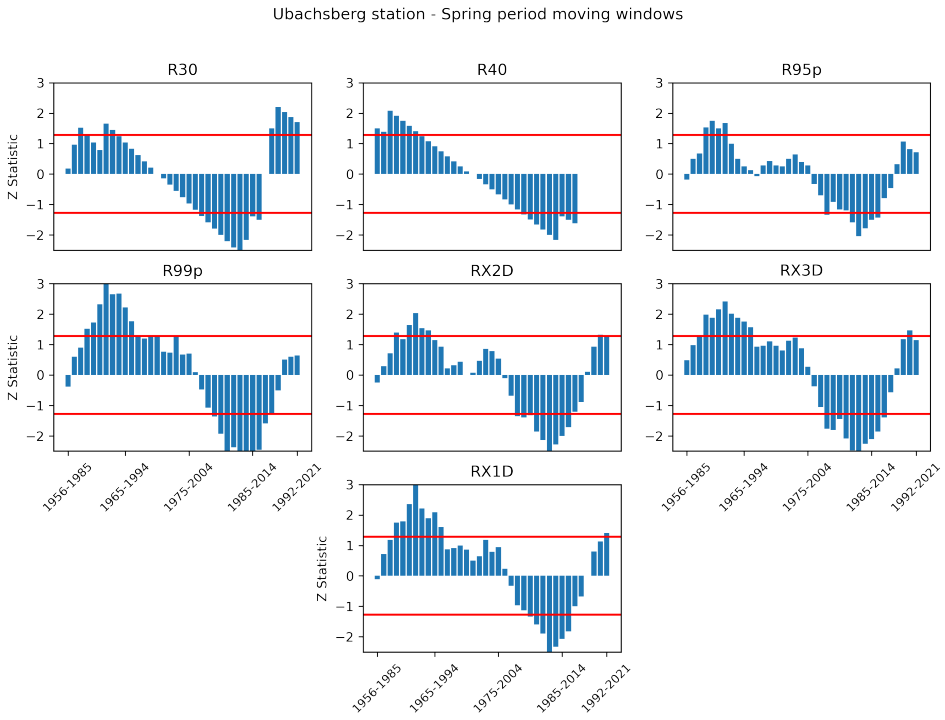

Figure 4.6: Z-statistic values calculated for each moving window for Ubachsberg in spring period. A shift from increasing to decreasing and again back to increasing trends is visible.

4.1.3. Trend stabilites

This section is devoted to the stability of statistically significant trends. The aim of this section is to continue the previous one by clarifying which significant directions are the most dominant in every station.

The results of the trend stabilities per station for the full year and seasonal periods are presented in Appendix A.2. The analysis follows the methodology as explained in Section 3.1.2 page 13. The most important results are summarized below.

In summer periods almost all stations in all indices show increasing stable trends (Figure A.11), while in some of them very strongly stable trends are also found. These results are aligned with the percentages of the significant trends, as illustrated in Figure 4.3a. As mentioned in Section 4.1.1, despite the fact that the difference between increasing and decreasing trends in summer is not clear, the statistically increasing trends are more and stronger. This explains the increasing stabilities. The very strongly stable trends in station Epen, in comparison to the other stations, are attributed to the short available time series (1981-2021). After the 1980s, a relatively strong-significant increase is observed in almost all extreme precipitation indices in summers, as explained in the previous section. Thus, almost all moving windows in Epen are statistically significant and increasing, leading to high percentages of time T as presented in Table 3.5.

Unstable trends are significantly more common than the other types of stabilities, for autumn (Figure A.14) and full year periods (Figure A.15). Considering the fact that significant trends in those periods are not clearly visible, as it is depicted in Figure 4.3d and Figure 4.3e, the stabilities are also barely visible as expected.

In spring (Figure A.12), stable decreases are recorded in R30. In the remaining indices mixed trends are found. There is no clear distinction between unstable and stable trends in the area.

For winter trends (Figure A.13), mixed stabilities are observed in the catchment. Stable increasing trends are more common than decreasing trends in indices RX1D, R95p, RX2D and RX3D, while the opposite applies to R30 and R40. It is worth mentioning that 5 out of 6 stations, all stations except Epen, show stable increasing trends in index R95p (”very wet days”). Again, the unstable trend in R95p in Epen is attributed to its recent record. Total precipitation is characterized by instabilities and poor increasing stabilities. For R99p there are no clear distinction between increasing and decreasing

stabilities.

4.2. Trend analysis of potential evaporation time series

4.2.1. Directions and magnitudes

Figure 4.7 shows the full-year annual evaporation values and the fitted linear model. A strong increase can be observed, which is statistically significant at α=0.01 (confidence interval 99%) as the Z-statistic value of the M-K test is 5.36. The Sen's slope β is equal to 1.82 mm/year. This means that the annual total potential evaporation has increased by approximately 100 mm since 1965.

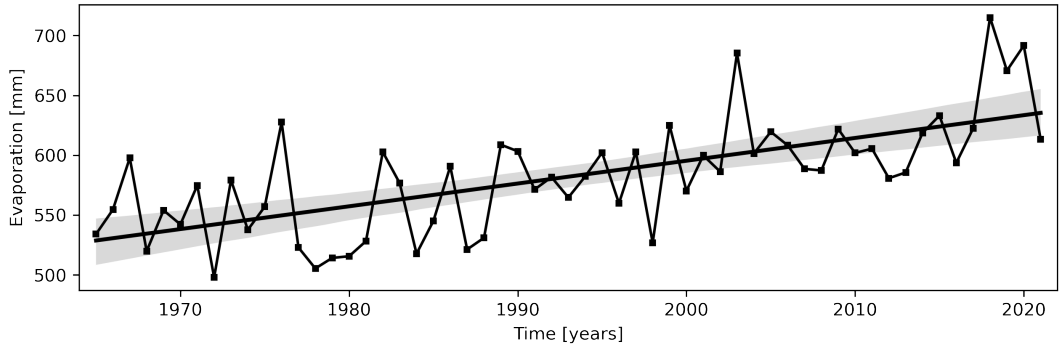

Figure 4.7: Annual evaporation in full year periods. The continuous line represents the linear trend fit using the least squares approach and the shaded area the uncertainty of the linear regression. A strong increase is visible.

Figure 4.8 presents the annual potential evaporation values per season. Table 4.1 contains the calculated Z-statistic values and Sen's slope per season. All seasons show statistically significant increases. Trends in summer and spring are statically significant at α=0.01 and have an increase of 0.87 and 0.7 mm/year, respectively. Winter and autumn are increasing at a significance level α=0.05 with a rate of 0.07 and 0.2 mm/year, respectively. Overall, considerable increases are reported for summer and spring and medium for autumn. Despite the increase in winter being statistically significant, the magnitude of the trend is considered negligible.

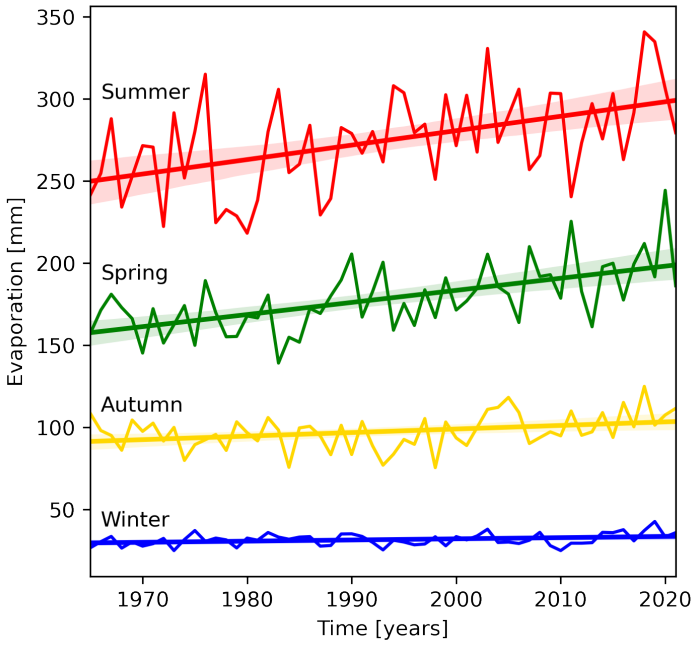

Figure 4.8: Annual evaporation in seasonal periods and the linear trend fits. Increases for summer and spring are visible.

Table 4.1: M-K Z-statistic values and calculated slopes per season for annual evaporation trends. Z-statistic values with a (*) are significant at α=0.01. The remaining values are significant at α=0.05.

	Z-statistic	Sen's slope (β) [mm/year]
Summer	3.57*	0.87
Winter	2.09	0.07
Spring	4.77*	0.7
Autumn	2.41	0.2

4.2.2. Variability of the trends

Figure 4.9 shows the Z-statistic values calculated for each 30-year moving window per season and in full year periods for the annual evaporation time series. As can be observed, the trends are consistently increasing and significant in almost all moving 30-year time frames for the full year, summer, spring, and autumn periods. For winter, only trends starting the last years (after the 1990s) are statistically significant and increasing, while in earlier periods insignificant trends in both directions are found.

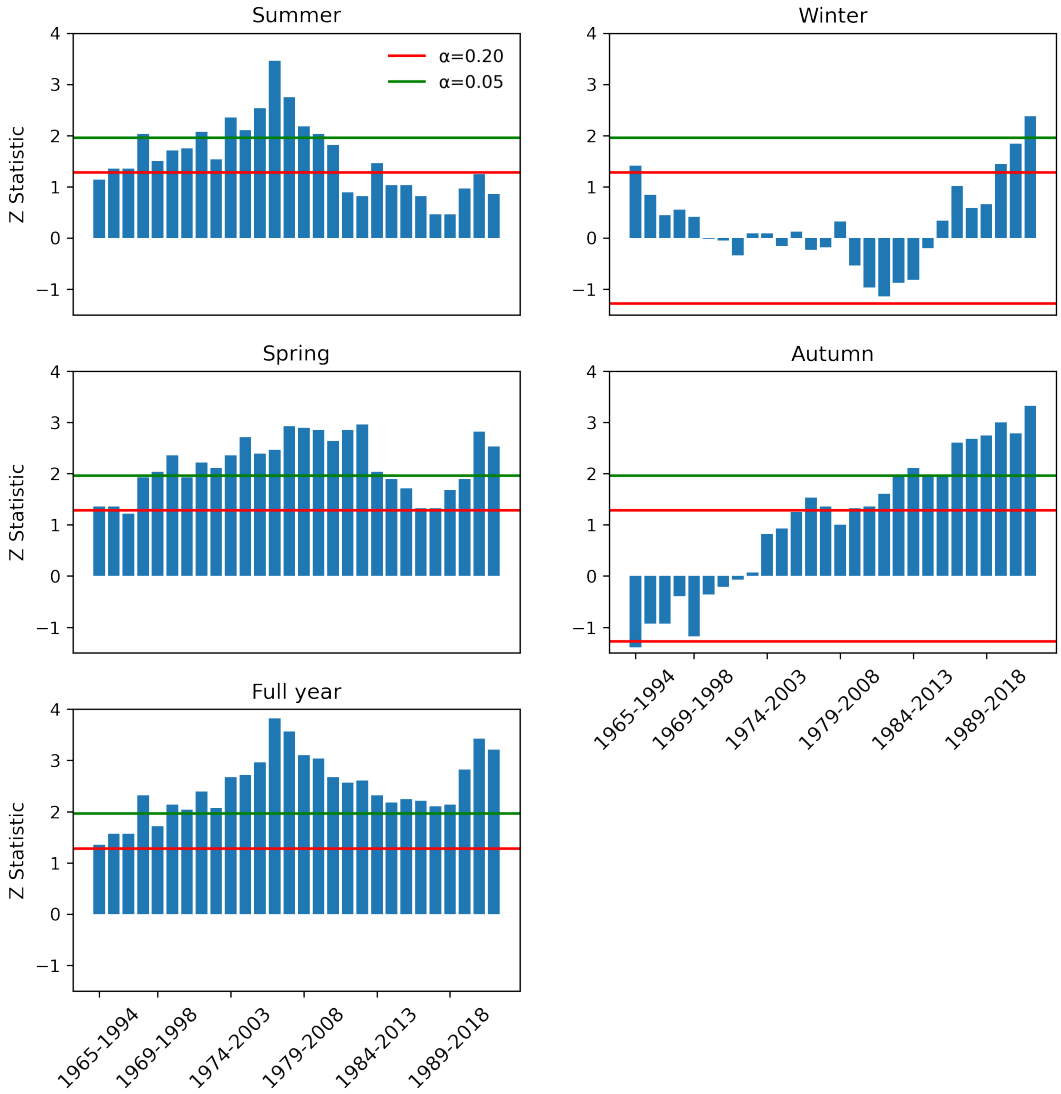

Figure 4.9: Calculated Z-statistic value for each moving period for annual evaporation time series in full year and seasonal periods. The horizontal lines represent two significance levels. The trends are very strong and increasing all over the studying period for full year, spring, summer and autumn.

4.2.3. Change points

Figure 4.10 shows the results of the change points found in spring, summer, and full year periods. A strong increase in mean values is observed in the three periods as expected. The change points are found almost in the same periods mainly near 1990.

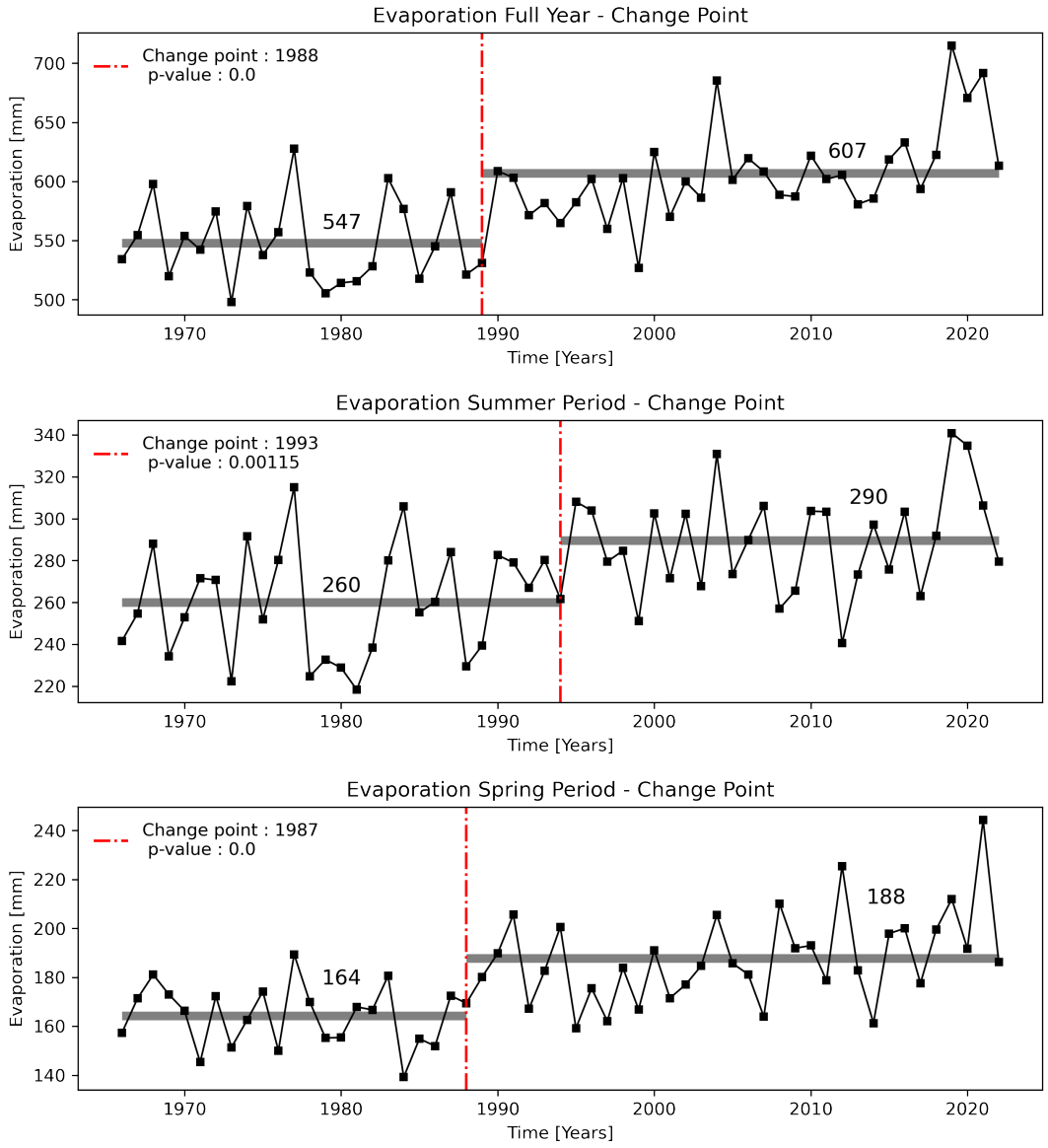

Figure 4.10: Change point results of full year, spring and summer periods in annual evaporation times series. The red vertical line represents the change point in the time series. The gray bold lines show the mean values before and after the change point. The numbers indicate the mean values for the two subsets. The plots show a considerable increase (change point) after the 1990s.

4.3. Land cover changes

4.3.1. Land use changes between 1990 and 2018

Whole catchment

The results for the whole catchment show that there are no significant changes between 1990 and 2018. More specifically, the built-up area has increased by 1% while at the same period the fraction of pasture has decreased at the same rate (Table 4.2). Insignificant changes are observed to the two remaining classes. The agricultural area remained almost the same and forests are slightly expanded

by 0.1%. Figure 4.11 illustrates the land cover maps for the year 1990 and 2018.

Table 4.2: Land use distribution in the years 1990 and 2018 for the Geul river catchment including its change

Land Use Class	1990 (in km^2)	%	2018 (in km^2)	%	Change (%)
Built-up area	54.2	16.1	58.0	17.1	1.0
Pasture	98.3	29.1	94.4	28.0	-1.1
Agricultural area	140.2	41.5	140.0	41.5	0.0
Forest	45.0	13.3	45.3	13.4	0.1
Total	337.7	100	337.7	100	

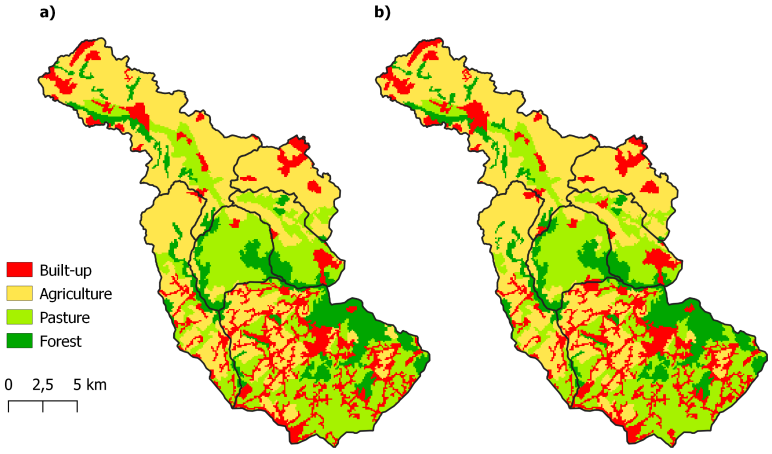

Figure 4.11: Land use map for the Geul river catchment for 1990 (a) and 2018 (b). Differences between the two periods are hardly distinguishable.

Subcatchments

Land use distribution in the years 1990 and 2018 and the percentage that each land class occupies per subcatchment can be seen in the Table 4.3. Small changes can be also seen for each sub-catchment. The most significant changes are observed in Meerssen and Selzerbeek.

A 20% increase of built-up area (from 9.2 to 11 km^2) is reported for Meerssen. Built-up area covered 11.4% of the sub-catchment in 1990 and 13.5% in 2018 (Table 4.3). Agricultural area decreased by 1.8 km^2 across Meerssen making up 64.6% of the whole sub-catchment (from 66.8% in 1990). An increase in forests (0.3 km^2) and a decrease in pastures (0.3 km^2) is also visible.

An increase of 1.1 km^2 in built-up area is visible for the Selzerbeek sub-catchment (20% in the class itself). The built-up area occupies 12.2% of the total sub-catchment in 2018, an increase of about 3.8% since 1990. Pasture area decreased with 7.1%, in terms of total subcatchment area, across Selzerbeek, which is the most significant loss in all sub-catchments. Forest is slightly reduced while agriculture is increased by 1.1 km^2.

Hommerich and Eyserbeek show similar patterns, with small gains in built-up area and agriculture, and losses in forest and pasture areas. Negligible changes are also observed for Sippenaken: increases in built-up and pasture (0.6 and 0.1 km^2) and decreases in agriculture and forest (0.5 and 0.2 km^2).

For the Gulp, a small increase can be seen in agriculture and forest, 0.45 and 0.35 km^2, respectively, while a decrease of about 0.75 km^2 is reported for pastures (10% decrease in the class itself).

Further information about land use changes in the whole catchment and per sub-catchment can be found in Appendix B.

4.3.2. Other human interventions

Flood mitigation measures have been implemented in the Geul area during the last 40 years. The local water board installed rainwater buffers on a large scale (more than 400), to increase the safety

Table 4.3: Land use distribution in the years 1990 and 2018 for each sub-catchment. Values in parentheses represent the percentage that each land cover class occupies in the sub-catchment.

	Area km^2 - 1990				Area km^2 - 2018			
	Built-up	Pasture	Agriculture	Forest	Built-up	Pasture	Agriculture	Forest
Sippenaken	32.6 (26.5%)	45.4 (36.9%)	23.4 (19.1%)	21.5 (17.5%)	33.2 (27.1%)	45.6 (37%)	22.9 (18.6%)	21.2 (17.3%)
Hommerich	0.40 (1.3%)	19.1 (62%)	3.80 (12.4%)	7.54 (24.3%)	0.74 (2.4%)	18.4 (59.7%)	4.20 (13.6%)	7.50 (24.3%)
Meerssen	9.2 (11.4%)	10.3 (12.7%)	54.5 (66.8%)	7.30 (9.0%)	11 (13.5%)	10.0 (12.4%)	52.7 (64.6%)	7.60 (9.5%)
Eyserbeek	4.12 (15.1%)	1.78 (6.6%)	20.9 (77.1%)	0.15 (0.7%)	4.26 (15.9%)	1.35 (5.1%)	21.2 (78.5%)	0.10 (0.4%)
Selzerbeek	2.40 (8.4%)	13.6 (47.3%)	8.2 (28.5%)	4.50 (15.7%)	3.50 (12.2%)	11.5 (40.2%)	9.30 (32.4%)	4.34 (15.2%)
Gulp	5.15 (11.1%)	8.0 (17.4%)	28.7 (62.3%)	3.90 (8.5%)	5.10 (11.2%)	7.25 (15.8%)	29.15 (63.5%)	4.25 (9.3%)

against flooding (van Heeringen et al., 2022). These buffers are mostly found in the small streams (tributaries), in dry valleys and in upstream parts of the catchment (places with steep slopes) (van Heeringen et al., 2022). These buffers are considered natural solutions for slowing down the water and boosting the storage capacities as they are not artificially controlled and are planned to drain the retained water within a day (van Heeringen et al., 2022). The only water retention basins that can be controlled manually are the reservoirs of Partij and Nijwiller (van Heeringen et al., 2022). In addition, in 2010 the restoration of the meander in the Geul from Mechelen to Gulpen took place by removing the channelized part (van Dijk, 2022).

It seems that an amount of water from urban areas is routed to a Waste Water Treatment Plant (WWTP) that is located outside the catchment (Tu, 2006). Furthermore, three retention areas of approximately 9000 m^3 in total are located in the Geul catchment and discharge to the WWTP (Agor, 2003). Furthermore, according to the water board a WWTP discharges mainly rural usage water to the Eyserbeek tributary, however its contribution to river flows is minor especially during high flows.

In addition, beer factories in the area extract large proportions of water (Agor, 2003). Losses of groundwater due to wells and decreases in water tables are also reported by Agor (2003).

4.4. Trend analysis of discharge time series

4.4.1. Annual maxima

Full year

Figure 4.12 illustrates the annual maximum discharges for the Geul and its tributaries. As can be observed, in extreme events Hommerich (discharge from the Belgian part) contributes a significant amount to the discharge at Meerssen, as their maxima discharges are almost the same.

As mentioned in Section 3.4.3, the M-K test is applied to every possible combination of longer than 30-year periods in the time series. The results of the multi-temporal analysis for annual maxima for full-year periods in Meerssen, Hommerich and Gulp are shown in Figure 4.13. Each pixel in the graph represents a fixed single period (minimum window length of 30 years) of start and end year. In each of those periods the M-K test is applied. The color represents the Z-statistic value of the test. Blue colors indicate downward trends and red increasing ones. The darker the color the more significant the trend is. Weak trends are those with Z-statistic values higher than 1.28 and strong trends with a Z value higher than 1.64 (or smaller than -1.28 and -1.64, respectively, for downward trends). The same definitions apply to the subsequent figures of multi-temporal trend analyses.

Mixed trends are observed at Meerssen. Most of them are positive tendencies but no statistically significant trends are found. Positive trends are more frequent than negative ones for Hommerich, however none of them is statistically significant. Weak positive trends are observed for the Gulp for

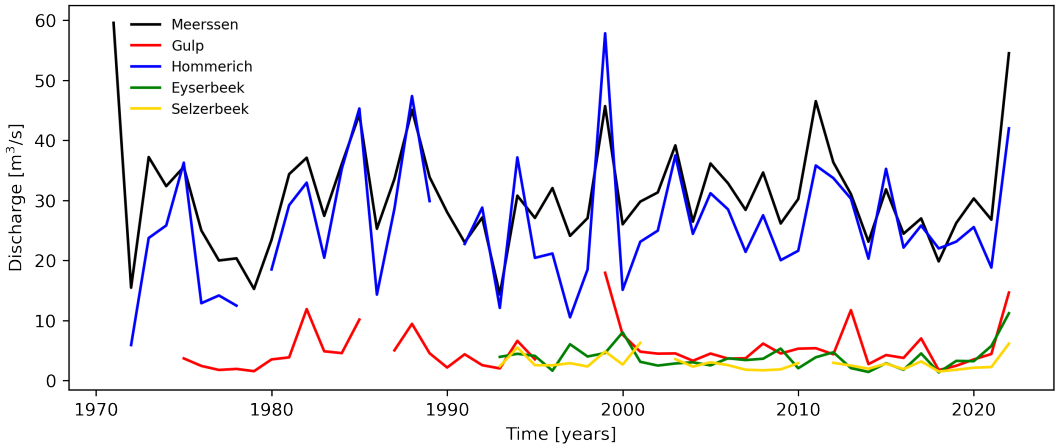

Figure 4.12: Time series of annual maximum discharge in the Geul and its tributaries. Annual maximum discharges at Hommerich and Meerssen are almost identical.

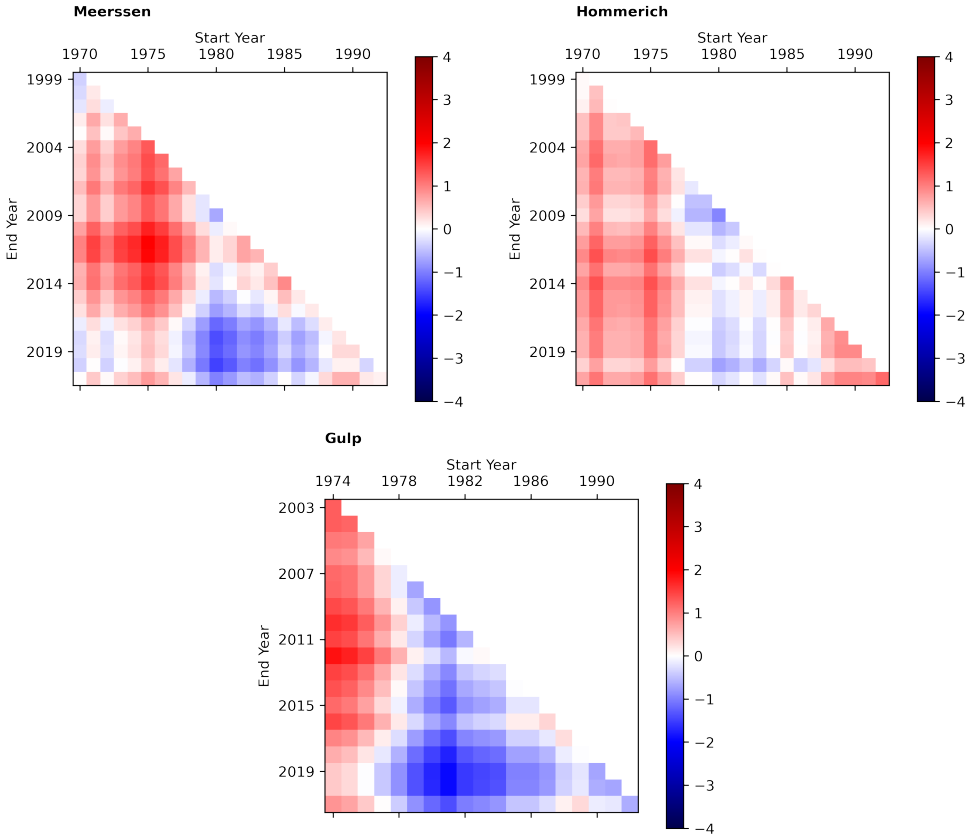

Figure 4.13: Multi-temporal trend analysis for the annual maximum discharges at Meerssen, Hommerich and the Gulp - full year period. Each pixel presents a fixed period, and the color indicates the value of the Z statistic. The same definitions apply to the subsequent figures. Mixed insignificant trends are observed.

periods starting between 1974 and 1977, but it seems that after that period the trends are moving towards a decreasing direction. Full-year annual maximum discharges in the Selzerbeek are moving downwards (statistically significant at the 20% level) while an insignificant decreasing tendency (Z = -0.6) is observed in the Eyserbeek.

Seasons

Meerssen

Figure 4.14 shows the annual maxima time series at Meerssen per season and Figure 4.15 the results of the multi-temporal trend analysis for the same period.

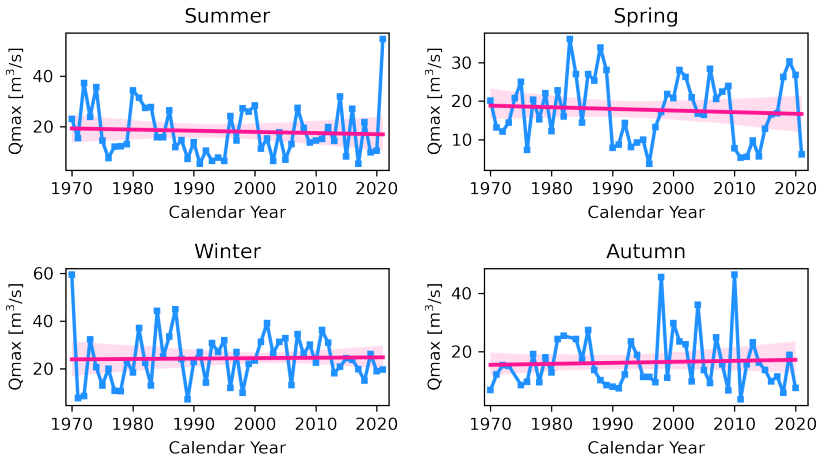

Figure 4.14: Seasonal annual maxima time series and linear fits for Meerssen.

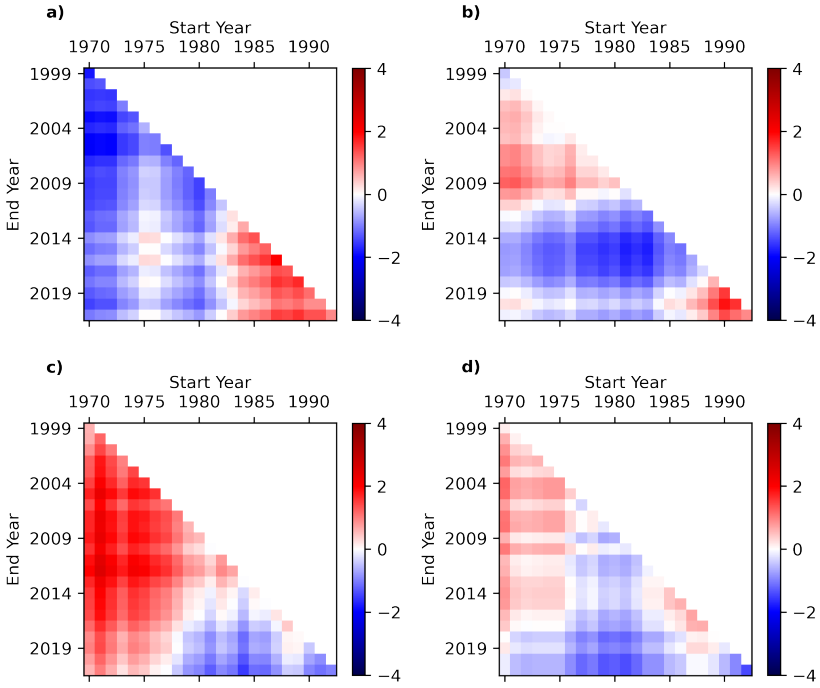

Figure 4.15: : Multi-temporal trend analysis for the annual maximum discharge at Meerssen. (a) summer; (b) spring; (c) winter; (d) autumn.

As can be observed from Figure 4.15, the annual discharges at the Meerssen station (which is the outlet of the catchment) show variability over the different seasons. For summer, despite the fact that weak negative trends are visible for the longest periods (Figure 4.15a), this changes to positive weak trends in the recent past (trends starting after 1980s). This result is in agreement with the extreme precipitation patterns in summers.

For spring, there is a shift from weak increasing tendencies to stronger negative ones, and back to strong increasing trends after 1989. This pattern seems to be similar to the extreme precipitation in spring (see Figure 4.6).

Strong increasing trends are found in the longest periods for winter (19% statistically significant at α=0.1) but this seems to have changed in the recent past to statistically insignificant decreasing tendencies. These patterns are again in agreement with the extreme precipitation in the area (see for example extreme precipitation moving windows in Valkenburg Figure A.1).

Mixed and non statistically significant trends are observed in autumn (Figure 4.15d), as it was expected, considering that the trends in extreme precipitation in autumn are unstable and their strength is (statistically) insignificant.

Hommerich

Figure 4.16 shows the annual maxima time series at Hommerich per season and Figure 4.17 the results of the multi-temporal trend analysis for the same period.

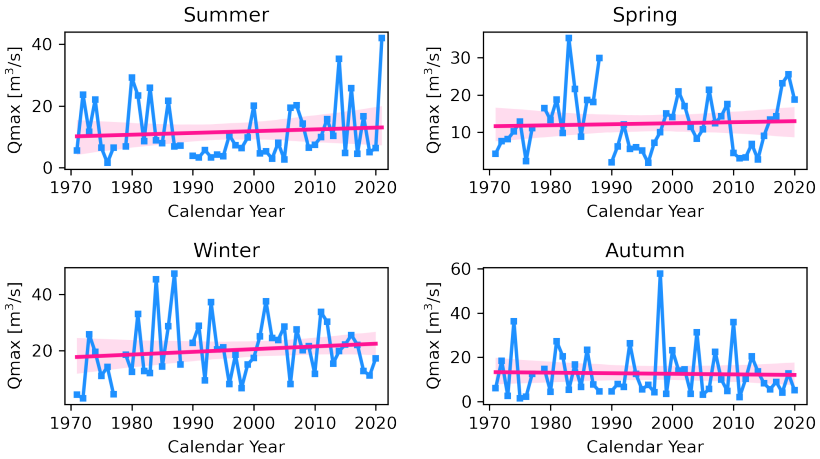

Figure 4.16: Seasonal annual maxima time series and linear fits for Hommerich.

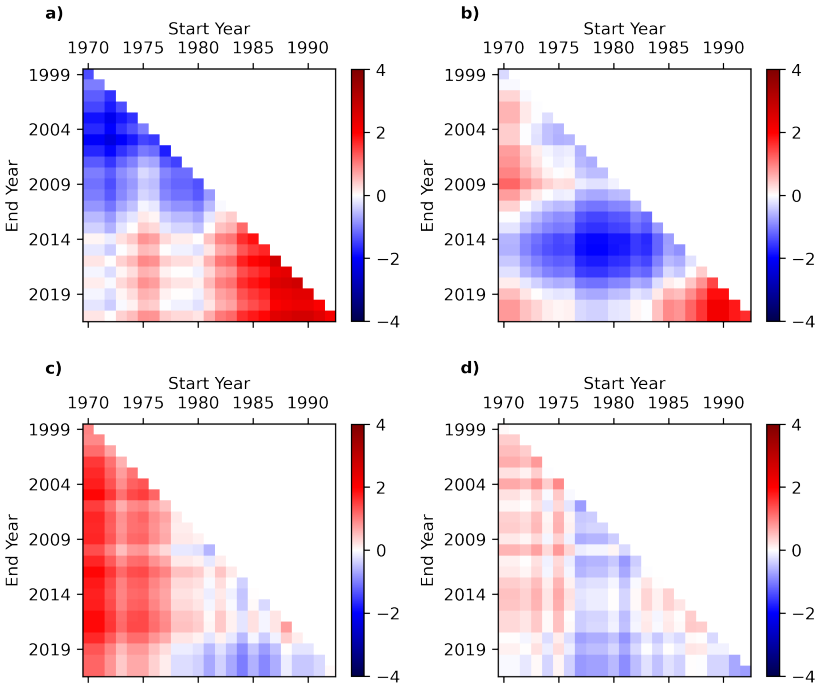

Figure 4.17: : Multi-temporal trend analysis for the annual maximum discharge at Hommerich. (a) summer; (b) spring; (c) winter; (d) autumn.

The Hommerich station shows similar patterns as Meerssen, however differences in trend strengths

are visible. Trends ending after 2019 are positive in summer. It should be mentioned that summer trends in the recent past, after 1985, show very strong increasing trends. Almost all of them are statistically significant at α=0.05 and some of them even at α=0.01. This division between trends (blue and red colors) indicates a strong change in the tendency. Similarly to Meerssen, spring shows mixed trends (shift from increasing to decreasing and again back to increasing) but this time the trends after 1987 are even stronger (significant at the 5% level). More than 20% of all periods exhibit significantly increasing trends at the 20% significance level in winter. The decreasing tendency in the recent past observed at Meerssen is also reflected at Hommerich, however it is considered negligible. Weak and insignificant trends are found in autumn.

Gulp

Figure 4.18 shows the annual maxima time series for the Gulp per season and Figure 4.19 the results of the multi-temporal trend analysis of the same period. Summer is characterized by insignificant and

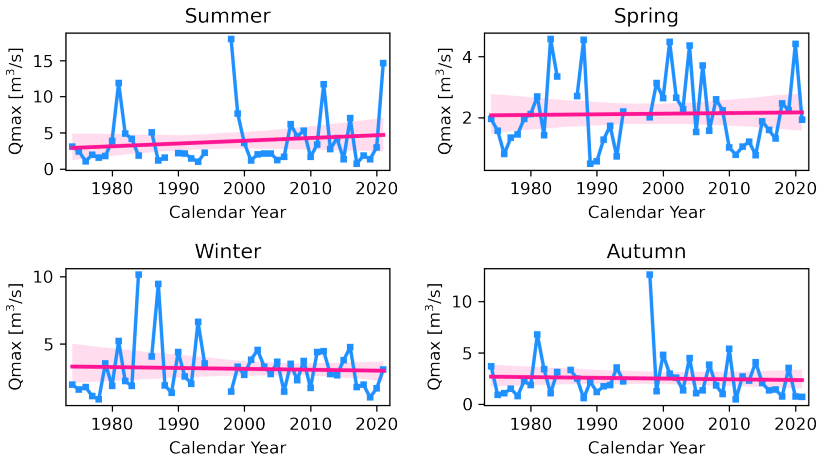

Figure 4.18: Seasonal annual maxima time series and linear fits for the Gulp.

mixed trends with only 2 statistically significant increasing trends (at the 20% level). Compared to the other two stations (Meerssen and Hommerich), for the Gulp increasing tendencies are more frequent than the decreasing ones. In spring, increasing trends are observed for periods ending before 2010, but after that period the tendencies are moving towards a weak decrease. For winter, increasing strong trends can be seen over the longest periods, however in the recent past, insignificant decreasing tendencies can be detected. All trends ending in the full period seem to be decreasing in autumn, with some mixed insignificant trends all over the time.

Eyserbeek and Selzerbeek

The Eyserbeek and the Selzerbeek show decreasing (statistically) insignificant directions in all seasons except autumn, in which statistically significant decreasing trends at the 5% level are observed (Table 4.4).

Table 4.4: Seasonal Z-statistic values for annual maximum discharges in Eyserbeek and Selzerbeek (** Significant at the 5% level). The only statistically significant trends are decreasing and found in autumn.

Season	Eyserbeek	Selzerbeek
Summer	-1.25	-1.13
Spring	0.00	-0.10
Winter	-1.11	-1.13
Autumn	-2.23**	-2.21**

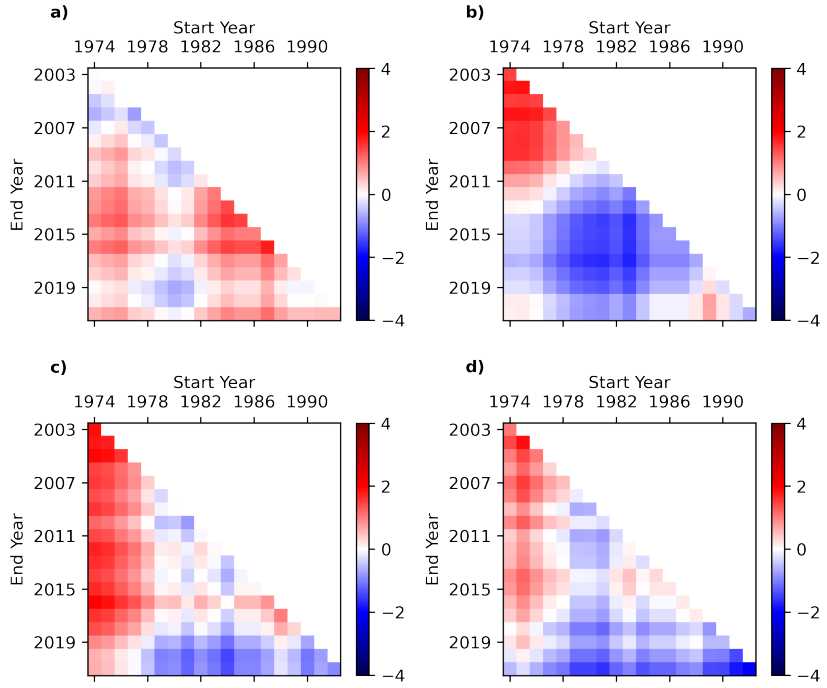

Figure 4.19: : Multi-temporal trend analysis for the annual maximum discharge in the Gulp. (a) summer; (b) spring; (c) winter; (d) autumn.

4.4.2. Annual mean

Full year

Figure 4.20 illustrates the annual mean discharges for the Geul and its tributaries. The results of the multi-temporal analysis for the annual mean discharges for full-year periods in Meerssen, Hommerich and the Gulp are shown in Figure 4.21.

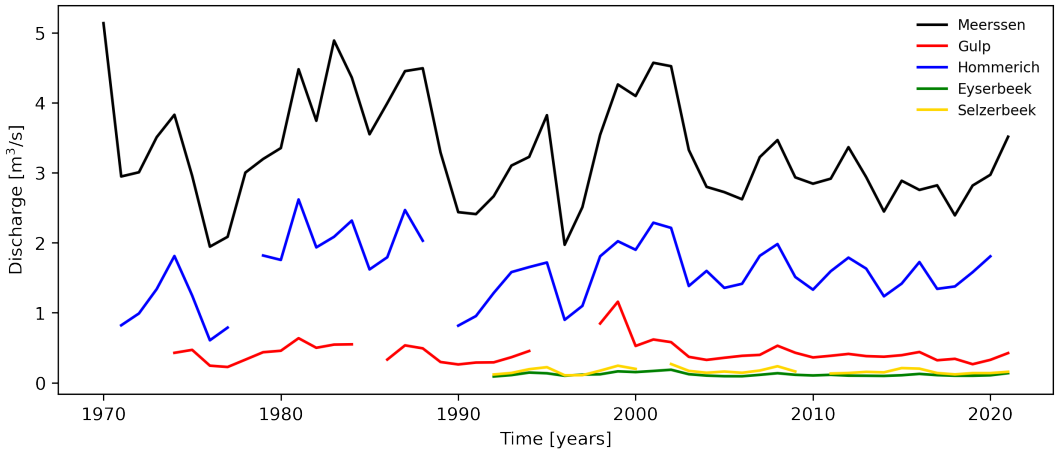

Figure 4.20: Time series of annual mean discharge in the Geul and its tributaries.

For the Meerssen station, the annual mean trends are negative all over the studying periods. Irrespective of the year, all trends starting after 1978 are negative and most of them statistically significant at α = 0.10 (16.6% of values). Some of the trends in the earlier series show increasing tendencies, although very weak. Hommerich and Gulp show similar patterns with more mixed trends. For Hommerich, the annual mean trends, starting from 1971 till the end of the period, are mostly very weak and positive, however for the periods starting from 1978-1985 till the 2021, strong decreasing trends can be observed. All trends ending after 2019 in the Gulp are weak decreasing tendencies, except

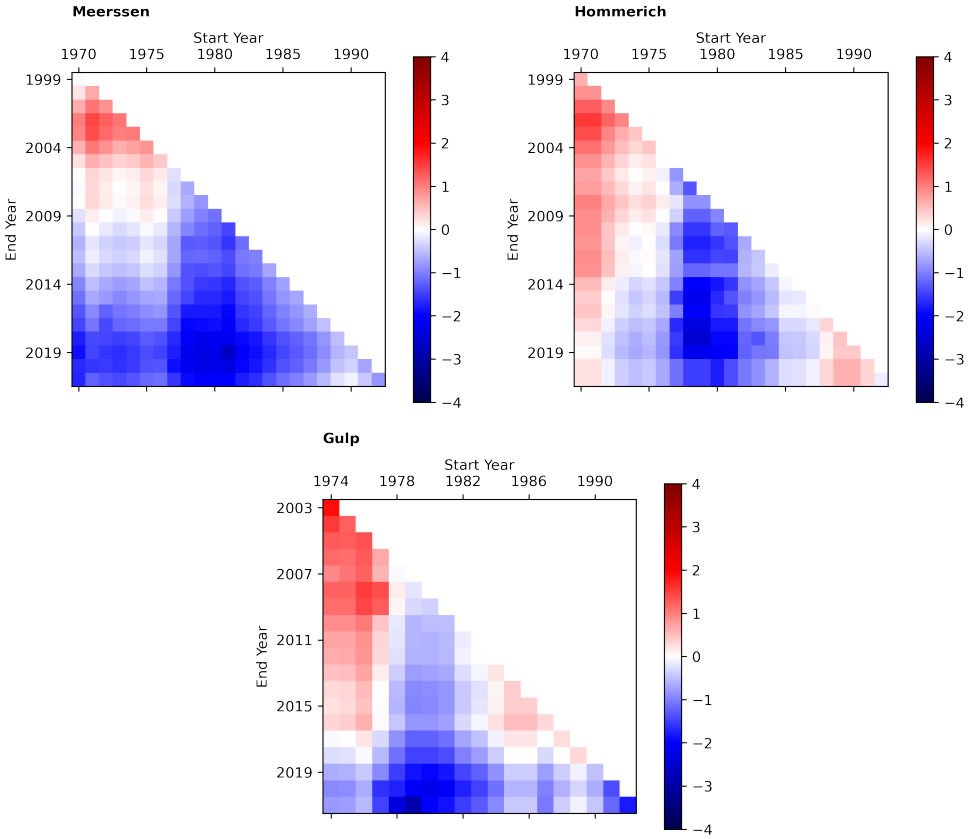

Figure 4.21: Multi-temporal trend analysis for the annual mean discharges in Meerssen, Hommerich and the Gulp.

those starting in 1980, 1981 and 1982, that are stronger. The mean annual discharges for Eyserbeek and Selzerbeek show negative insignificant tendencies (Z-statistic value -1.14 and -0.81, respectively) between 1992-2021.

Seasons

Meerssen

Figure 4.22 shows the annual mean time series at Meerssen per season and Figure 4.23 the results of the multi-temporal trend analysis for the same period. Regarding the mean flows in Meerssen,

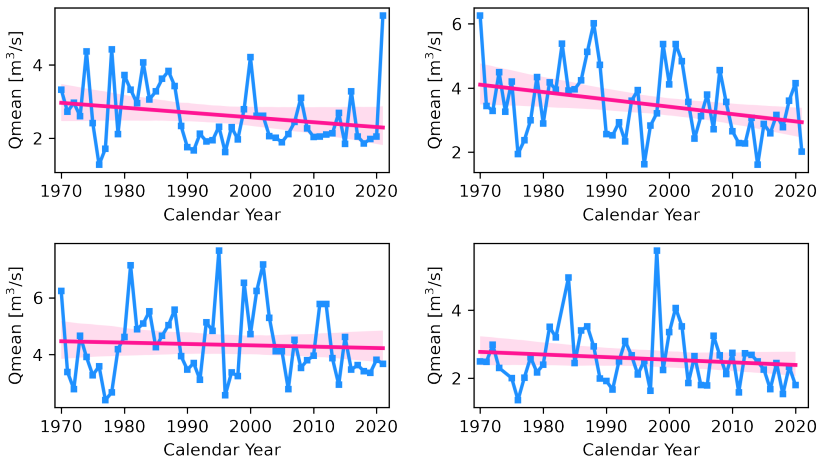

Figure 4.22: Seasonal annual mean time series and linear fits for Meerssen.

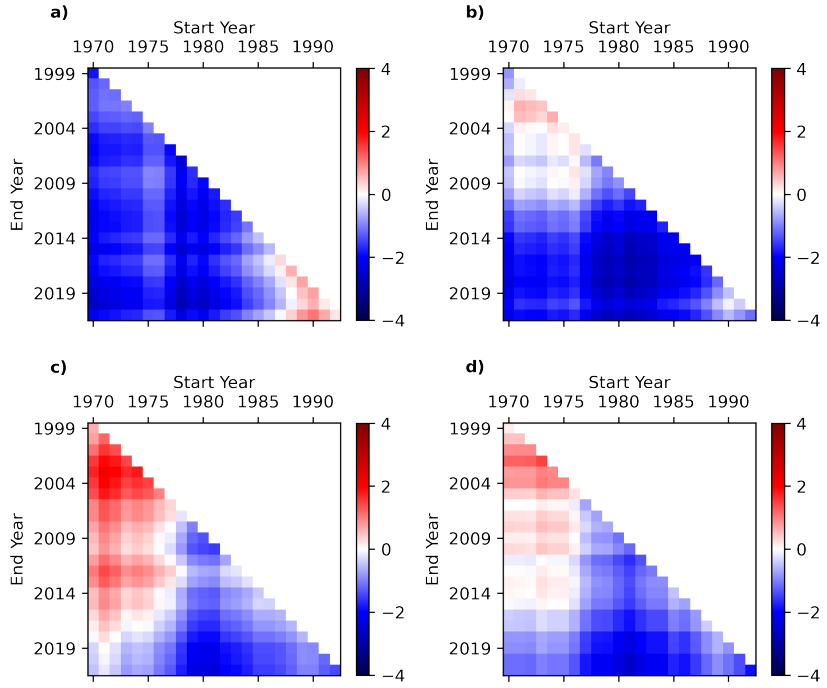

Figure 4.23: : Multi-temporal trend analysis for the annual mean discharges in Meerssen. (a) summer; (b) spring; (c) winter; (d) autumn.

it can be stated that the seasons show a broadly similar pattern in contrast to the annual seasonal maxima. Strong decreasing trends are visible in summer and spring all for all periods. In spring, 61.6% of all multi-temporal windows display statistically significant decreasing trends at α=0.2 and 36.2% of them at α=0.05, while 25.4% are statistically significant at α=0.05 in summer. Winter and autumn show more mixed trends. All trends ending after 2015 are decreasing trends, while most of them are increasing before that period (stronger in winters). It should be stated that all trends in the recent past are decreasing trends.

Figure 4.24 shows the change points found for Meerssen. A decrease in mean values is visible for spring and summer in 1989. The decrease in mean flows coincides with the increase in the evaporation time series (see Figure 4.10).

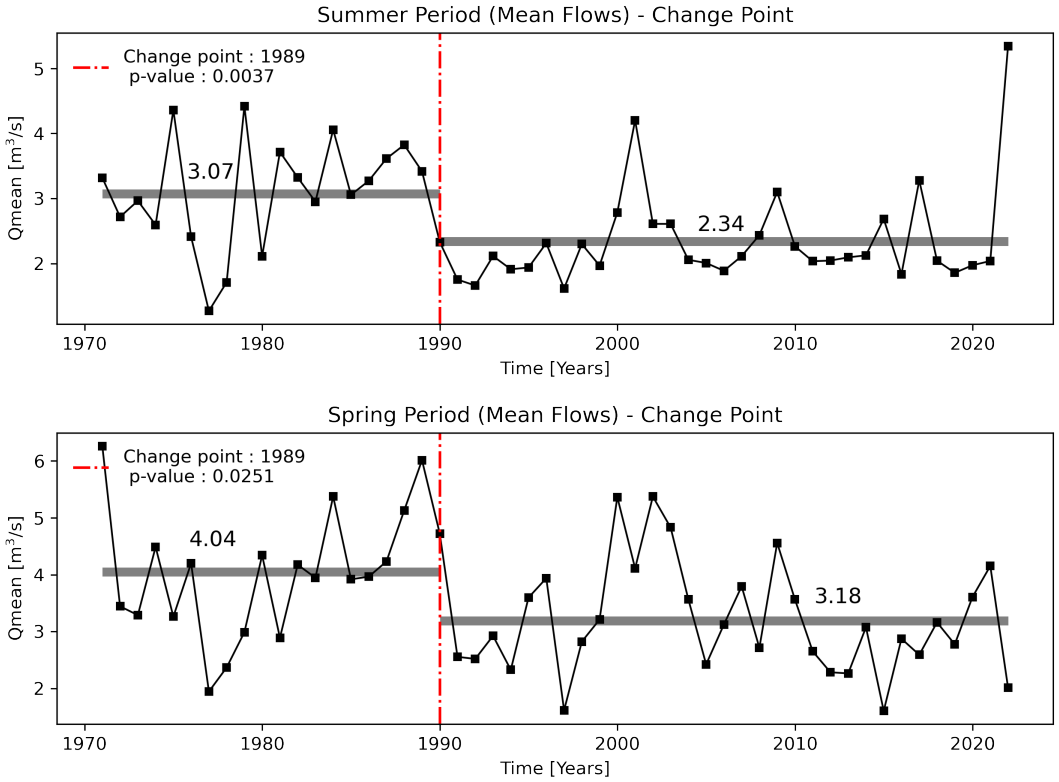

Figure 4.24: Change point results for summer and spring periods in annual mean discharge times series. The plots show a considerable decrease (change point) after 1990.

Hommerich

Figure 4.25 shows the annual mean time series at Hommerich per season and Figure 4.26 the results of the multi-temporal trend analysis for the same period. A large similarity is observed between the

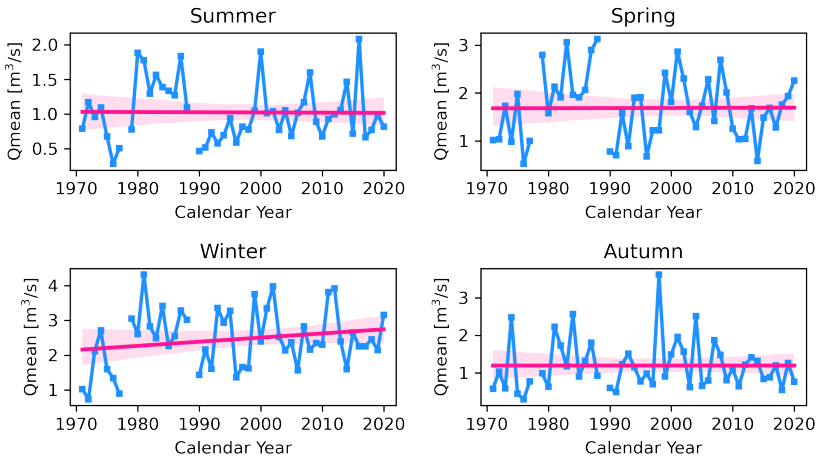

Figure 4.25: Seasonal annual mean time series and linear fits for Hommerich.

temporal variabilities of annual maximum and mean discharges at Hommerich. Insignificant, mainly decreasing, trends are observed in summer, however the last 40 years the mean values indicate an increase which is statistically significant (nine moving windows significant at α=0.05). Mainly increasing tendencies are found for the longest periods in the other seasons, moving towards an increasing direction (more significant in winter) and again back to insignificant downward tendencies.

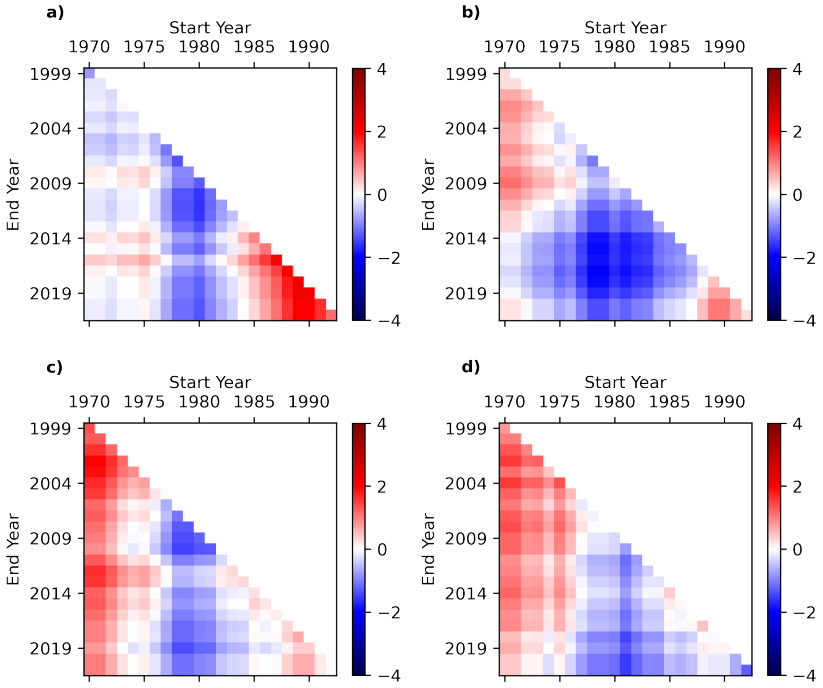

Figure 4.26: : Multi-temporal trend analysis for the annual mean discharges at Hommerich. (a) summer; (b) spring; (c) winter; (d) autumn.

Gulp

Figure 4.27 shows the annual mean time series for the Gulp per season and Figure 4.28 the results of the multi-temporal trend analysis for the same period. Decreasing trends are more frequent than the

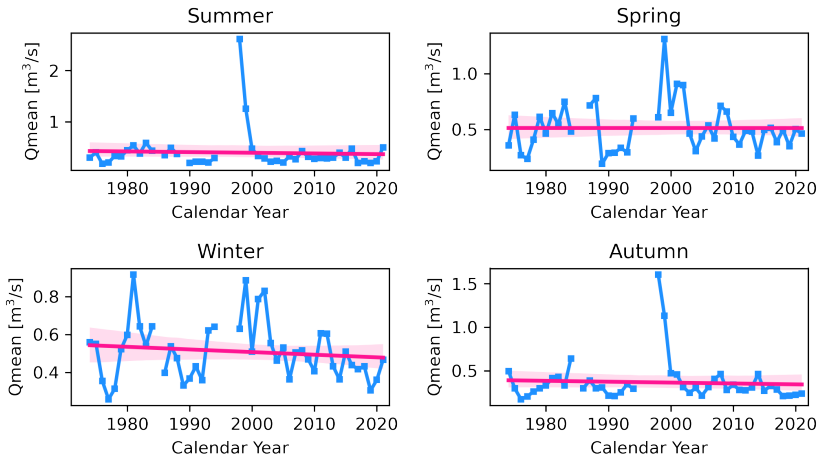

Figure 4.27: Seasonal annual mean time series and linear fits for the Gulp.

increasing trends in the Gulp. Strong decreasing trends are observed for all periods ending after 2018 for summer, winter and autumn, while insignificant mixed trends (mainly upwards tendencies) are seen in spring.

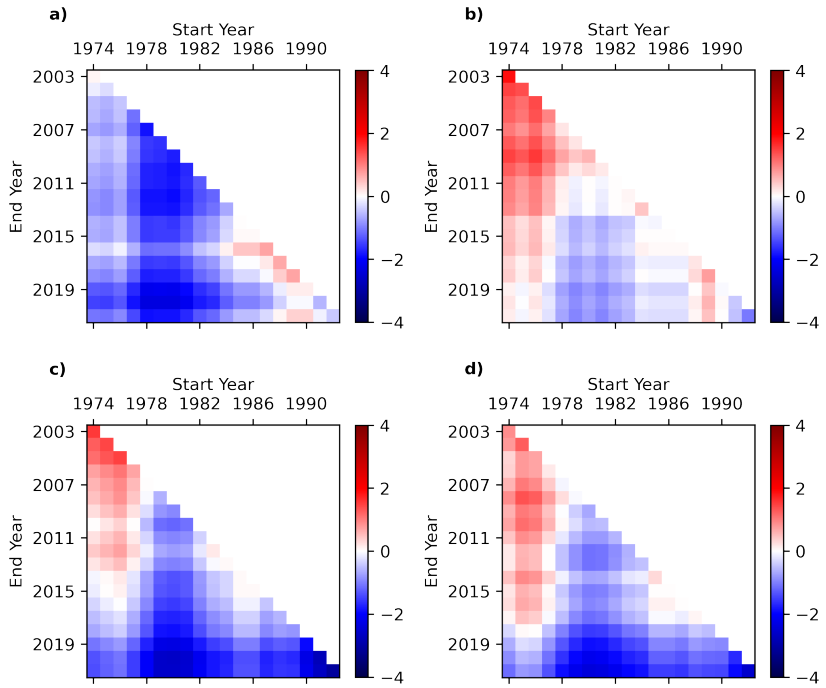

Figure 4.28: : Multi-temporal trend analysis for the annual mean discharges for the Gulp. (a) summer; (b) spring; (c) winter; (d) autumn.

Eyserbeek and Selzerbeek

The only statistically significant trends in Eyserbeek and the Selzerbeek are observed in autumn (Table 4.5). The other seasons show insignificant decreasing tendencies except from the summer period in the Selzerbeek, which moves upwards.

Table 4.5: Seasonal Z-statistic values for annual mean discharges for the Eyserbeek and Selzerbeek (** Significant at the 5% level, * significant at the 10% level). The only statistically significant trends are found in autumn.

Seasons	Eyserbeek	Selzerbeek
Summer	-1.11	0.93
Spring	-0.64	0.00
Winter	-0.96	-0.97
Autumn	-1.96**	-1.88*

4.5. Attribution and Validation

4.5.1. Maximum flow variability attribution

Figures 4.29 and 4.30 show the results of the correlations of Sen's slopes in moving windows between extreme precipitation indices and annual maximum discharges (as described in Section 3.5.1) for Meerssen and Hommerich, respectively. Each dot in the graphs represents the correlation value of a rainfall station for an extreme precipitation index with the corresponding slopes in annual maximum discharges. The station Epen is not included as it has a record from 1981. Only correlations for summers, winters and springs are investigated, as those periods contain statistically significant trends. Autumn is not included in the analysis as only insignificant trends are found. Insignificant trends result in zero slopes. The R99p index is not included for winter and spring because it has many zero values.

High positive correlations between extreme precipitation indices and annual maximum discharges in both Meerssen and Hommerich can be observed for the three studied seasons. Correlations for winter are very high for all stations in every extreme precipitation index, close to 0.8, for both Meerssen and Hommerich. For summers, also positive strong correlations are observed with small fluctuations

between indices and stations. Index RX3D shows the greatest correlation in all stations, with values higher than 0.8. There are stations that have correlation values higher than 0.9. Similar patterns are observed for spring.

Overall, strong positive correlations in moving period slopes are observed between extreme precipitation indices and maximum discharges in the Geul river catchment. The majority of the precipitation stations show a correlation coefficient close to 0.8. This means that the annual maximum discharges change at the same rate as extreme precipitation in directions, magnitudes and time frames, indicating that the variability in high flows comes mainly from the variability of extreme precipitation.

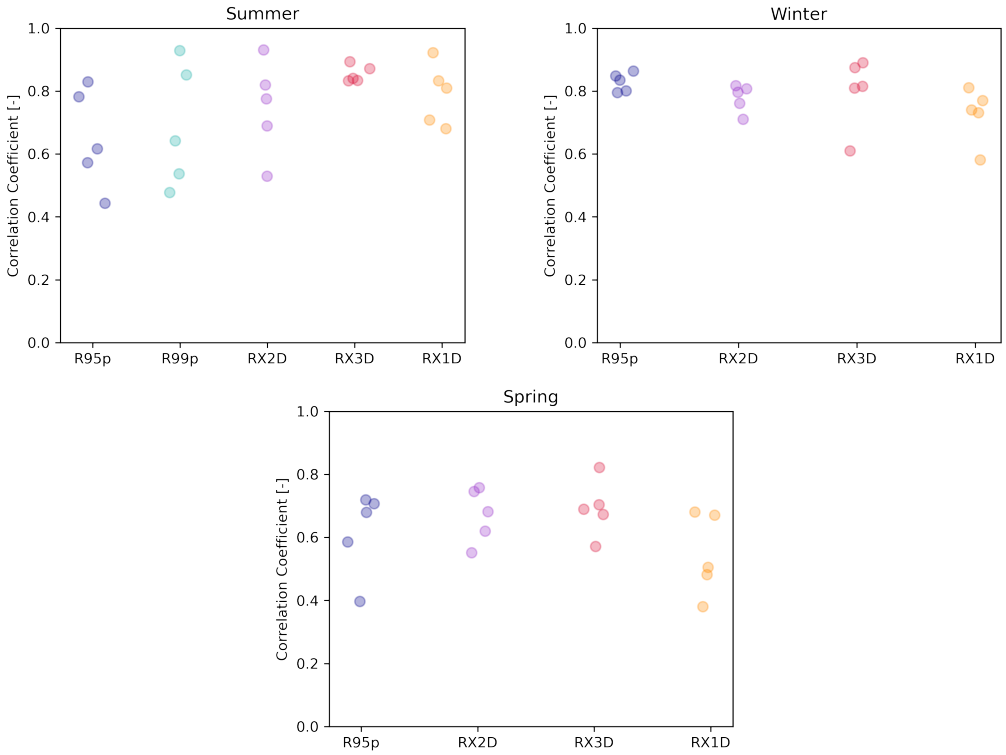

Figure 4.29: Correlation coefficients between extreme precipitation indices and annual maximum discharge at Meerssen, for the calculated slopes in the moving windows. The dots show the exact values per rainfall station. Strong positive correlation values are visible.

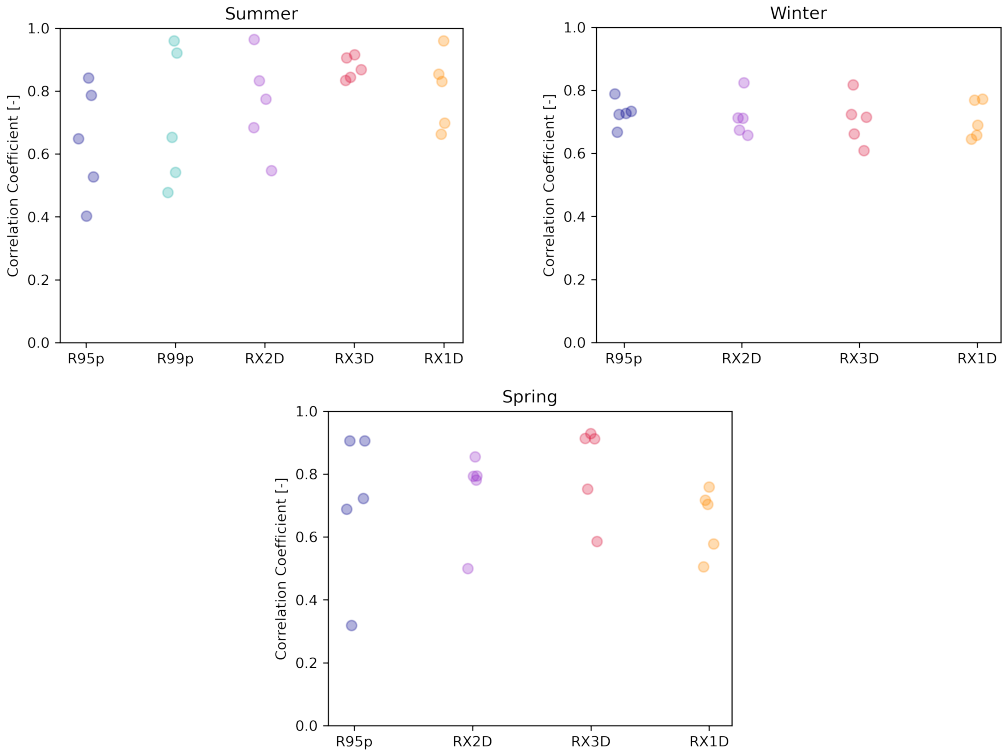

Figure 4.30: Correlation coefficients between extreme precipitation indices and annual maximum discharge at Hommerich, for the calculated slopes in the moving windows. Strong positive correlation values are visible.

4.5.2. Mean flow attribution

Table 4.6 and Figure 4.31 show the results of the attribution of changes in stream flows to LUC and CC in the Geul river catchment. A simultaneous decrease in P_{ex} and increase in E_{ex} are visible. Both P and ET increased, however the increase in ET is higher compared to P, and causes the decrease in P_{ex}. On the other hand, the higher increase in ET_0 in comparison to ET leads to an increase in E_{ex}. The long-term constant aridity index of the catchment is equal to 0.67. The angle θ of 63° of the gradient M1-M2 (baseline and altered period) relative to the constant aridity index, indicates that the CC (changes in P and ET_0) has a larger impact on changes in stream flows compared to LUC (as it creates a movement perpendicular to the aridity index see Section 3.5.2). The low value of the length of the vector R (arrow M1-M2 in Figure 4.31) indicates that the magnitude of the combined changes is relatively small. The proportion of changes in mean discharge flows attributed to LUC and CC is estimated to be 34 and 66%, respectively.

Table 4.6: Analytical values calculated for the attribution of changes. P, Q, ET_0 and ET are the mean annual precipitation totals, discharge, potential evaporation totals and evapotranspiration totals in mm, respectively. P_{ex} is the proportion of excess water and E_{ex} the proportion of excess energy. R is the length of the vector between the two periods and θ is the angle (in degrees) of changes relative to the constant long-term aridity index. R_{LUL} and R_{CC} are the relative attribution of changes in stream flows to land use and climate change, respectively (see Section 3.5.2).

Period	P [mm]	Q [mm]	ET_0 [mm]	ET [mm]	P_{ex} [-]	E_{ex} [-]	R [-]	θ [°]	R_{LUL} [%]	R_{CC} [%]
1970-1981	830.4	306.9	541.9	523.5	0.37	0.03				
2010-2021	871.5	269.7	627.7	601.8	0.31	0.04	0.061	63	34	66

4.5.3. Validation

Many of the reported results can be supported using the data from Sections 4.5.1 and 4.5.2.

The maximum flow variability attribution results (Section 4.5.1) support the statement presented in Section 4.4.1 that the variability of the annual maximum discharges is in agreement with the variability

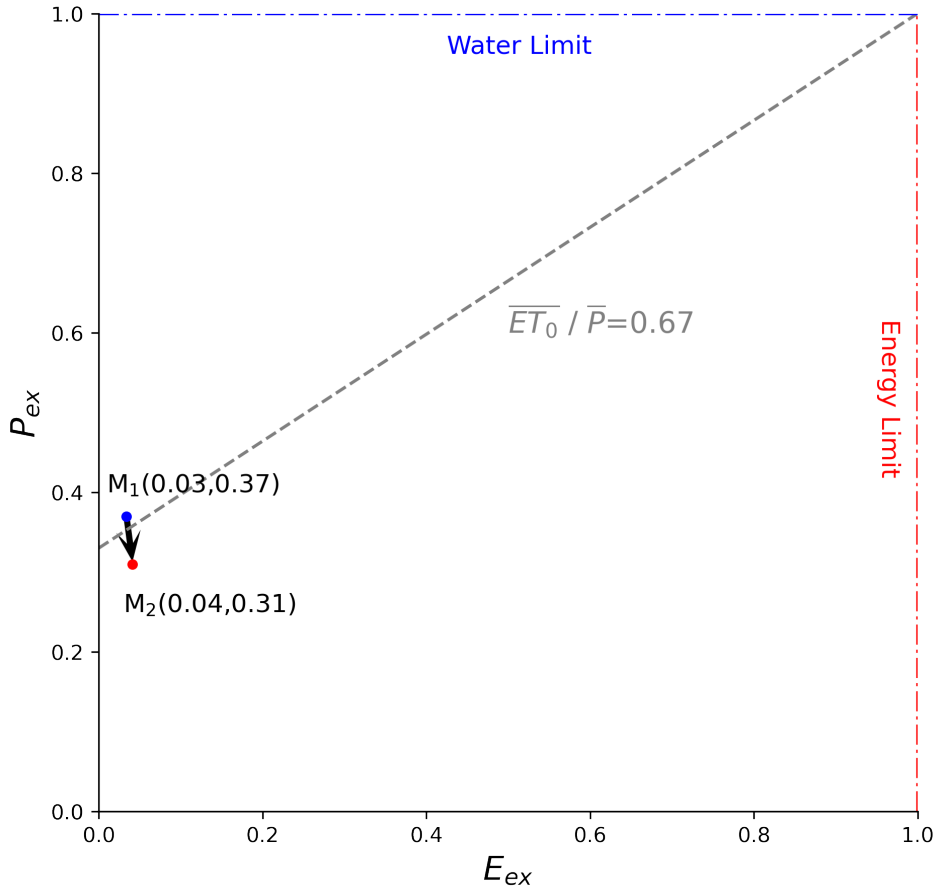

Figure 4.31: Visualization of the changes of the proportions of excess water (P_{ex}) and energy (E_{ex}) relative to the long term aridity index ($\overline{ET_0}$ / $\overline{P}$). The arrow indicates the direction of change between M1, which represents the baseline period 1970-1981, and M2, which represents the altered period 2010-2021. The change away of the constant aridity index indicates that climate change has a larger contribution, in comparison to land use changes, on mean flow alternations. Although, overall, at the scale of the entire graph, the change appears to be small

of the extreme precipitation in the area.

The mean flow attribution results (Section 4.5.2) support the following statements in both land use change and trend analysis:

1. The total precipitation is slightly increasing (presented in Section 4.1.1), the annual mean discharges are significantly decreasing (presented in Section 4.4.2) and potential evaporation is considerably increasing (presented in Section 4.2). All these statements are supported by the calculated values in Table 4.6.

2. The change points between the increase in potential evaporation (see Figure 4.10) and the decrease in annual mean discharges (see Figure 4.24) coincide, indicating that the potential evaporation rate may influence considerably the mean flows. This is verified by the large attribution of climate change to stream flow alterations (Table 4.6 and Figure 4.31).

3. The land use changes between 1990 and 2018 are not significant. This is consistent with the relatively low contribution of land use change to stream flow alterations (see Table 4.6). In addition, specific land use changes and human interventions presented, for example increase in forest area, re-direction of rainfall water to a WWTP outside the catchment, retention areas etcetera, seem logical as the Q values decrease.

5

Discussion

In this chapter, the main findings of this research are summarized and their implications are discussed. In addition, the methodology followed in Chapter 3 includes assumptions and uncertainties that must be addressed in order to be able to assess the quality of the reported results in Chapter 4. Section 5.1 summarizes the implications and the meaning of the results. Subsequently, the limitations of the applied methodology and the sources of uncertainty are presented in Section 5.2. Lastly, Section 5.3 provides guidance and recommendations based on the interpretation and the meaning of the results.

5.1. Implications

The statistical results obtained in Section 4.1 demonstrate some intriguing variations in the Geul catchment's precipitation regimes across the studied periods. The most notable change is the increase in very and extremely wet days (R95p and R99p). This increase constitutes the most significant change as it is also visible in the full-year period analysis (see Figure 4.1e). This is in line with the statistically significant increase of R95p all over the Netherlands (also including the Valkenburg station), reported by Lukić et al. (2018). The stable increase in R95p comes mainly from winters. The analysis of extreme precipitation in the winter season for the Geul catchment shows a stable and strong increase in most extreme indices, especially on very wet days (R95p) and maximum k-day precipitation sums (RXkD). The rise in severe precipitation is caused mostly by more rain on already wet days. This is a crucial finding as prolonged rainfall events have impacted the catchment and caused floods mainly in winters. These results are in agreement with previous studies in the Geul, the Netherlands but also in northwest Europe. Tu (2006) reported that the winters in the Geul and the Meuse have become wetter due to increases in the frequency of very wet days and multi-day precipitation extremes. Buishand et al. (2013) reported considerable increases in winter mean precipitation in the Netherlands. Gellens (2000) found considerably increasing trends in multi-day extreme precipitation in Belgium. Overall, trends in the Geul catchment are moving toward more wet conditions and frequent extreme events.

Furthermore, in this study, a significant and stable increase is found for trends starting mainly after 1980 for summer periods, where increases are visible for every extreme index and total precipitation. The frequency of very heavy and severe precipitation days increased in the recent past only in summers, as reflected in R30 and R40. These extreme events are characterized by limited occurrence in the catchment (as was also reported by Tu, 2006) and are mainly observed in the summer periods in the form of short and intense showers. The results of this thesis also reveal considerable increases on very wet days (R95p and R99p) and extreme precipitation in one, two, and three consecutive days (RX-k-D indices) for summer. This finding is important as it shows that, except for the intense showers in summers, the effects of heavy storms in combination with wet antecedent conditions should be also taken into account. This can be associated with the recent flood events of which most occurred in summer periods. The increase in extreme precipitation in summers is in agreement with the recent KNMI report, which shows that the heavy summer showers become more extreme (KNMI, 2021). The results are also partly supportive to the study of Buishand et al. (2013). Buishand et al. (2013) reported a considerable increase in total precipitation and extreme events (R30) in summers after 1980 in the Netherlands but mainly for coastal areas, while they mentioned that changes in the southeast part of

the country are lower. On the other hand, Tu (2006) reported a decrease in annual maximum summer precipitation for the Geul using a change-point test and a precipitation record from 1952 to 2001. This difference has three main explnations. First of all, Tu (2006) used a shorter record from 1952 to 2001 in comparison to the current study. Statistical tests for trend detection can be heavily affected by the studying period in which changes are calculated. Many of the extreme events occurred in the last 20 years in summers. Secondly, he defined summer periods from May-October while here summers are defined as the three regular months (June, July, and August). Finally, Tu (2006) used a different statistical test as compared to this study, which uses the M-K test in a multi-temporal way. As it is shown in this study, two statistically significant and opposite directions are identified for summer periods (see Figure 4.5 and/or Table A.1). Thus, the decreasing change point of Tu (2006) seems reasonable as the period 1951-2001 contains stronger decreasing than increasing trends.

No changes in autumn are observed in both extreme and total precipitation. The results in precipitation trend analysis for autumn periods support the theory of generally unchanged autumn total precipitation in the Meuse catchment (Tu, 2006). Springs show great variability and mixed trends. The very intense precipitation events (R30 and R40) are decreasing while for the other indices no clear patterns can be extracted. The total precipitation in spring shows more frequent downward trends in comparison to increases, indicating a decreasing tendency. Agor (2003) concluded that spring in the Geul has become wetter in the period 1952-2001 due to a change point in March. On the other hand Tu (2006) reported no trends in total precipitation in the Geul for spring in the period 1952-2001. Both studies are based on change point tests.

Furthermore, an important aspect of extreme precipitation trend analysis that needs to be addressed is the annual maximum precipitation RX1D (Figure 4.3e). As mentioned in Section 4.1.1, the percentages of statistically decreasing trends in RX1D are higher compared to increasing in full-year periods, however the difference and the total percentages are considered too small to indicate directions. This is also visible in the unstable trends found in Section 4.1.3 (Figure A.15). This pattern indicates that there are no significant changes over the past century in heavy thunderstorms for small aggregation levels (1-day interval). This pattern is in agreement with the study of Vaes et al. (2002) who reported a small decreasing tendency for small aggregation levels in Belgium. This finding also partly agrees with the results of Tu (2006) that there is a decreasing change point in the annual maximum precipitation. Despite the fact that the annual maximum precipitation has not changed in full periods, the characteristics of extreme precipitation, like the intensity and the frequency (i.e extreme showers in summers as reflected by R30), the prolonged very wet days (i.e R95p and R99p in all periods), and the consecutive maximum precipitation (i.e RXkD in winter and summer), have considerably increased. Some of the changes are only visible in seasonal patterns, while no considerable changes (except R95p and R99p) are observed in full year periods. These findings show the importance and relevance of ETCCDI indices in identifying extreme precipitation patterns and variations. In addition, the value of investigating trends not only in every season but also in full year periods is highlighted.

In this study, a correlation methodology is proposed in order to investigate to what extent extreme precipitation affects maximum discharges. Instead of correlating the variables in a fixed time frame, the rates of change over all moving windows between extreme precipitation indices and extreme discharge is evaluated. The results show that the variability of annual maximum discharges is quite similar to the variability of extreme precipitation. This is also visible in the seasonal multi-temporal trend analysis results, for example decreasing trends are visible before the 1980s in summer, while this pattern is reversed to statistically significant increases for trends starting after that period, similar to the extreme rainfall patterns. The largest correlation is observed between the index RX3D and maximum discharges. This may indicate that the extreme discharges are affected to a great extent by extreme precipitation on many consecutive days. This is probably related to catchment dynamics (response time) and storage capacity. This finding is important as the role of the water retention basins during prolonged rainfall events is not clearly analysed. These basins may have negative consequences if they are full and spill during the wrong time.

The mean flows in the Geul are generally decreasing (with some exceptions in winter). The decreasing change points found for spring and summer are identical with the results of Agor (2003) and Tu (2006) and coincide with the increasing change points found in potential evaporation trends. The total precipitation in the area slightly increased, while evaporation is increasing by a significant amount (1.82 mm/year). This finding is in agreement with the recent study of Huang et al. (2021), in which they reported an increase in potential evaporation in the Netherlands of about 1.66 mm/year for 1965-2019.

The increase in potential evaporation mainly comes from increases in summer and spring. The huge increase in potential evaporation reveals the severe drought years observed in the past (for example the severe drought of 2018 which is the highest value in the 1965-2021 time series, see Figure 4.7) and indicates that droughts may become more frequent and severe in future. KNMI also recently reported that droughts have significantly increased in summer and spring. The land-use changes from 1990 to 2018 are negligible. All these results are verified by an attribution analysis which shows that climate change has a larger contribution to mean flow alterations in the catchment due to the huge increase in potential evaporation. Contrary to the hypothesised association of Agor (2003) that the increase in "water loss" (precipitation minus discharge) is attributed to human interventions and losses from the catchment, this study attributes the decrease in mean flows mainly to climate variability. The main human interventions responsible for the mean flow reductions seem to be the large groundwater abstractions (mainly in summers), the water management practices and the reforestation. In general, the effects of land use and human interventions are only evident in mean flows and are not visible or could not be detected in extreme discharges. The extreme discharges mainly come from climate variability, especially in the recent past. The effects of land use seem to be overshadowed by climate variability.

5.2. Limitations and uncertainty

5.2.1. Precipitation

For the trend analysis in precipitation time series, records of daily precipitation are used that come from the Netherlands KNMI manual rain gauge network. Long precipitation time series may have been influenced by instrumental modifications and station relocations throughout the recording period. As mentioned in Section 3.1.1, the data are considered to be of high quality, as KNMI performs regular quality tests. In addition to that, two homogeneity tests are applied to monthly sums. In general, it is assumed that the analyzed precipitation time series in this research are not affected by instrumental and location alterations, so the trends that are found can be attributed to climate and not to human interventions.

Stations in the most upstream parts, with higher altitudes in Belgium, are not considered, as their time series lengths are too short. Higher amounts of precipitation are expected in those areas. Had Belgian stations with long time series been provided, a more accurate image of precipitation trends in the whole catchment would have been achieved. In general, the results show that there is no significant spatial variability of trends in the area, so similar patterns are expected for most upstream parts. A small difference is observed at the Noorbeek station, which is located outside the catchment.

The records of the precipitation stations slightly differ and mainly start in the 1950s, except for the Epen station which has a record from 1981. Ideally, the stations should have exactly the same time records, so the trend-strength percentage index p (see Equation 3.5) could have been expressed more appropriately. However, the index has high relevance and is considered vital for the study (it is catchment-based rather than station-based as Epen is also included). The differences in time records in the 5 out of 6 stations are negligible, as the records in three stations start in 1951, one starts in 1956, and the other in 1958. The station Epen has no considerable impact on the index relevance as it counts only for the 12 out of 210 studied moving windows in N_T (see Equation 3.5). Figure 5.1 shows the calculated percentages for spring periods with and without including station Epen in trend-strength percentage calculations. As can be observed differences are hardly visible. The use of Epen station in index p must be seen as an advantage because it adds value to the recent trends (it is like a slight weight is placed on the trends starting after 1980). In addition, station Epen is needed to identify recent patterns, as mentioned many times in this report, especially in the stability section results (Section 4.1.3). Furthermore, an identical time record for all stations could facilitate expressing the long-term variability in a more accurate way, for example as a percentage of stations that have significant increasing or decreasing trends in every moving window, rather than an average behavior as reported in this study (Section 4.5.1). In general, the effect of the differences in time records on the relevance of the results is considered negligible but it should be kept in mind.

Indices R30 and R40 represent annual counts of exceedances. These events are rare (especially R40) in the catchment and are mainly observed in summers in the form of intense showers as mentioned above. Their values range between 0 and 5. This is why Sen's slope is not calculated for R30 and R40. Most of the counts are equal to 0, especially in the seasonal trend analysis, making the M-K test unstable. In this regard, a different trend test and assumptions for slopes could have been used for

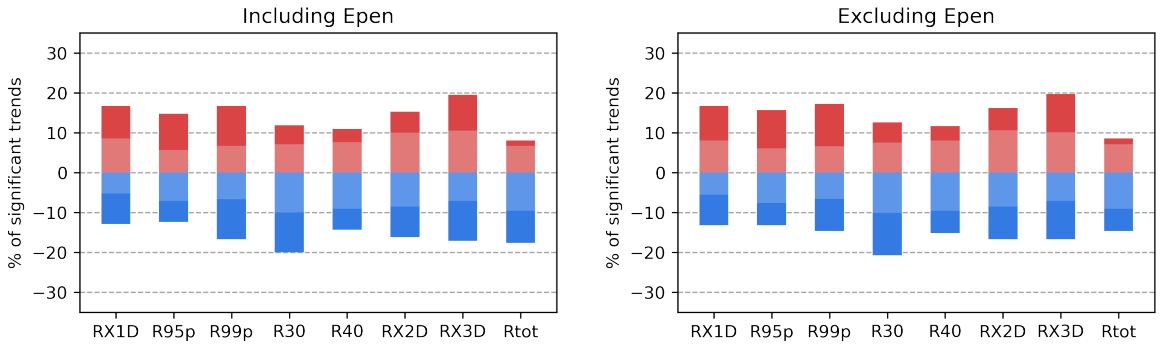

Figure 5.1: Percentages of statistically significant trends calculated for each station in spring, with and without including station Epen. Almost identical percentages can be seen.

example considering that the number of exceedances follows a Poisson distribution.

The precipitation trend analysis is used for the identification of directions, stabilities, and temporal variabilities. Although this study provides an indication of the rate of change in summers (see Table A.2), slopes of statistically significant trends are not considered. A stable and statistically significant trend might be irrelevant because of its low rate of change. Overall, this study focuses on trend variability rather than actual magnitudes.

5.2.2. Evaporation

For the potential evaporation trend analysis, only the meteorological station in Maastricht is used. Thus, this station is considered representative of the whole catchment. In reality, the potential evaporation values may slightly differ in most upstream parts of the catchment as the height increases. No large discrepancies are expected due to this assumption in the potential evaporation values of the area, as the average potential evaporation value of the catchment would be more or less the same. This assumption does not affect the trend analysis results. In general, it is important to note that the translation from potential to actual evaporation does depend on land use.

5.2.3. Land use

In general, it is essential to note that the aggregated percentages of large land cover groups cannot sufficiently depict land use changes, especially in small-scale catchments like the Geul. In addition, changes in agricultural crops, that could have potentially impacted the flows, are not visible in the used land cover data sets. Furthermore, the land cover maps used in this thesis have low resolution (100 m) and as a result interventions on smaller scales, for example buffer zones, are not visible. The studying period from 1990 to 2018 is considered short, as significant changes are reported mainly before 1980. Overall, the land use change detection in this study is essential as it provides the recent general tendencies in the area.

5.2.4. Discharge

It must be acknowledged that the results produced for all stations and especially stations Hommerich and Gulp, are subject to significant uncertainty. Some of the trends in mean flows may be related to inconsistencies in discharge data from those locations. During a period of transition, changes in gauge position, equipment and monitoring frequencies, and stage-discharge relations can cause sudden variations in flow rates and these changes might have altered discharge characteristics of the stream. For example, the stage-discharge relations used are very uncertain especially during extremely high flows and have been changed many times in the past (see Subsection 3.4.2). In addition, in the aforementioned stations, there are missing values that lead to exclusion of years in the statistical analysis. These changes can be more visible in mean flow trends where the values are low in contrast to high flows. Change point tests are sensitive to those alternations.

For the reasons discussed above, only the Meerssen station is considered for change point tests. The long-term measurements of station Meerssen at the outlet of the catchment are considered reliable. Agor (2003) reported that, despite the changes in gauging techniques in 1978, the data in Meerssen

do not reveal any inhomogeneities based on a double mass plot between Meerssen and the Gulp. In general, no considerable differences are detected between the different stations and the total response of the catchment at Meerssen, indicating that the measuring changes have likely not affected the overall directions. The only significant difference is observed in mean flows between Hommerich and Meerssen. There is evidence that this difference is attributed to the relocations and the uncertainties in the measurement techniques in Hommerich, but it should be further investigated.

5.2.5. Attribution

The attribution of the mean flow results is based on the initial framework proposed by Tomer and Schilling (2009) as modified by Renner et al. (2014) and Marhaento et al. (2017). Although considerable effects of LUC and CC on mean discharge flows are evident, the magnitude of the changes (R-value in Figure 3.5) is relatively low. This may indicate that the stream flow changes may be also affected by other factors (besides CC and LUC), for example, area size, slopes, soil moisture etcetera. The proposed framework provides a quantitative assessment for attributing changes in stream flows to LUC and CC, however, it uses significant assumptions that do not represent the real world. The initial framework proposed by Tomer and Schilling (2009) is based on the assumption that CC only affects precipitation and potential evaporation, while LUC only affects actual evaporation. In this approach, the fundamental concept ignores the real-world complex relations in which changes in evaporation are driven by a combination of both CC and LUC. Renner et al. (2014) tried to make the framework more realistic by imposing that alterations in the water supply have similar effects as alterations in the energy supply but in opposite directions. In their framework, the attribution of alterations in discharges to CC can interfere with LUC, if for example both precipitation and potential evaporation increase or decrease in the same direction. This framework improves the results of attribution, but the uncertainty is still evident (Marhaento et al., 2017). Furthermore, the framework used in this study highly depends on the data quality. Concepts like excess energy and water show great sensitivity to data time series (Marhaento et al., 2017; Renner et al., 2014; Tomer & Schilling, 2009) and can be influenced by them. As mentioned in Section 5.2.1 areal average precipitation is not 100% accurate as upstream stations are not included. In addition, potential evaporation is just taken from one station (Section 5.2.2). Discharge measurements at the outlet of the catchment at Meerssen may introduce extra errors in the calculations (Section 5.2.4). Overall, it is vital to mention that the attribution analysis must be seen as an indication of the dominant driving force of the mean flow changes and not as an exact number. Although a precise attribution is impossible due to the assumptions employed (and actually in any case), the directions of the proportions of excess water and energy in relation to the constant aridity index can offer a reasonable clue (Marhaento et al., 2017). In the current study, long and annual records are used so random errors in hydro-meteorological variables can be reduced. In addition, the results of the attribution are in agreement with the results of the trend analysis and land use change detection as expected, indicating that climate change has a larger contribution to mean flow changes in comparison to LUC.

5.3. Guidance and recommendations

The results of this study support the rainfed nature of the Geul river, as there is a strong indication that variability of extreme discharges comes mainly from climate variability. The variability of the rates of change in extreme precipitation indices (e.g. RX3D) is almost identical to the rates of change in extreme discharge. Events that impacted the catchment in the past (both in summer and winter) and revealed significant failures are increasing both in magnitude and frequency. Thus, climate change should be taken seriously into account in the area and should be incorporated into flood designs. Furthermore, floods and droughts should be considered interconnected hazards and must be evaluated at the same time to ensure a balance between water availability during dry periods and flood safety during wet periods. This could facilitate improving resilience against natural hazards and provide adaptation strategies to a changing climate.

According to the local water board, no substantial artificial interventions influencing the flow and storage of the Geul have been implemented since 2014 (van Dijk, 2022). Almost none of the current measures reduced the peak discharges during the recent flood event of July 2021 (van Dijk, 2022). The Geul is vulnerable to erosion and flooding and extreme events are expected to be more extreme and more frequent. Thus, action is needed. Action and solutions should be in an integrated framework

that includes aspects that seem to cause the hazard, for example, climate change (extremes more intense and frequent etc.), land use changes (intensification of agriculture, urbanization, mining activities etc.), flood protection levels (low safety standards, etc.), governance-crisis response (few early warning signs, position of critical infrastructure, evacuation, etc.) and so on. Apart from the main suggestion to incorporate climate change into flood design there are also attractive suggestions related to the aforementioned problems, for example biodiversity policies, use of abandoned mining areas, better drainage facilities to agricultural areas, retention areas upstream that can increase the safety levels, international cooperation between the Netherlands and Belgium, etc.

Furthermore, the results of this study can be used as an indication of the assessment of changes in hydroclimatic variables in the Meuse river catchment, as the Geul is one of its main tributaries. In addition, the results of the precipitation and evaporation trend analyses can facilitate the evaluation of climate change effects on precipitation regimes and droughts all over the Netherlands, especially in the recent past. The use of a multi-temporal approach is useful and is recommended for identifying variabilities, recent directions but also long-term trends. In addition, the correlation methodology proposed for investigating the rates of change all over the study periods adds value to the multi-temporal trend analysis. Overall, it seems promising and is recommended to be tested also in other cases and for different variables.

6

Conclusions and future directions

6.1. Conclusions

The main objective of this research was to investigate the temporal variability of hydrometeorological variables trends and the main land use changes in the Geul river catchment. Thus, this study aimed to improve understanding of climate change and human intervention impacts on the hydrological response of the Geul. Therefore, this thesis initially investigated the trends in (extreme) precipitation in the area by studying their long term-variability, their strengths, their stabilities, and directions. Then, the trends in potential evaporation and the main land use changes/human intervention in the catchment have been identified. Subsequently, the spatial and temporal variability of runoff patterns has been reported. Finally, the correspondence between extreme precipitation and annual maximum discharges was investigated by proposing a new correlation methodology, and the alternations in mean flows were attributed to climate change and land use changes. In order to conclude this thesis, the research questions presented in Section 1.2 are revisited.

Question 1: ***What are the temporal variability, the stability, and the trend directions of the extreme and total precipitation in the Geul River catchment?***

The winters are becoming wetter. This becomes evident by the stable and strong upward trends in "very wet days" all over the area. Strong and relatively stable increases are also observed in winter maximum precipitation sums for k-day intervals (RX1D, RX2D, and RX3D). A small increase (poor stability) in total precipitation in winters is also visible. Very heavy and severe precipitation days seem to be rare events and not observed in winters. The rareness of those events causes significant and stable decreases in R30 (number of days when precipitation exceeds 30 mm) and R40 (number of days when precipitation exceeds 40 mm) indices. These decreases are mainly visible in the recent past for trends starting after the 1980s. Overall, it seems that the Geul river catchment becomes wetter in winter due to multi-day precipitation extremes and the increase in precipitation on wet days larger than the 95th percentile (R95p).

Despite the fact that most of the precipitation indices show decreases from 1951 to 1980 in summer, statistically significant, strong, and stable increasing trends are observed in all extreme precipitation indices since the 1980s. The frequency of very heavy and severe precipitation days increased in the recent past, as it is reflected in R30 and R40. These extreme events are characterized by limited occurrence in the catchment and are mainly observed in the summer periods in the form of short and intense showers. In addition, considerable increases on very wet days and extreme precipitation in one, two, and three consecutive days (RX-k-D indices) are found for summer periods in the last 40 years. Thus, both the magnitudes and the duration of extreme precipitation are moving upwards. Heavy storms in combination with wet antecedent conditions can cause large flooding and these conditions are moving towards an increase in summers. In addition, the total precipitation appears to have increased over the last years in summers but this increase is statistically insignificant.

No changes are observed in autumn, as all precipitation indices show unstable and non-significant trends in the area.

In spring, mixed trends are observed. A shift from increasing to decreasing and then back to increas-

ing for trends starting in the recent past is observed. Overall, indices R30, R40, and total precipitation are decreasing, while there is no clear distinction in the remaining indices.

Despite the fact that notable changes in seasonal precipitation regimes are reported across the studied periods, no considerable changes are found for full year periods. Extreme and total precipitation show unstable and statistically insignificant trends for full years. The only exception is observed in very wet days in the downstream part of the catchment (stations Maastricht, Valkenburg and Ubachsberg) where a stable and statistically significant increase is visible.

Question 2: ***What are the temporal variability, the magnitudes, and the trend directions of the potential evaporation in the catchment?***
The potential (reference) evaporation is significantly, strongly, and consistently increasing all over the study period. The rate of change for is 1.82 mm/year, which means that the potential evaporation has increased more than 100 mm since 1965. Considerable increases are reported for summers and springs (0.87 mm/year and 0.7 mm/year, respectively) and medium for autumns (0.2 mm/year). The increase in potential evaporation in winters is statistically significant, however the rate of change is low (0.07 mm/year). While for the other seasons the increases in evaporation are consistent in all moving periods, the trends in winter are statistically significant only in the recent past (trends starting after 1988). This indicates that in the last 30 years a significant increasing direction has been detected for winters.

Question 3: ***What are the most important land-use changes and human interventions in the area?***
The urbanization, the intensification of agricultural areas, and the groundwater abstractions are the most important changes in the Geul river catchment. These changes dominated between 1950 and 1970. There do not appear to be significant changes in the whole Geul river catchment from 1990 to 2018. During the period 1990-2018, the built-up area increased by 1%, while pastures decreased at the same rate. The agricultural area remained the same, while a small increase in the forest of 0.1% is observed.

Question 4: ***What are the spatial and temporal variability and directions of the extreme and mean discharge trends in the Geul river catchment?***

Annual maximum discharges
For full year periods, the annual maximum discharges at the outlet of the catchment at Meerssen have increasing tendencies, however, most of them are statistically insignificant. During extreme precipitation events, Hommerich contributes to a significant amount of discharge in Meerssen, as the annual maximum discharges, the variability, and the directions of the trends in the two locations are similar. The summer maximum discharges show weak decreasing tendencies over the longest periods, but this changes to increasing weak trends (mainly statistically significant at α=0.2) for periods starting after the 1980s. The winter maximum discharges are significantly increasing (19% of the tested cases are significant at α=0.1) but in the recent past (trends after the 1980s), statistically insignificant decreasing tendencies are observed. The maximum discharges in spring are decreasing, but this pattern is reversed in the recent past moving towards an increase. No pattern is identified for autumn as mixed and insignificant trends are found.

The Hommerich station, which measures the discharge coming from the Belgian part of the Geul catchment, has similar temporal variability in the trend directions as Meerssen. However, the magnitudes of the increases are even higher, especially in summer, when strong and significant upward trends have been observed in the recent past. Almost all summer trends starting after 1985 are statistically significant at α=0.05 and some of them even at α=0.01. The winter maximum annual discharges are constantly moving upward (most of the cases are significant at α=0.20). Only increasing tendencies are reported in full-year periods but they are not statistically significant.

Annual maximum discharges in the Gulp are continuously increasing in summers but this increase is insignificant and weak (no trends are detected even at 20% significance level). For winter, increasing strong trends are found for longer periods, however, insignificant decreasing tendencies are visible in the recent past. Increasing trends are found for periods ending before 2010 in spring, but after that period the tendencies are moving towards a weak decrease. Statistically significant decreases are

found for the longer period in autumn but this pattern is considered unstable, as mixed statistically insignificant tendencies are observed all over the time combinations.

The only statistically significant trends for the Eyserbeek and the Selzerbeek are decreasing (both at the 5% level), and are found during autumn periods.

Annual mean discharges
Mean discharges show significantly and strong decreasing trends in Meerssen, in all periods except winter, which shows mainly increasing tendencies over longer periods and downward strong trends in the recent past. Significant decreases in average mean flows are found in summer (from 3.07 m^3/s to 2.4 m^3/s) and spring (from 4.04 m^3/s to 3.18 m^3/s) after 1989. Similar patterns as those in Meerssen are reported in the Gulp for winter, summer, and autumn periods, however, insignificant tendencies are found for spring. Although the Hommerich station shows similar patterns to Meerssen in the annual maxima, it seems that the patterns of annual mean discharges are moving differently. Mean discharges in Hommerich have a similar tendency as maximum discharges. This difference may be caused by differences in locations and measuring techniques at the station and not due to climate or land use changes, however further investigation is required. The only statistically significant trends for the Eyserbeek and the Selzerbeek are decreasing (at 5 and 10% level, respectively), and are found during autumn periods.

Question 5: ***To what extent is the variability of the runoff patterns affected by climate variability and human interventions?***
The variations in the maximum discharges in the area can be largely explained by the variations in the extreme precipitation in the area. The annual maximum discharge variability follows the directions and magnitudes of extreme precipitation, as the rate of change between extreme rainfall and extreme discharge (annual maximum) is quite similar. The increased frequencies and magnitudes in the recent past in the Geul are a reflection of the climate variability. The effect of land use changes in the extreme discharges seems to be less important or probably is overshadowed by climatic variability for the studying time frame from 1970 to 2021.

Changes in mean stream flows of the Geul river catchment for the period 1970-2021 can be attributed mainly to climate change and secondary to land use changes/human interventions, as indicated by the relative attribution percentages. The results of the statistical trend analyses show that climate has significantly changed and especially potential evaporation, which seems to contribute to a great extent to the decrease in flows. At the same time, land use has not significantly altered. Human interventions that may have slightly affected the stream flows could be the groundwater abstractions, increase in forested area, and general hydraulic and water management practices in downstream areas, e.g. retention areas.

6.2. Future research directions

This thesis has presented several aspects of work that could be further investigated. The following indicates the most important, forming the future research directions.

Precipitation variability and large-scale atmospheric circulation: The principal driver of regional fluctuations in temperature, precipitation, and other climatic variables is atmospheric circulation, particularly in the mid-latitudes (Slonosky et al., 2000). In this thesis variations in Geul catchment's precipitation regimes are found across the studied periods. Some of these patterns may be a result of alterations in atmospheric circulation patterns, for example North Atlantic Oscillation (NAO) and Grosswetterlagen system. An analysis connecting synoptic data and climatological data can improve our perception of precipitation variabilities in the Geul catchment area.

Hydrological response of the Geul to climate change: According to the KNMI increases in dry springs and summers and more extreme summer showers are the climate risks for the Netherlands the next years (KNMI, 2021). These climate scenarios are in line with the trends found in this study. One of the main findings of this thesis is that climate variability affects to a great extent the runoff patterns in the Geul. As a result, it becomes evident that projected changes in precipitation and temperature characteristics due to climate change are expected to have significant impacts on the hydrological regime. For this reason, it is important to study the hydrological response of the Geul based on likely future high resolution climate scenarios.

Tracers and process-based hydrological modeling: In this thesis, the effects of land use changes on runoff patterns of the Geul are not visible (or could not be detected), especially in maximum discharges. Further research is suggested to increase our understanding of human interventions on the Geul. One aspect of this could be the use of tracers and geophysical approaches together with process-based hydrological models. State-of-the-art tracers can facilitate our understanding of hydrological processes and runoff partitioning (Smith et al., 2021) in the area, especially upstream of the Geul (which is urbanized and sensitive to land use changes) and in tributaries like the Gulp, for which there is evidence that the topographic divide leads to losses (Agor, 2003; Dautrebande et al., 2000).

Bibliography

Abbott, B. W., Bishop, K., Zarnetske, J. P., Minaudo, C., Chapin, F., Krause, S., Hannah, D. M., Conner, L., Ellison, D., Godsey, S. E., et al. (2019). Human domination of the global water cycle absent from depictions and perceptions. *Nature Geoscience*, *12*(7), 533–540.

Agor, M. L. C. (2003). *Assessment of the long-term rainfall runoff relation of the Geul catchment* (Master's thesis). UNESCO–IHE Institute for Water Education, The Netherlands.

Ahmad, I., Tang, D., Wang, T., Wang, M., & Wagan, B. (2015). Precipitation trends over time using Mann-Kendall and Spearman's rho tests in Swat river basin, Pakistan. *Advances in Meteorology*, *2015*.

Alexandersson, H. (1986). A homogeneity test applied to precipitation data. *Journal of Climatology*, *6*(6), 661–675.

Alexandersson, H., & Moberg, A. (1997). Homogenization of Swedish temperature data. Part I: Homogeneity test for linear trends. *International Journal of Climatology: A Journal of the Royal Meteorological Society*, *17*(1), 25–34.

Armstrong, M. (2013). *Geostatistics: Proceedings of the Third International Geostatistics Congress September 5–9, 1988, Avignon, France* (Vol. 4). Springer Science & Business Media.

Asselman, N., van Heeringen, K.-J., de Jong, J., & Geertsema, T. (2022). *Juli 2021 overstroming en wateroverlast in Zuid-Limburg:Eerste bevindingen voor Valkenburg, Geulmonding, Roermonding en Eygelshoven* (tech. rep.). Deltares, report 1207700-000-ZWS-0019, The Netherlands.

Auer, I., Böhm, R., Jurković, A., Orlik, A., Potzmann, R., Schöner, W., Ungersböck, M., Brunetti, M., Nanni, T., Maugeri, M., et al. (2005). A new instrumental precipitation dataset for the greater Alpine region for the period 1800–2002. *International Journal of Climatology: A Journal of the Royal Meteorological Society*, *25*(2), 139–166.

Bhatti, A. S., Wang, G., Ullah, W., Ullah, S., Fiifi Tawia Hagan, D., Kwesi Nooni, I., Lou, D., & Ullah, I. (2020). Trend in extreme precipitation indices based on long term in situ precipitation records over Pakistan. *Water*, *12*(3), 797.

Blöschl, G., Gaál, L., Hall, J., Kiss, A., Komma, J., Nester, T., Parajka, J., Perdigão, R. A., Plavcová, L., Rogger, M., et al. (2015). Increasing river floods: Fiction or reality? *Wiley Interdisciplinary Reviews: Water*, *2*(4), 329–344.

Blöschl, G., Hall, J., Parajka, J., Perdigão, R. A., Merz, B., Arheimer, B., Aronica, G. T., Bilibashi, A., Bonacci, O., Borga, M., et al. (2017). Changing climate shifts timing of European floods. *Science*, *357*(6351), 588–590.

Bouaziz, L. J. E. (2021). *Internal processes in hydrological models: A glance at the Meuse basin from space* (PhD dissertation). Delft University of Technology, The Netherlands.

Brandsma, T., Beersma, J. J., van den Brink, J. W., Buishand, T. A., Jilderda, R., & Overeem, A. (2020). *Correction of rainfall series in the Netherlands resulting from leaky rain gauges* (tech. rep.). Royal Netherlands Meteorological Institute (KNMI).

Buishand, T. A. (1984). Tests for detecting a shift in the mean of hydrological time series. *Journal of Hydrology*, *73*(1-2), 51–69.

Buishand, T. A., De Martino, G., Spreeuw, J., & Brandsma, T. (2013). Homogeneity of precipitation series in the Netherlands and their trends in the past century. *International Journal of Climatology*, *33*(4), 815–833.

Buishand, T. A. (1982). Some methods for testing the homogeneity of rainfall records. *Journal of Hydrology*, *58*(1-2), 11–27.

Caloiero, T., Filice, E., Coscarelli, R., & Pellicone, G. (2020). A homogeneous dataset for rainfall trend analysis in the Calabria region (Southern Italy). *Water*, *12*(9), 2541.

Cappuyns, V., Swennen, R., Vandamme, A., & Niclaes, M. (2006). Environmental impact of the former Pb–Zn mining and smelting in East Belgium. *Journal of Geochemical Exploration*, *88*(1-3), 6–9.

Casanueva, A., Rodríguez-Puebla, C., Frías, M., & González-Reviriego, N. (2014). Variability of extreme precipitation over Europe and its relationships with teleconnection patterns. *Hydrology and Earth System Sciences*, *18*(2), 709–725.

Ceola, S., Laio, F., & Montanari, A. (2014). Satellite nighttime lights reveal increasing human exposure to floods worldwide. *Geophysical Research Letters*, *41*(20), 7184–7190.

Cheng, C., Yang, Y. E., Ryan, R., Yu, Q., & Brabec, E. (2017). Assessing climate change-induced flooding mitigation for adaptation in Boston's Charles River watershed, USA. *Landscape and Urban Planning*, *167*, 25–36.

Dai, A. (2013). Increasing drought under global warming in observations and models. *Nature Climate Change*, *3*(1), 52–58.

Dautrebande, S., Leenaars, J., Schmitz, J., & Vanthournout, E. (2000). *Pilot project for the definition of environment-friendly measures to reduce the risk for flash floods in the Geul River catchment* (tech. rep.). Technum, University of Liège and CSO Environmental Consultancy.

De Bruin, H., & Stricker, J. (2000). Evaporation of grass under non-restricted soil moisture conditions. *Hydrological sciences journal*, *45*(3), 391–406.

De Laat, P., & Agor, M. (2003). Geen toename piekafvoer Geul. *H2O*, (9), 25–27.

De Moor, J., Kasse, C., Van Balen, R., Vandenberghe, J., & Wallinga, J. (2008). Human and climate impact on catchment development during the Holocene—Geul River, the Netherlands. *Geomorphology*, *98*(3-4), 316–339.

Dejonghe, L., Ladeuze, F., & Jans, D. (1993). Atlas des gisements plombo-zincifères du synclinorium de Verviers (Est de la Belgique). *Mémoire-Service géologique de Belgique*, *33*, 1–148.

Di Baldassarre, G., Montanari, A., Lins, H., Koutsoyiannis, D., Brandimarte, L., & Blöschl, G. (2010). Flood fatalities in Africa: From diagnosis to mitigation. *Geophysical Research Letters*, *37*(22).

Dos Santos, C. A., Neale, C. M., Rao, T. V., & Da Silva, B. B. (2011). Trends in indices for extremes in daily temperature and precipitation over Utah, USA. *International Journal of Climatology*, *31*(12), 1813–1822.

Douglas, E., Vogel, R., & Kroll, C. (2000). Trends in floods and low flows in the united states: Impact of spatial correlation. *Journal of Hydrology*, *240*(1-2), 90–105.

Driessen, T., Hurkmans, R., Terink, W., Hazenberg, P., Torfs, P., & Uijlenhoet, R. (2010). The hydrological response of the Ourthe catchment to climate change as modelled by the HBV model. *Hydrology and Earth System Sciences*, *14*(4), 651–665.

Dutoo, D. (1994). Het Belgische Stroombekken. *Onderzoek watersnood maas, achtergrondrapport 1*. Water-loopkundig Laboratorium Delft/Delft Hydraulics, Delft.

Engelen, F. (1976). Delfstoffen en hun invloed op politieke beslissingen. het ontstaan van het neutrale gebied Moresnet en de geschiedenis van de mijnbouw in dit gebied. *Grondboor & Hamer*, *30*(1), 20–31.

Gellens, D. (2000). Trend and correlation analysis of k-day extreme precipitation over Belgium. *Theoretical and Applied Climatology*, *66*(1), 117–129.

Gocic, M., & Trajkovic, S. (2013). Analysis of changes in meteorological variables using Mann-Kendall and Sen's slope estimator statistical tests in Serbia. *Global and Planetary Change*, *100*, 172–182.

Grandry, M., Gailliez, S., Brostaux, Y., & Degré, A. (2020). Looking at trends in high flows at a local scale: The case study of Wallonia (Belgium). *Journal of Hydrology: Regional Studies*, *31*, 100729.

Haddeland, I., Heinke, J., Biemans, H., Eisner, S., Flörke, M., Hanasaki, N., Konzmann, M., Ludwig, F., Masaki, Y., Schewe, J., et al. (2014). Global water resources affected by human interventions and climate change. *Proceedings of the National Academy of Sciences*, *111*(9), 3251–3256.

Hall, J., Arheimer, B., Borga, M., Brázdil, R., Claps, P., Kiss, A., Kjeldsen, T., Kriaučiūnienė, J., Kundzewicz, Z. W., Lang, M., et al. (2014). Understanding flood regime changes in europe: A state-of-the-art assessment. *Hydrology and Earth System Sciences*, *18*(7), 2735–2772.

Hamed, K. H., & Rao, A. R. (1998). A modified Mann-Kendall trend test for autocorrelated data. *Journal of Hydrology*, *204*(1-4), 182–196.

Hannaford, J., Buys, G., Stahl, K., & Tallaksen, L. (2013). The influence of decadal-scale variability on trends in long European streamflow records. *Hydrology and Earth System Sciences*, *17*(7), 2717–2733.

Hannaford, J., Mastrantonas, N., Vesuviano, G., & Turner, S. (2021). An updated national-scale assessment of trends in UK peak river flow data: How robust are observed increases in flooding? *Hydrology Research*, *52*(3), 699–718.

Hellwig, J., & Stahl, K. (2018). An assessment of trends and potential future changes in groundwater-baseflow drought based on catchment response times. *Hydrology and Earth System Sciences*, *22*(12), 6209–6224.

Hirabayashi, Y., Mahendran, R., Koirala, S., Konoshima, L., Yamazaki, D., Watanabe, S., Kim, H., & Kanae, S. (2013). Global flood risk under climate change. *Nature Climate Change*, *3*(9), 816–821.

Huang, Y., Weis, J., Vereecken, H., & Hendricks Franssen, H.-J. (2021). Long-term trends in agricultural droughts over Netherlands and Germany: How extreme was the year 2018? *Hydrology and Earth System Sciences Discussions*, 1–27.

Hussain, M., & Mahmud, I. (2019). Pymannkendall: A python package for non parametric Mann Kendall family of trend tests. *Journal of Open Source Software*, *4*(39), 1556.

Imfeld, N., Sedlmeier, K., Gubler, S., Correa Marrou, K., Davila, C. P., Huerta, A., Lavado-Casimiro, W., Rohrer, M., Scherrer, S. C., & Schwierz, C. (2021). A combined view on precipitation and temperature climatology and trends in the southern Andes of Peru. *International Journal of Climatology*, *41*(1), 679–698.

IPCC. (2021). Summary for policymakers. In V. Masson-Delmotte, P. Zhai, A. Pirani, S. L. Connors, C. Péan, D. Berger, N. Caud, Y. Chen, L. Goldfarb, M. I. Gomis, M. Huang, K. Leitzell, E. Lonnoy, J. B. R. Matthews, T. K. Maycock, T. Waterfield, O. Yelekçi, R. Yu, & B. Zhou (Eds.), *Climate change 2013: The physical science basis. contribution of working group i to the Sixth Assessment Report of the Intergovernmental Panel on Climate Change*. Cambridge University Press.

Kang, H. M., & Yusof, F. (2012). Homogeneity tests on daily rainfall series. *Int. J. Contemp. Math. Sciences*, *7*(1), 9–22.

Karamage, F., Zhang, C., Fang, X., Liu, T., Ndayisaba, F., Nahayo, L., Kayiranga, A., & Nsengiyumva, J. B. (2017). Modeling rainfall-runoff response to land use and land cover change in Rwanda (1990–2016). *Water*, *9*(2), 147.

Kendall, M. G. (1955). *Rank Correlation Methods: By Maurice G. Kendall.* Hafner.

Klein Tank, A., Wijngaard, J., Können, G., Böhm, R., Demarée, G., Gocheva, A., Mileta, M., Pashiardis, S., Hejkrlik, L., Kern-Hansen, C., et al. (2002). Daily dataset of 20th-century surface air temperature and precipitation series for the European Climate Assessment. *International Journal of Climatology: A Journal of the Royal Meteorological Society*, *22*(12), 1441–1453.

KNMI. (2021). *Klimaatsignaal'21: Hoe het klimaat in Nederland snel verandert* (tech. rep.). Royal Netherlands Meteorological Institute (KNMI).

Kreienkamp, F., Philip, S., Tradowsky, J., Sarah, F., Lorenz, P., Arrighi, J., Belleflamme, A., Bettmann, T., Caluwaerts, S., Chanal, S., et al. (2021). Rapid Attribution of Heavy Rainfall Events Leading to the Severe Flooding in Western Europe during July 2021; World Weather Attribution: 2021.

Leenaers, H. (1989). *The dispersal of metal mining wastes in the catchment of the River Geul (Belgium-The Netherlands)* (Doctoral dissertation). Koninklijk Nederlands Aardrijkskundig Genootschap.

Lehmann, J., Coumou, D., & Frieler, K. (2015). Increased record-breaking precipitation events under global warming. *Climatic Change*, *132*(4), 501–515.

Lucassen, E., Van Kempen, M., Roelofs, J., & Van der Velde, G. (2010). Decline in metallophytes in tertiary polluted floodplain grasslands in the Netherlands: Experimental evidence for metal and nutritional changes in soil as driver factors. *Chemistry and Ecology*, *26*(4), 273–287.

Lukić, T., Basarin, B., Micić, T., Bjelajac, D., Maris, T., Marković, S. B., Pavić, D., Gavrilov, M. B., & Mesaroš, M. (2018). Rainfall erosivity and extreme precipitation in the Netherlands. *IDŐJÁRÁS / QUARTERLY JOURNAL OF THE HUNGARIAN METEOROLOGICAL SERVICE*, *122*(4), 409–432.

Lupikasza, E. (2010). Spatial and temporal variability of extreme precipitation in Poland in the period 1951–2006. *International Journal of Climatology: A Journal of the Royal Meteorological Society*, *30*(7), 991–1007.

Łupikasza, E. B., Hänsel, S., & Matschullat, J. (2011). Regional and seasonal variability of extreme precipitation trends in southern Poland and central-eastern Germany 1951–2006. *International Journal of Climatology*, *31*(15), 2249–2271.

Mangini, W., Viglione, A., Hall, J., Hundecha, Y., Ceola, S., Montanari, A., Rogger, M., Salinas, J. L., Borzì, I., & Parajka, J. (2018). Detection of trends in magnitude and frequency of flood peaks across Europe. *Hydrological Sciences Journal*, *63*(4), 493–512.

Mann, H. B. (1945). Nonparametric tests against trend. *Econometrica: Journal of the econometric society*, 245–259.

Marhaento, H., Booij, M. J., & Hoekstra, A. Y. (2017). Attribution of changes in stream flow to land use change and climate change in a mesoscale tropical catchment in Java, Indonesia. *Hydrology research*, *48*(4), 1143–1155.

McMillan, H., Montanari, A., Cudennec, C., Savenije, H., Kreibich, H., Krueger, T., Liu, J., Mejia, A., Van Loon, A., Aksoy, H., et al. (2016). Panta Rhei 2013–2015: Global perspectives on hydrology, society and change. *Hydrological Sciences Journal*, *61*(7), 1174–1191.

Menne, M. J., & Williams Jr, C. N. (2009). Homogenization of temperature series via pairwise comparisons. *Journal of Climate*, *22*(7), 1700–1717.

Min, S.-K., Zhang, X., Zwiers, F. W., & Hegerl, G. C. (2011). Human contribution to more-intense precipitation extremes. *Nature*, *470*(7334), 378–381.

Moberg, A., & Jones, P. D. (2005). Trends in indices for extremes in daily temperature and precipitation in central and western Europe, 1901–99. *International Journal of Climatology: A Journal of the Royal Meteorological Society*, *25*(9), 1149–1171.

Moberg, A., Jones, P. D., Lister, D., Walther, A., Brunet, M., Jacobeit, J., Alexander, L. V., Della-Marta, P. M., Luterbacher, J., Yiou, P., et al. (2006). Indices for daily temperature and precipitation extremes in Europe analyzed for the period 1901–2000. *Journal of Geophysical Research: Atmospheres*, *111*(D22).

Montanari, A., Young, G., Savenije, H., Hughes, D., Wagener, T., Ren, L., Koutsoyiannis, D., Cudennec, C., Toth, E., Grimaldi, S., et al. (2013). "panta Rhei—everything flows": Change in hydrology and society—the IAHS scientific decade 2013–2022. *Hydrological Sciences Journal*, *58*(6), 1256–1275.

Murphy, C., Harrigan, S., Hall, J., & Wilby, R. L. (2013). Climate-driven trends in mean and high flows from a network of reference stations in Ireland. *Hydrological Sciences Journal*, *58*(4), 755–772.

Murphy, C., Wilby, R. L., Matthews, T. K., Thorne, P., Broderick, C., Fealy, R., Hall, J., Harrigan, S., Jones, P., McCarthy, G., et al. (2020). Multi-century trends to wetter winters and drier summers in the England and Wales precipitation series explained by observational and sampling bias in early records. *International Journal of Climatology*, *40*(1), 610–619.

New, M., Hewitson, B., Stephenson, D. B., Tsiga, A., Kruger, A., Manhique, A., Gomez, B., Coelho, C. A., Masisi, D. N., Kululanga, E., et al. (2006). Evidence of trends in daily climate extremes over southern and west africa. *Journal of Geophysical Research: Atmospheres*, *111*(D14).

NOS. (2021). *400 miljoen euro schade door overstroming Valkenburg, 2300 huizen beschadigd*. Retrieved December 15, 2021, from https://nos.nl/artikel/2390198-400-miljoen-euro-schade-door-overstroming-valkenburg-2300-huizen-beschadigd

Oki, T., & Kanae, S. (2006). Global hydrological cycles and world water resources. *Science*, *313*(5790), 1068–1072.

Ongoma, V., Chen, H., Gao, C., Nyongesa, A. M., & Polong, F. (2018). Future changes in climate extremes over equatorial east africa based on cmip5 multimodel ensemble. *Natural Hazards*, *90*(2), 901–920.

Önöz, B., & Bayazit, M. (2003). The power of statistical tests for trend detection. *Turkish Journal of Engineering and Environmental Sciences*, *27*(4), 247–251.

Pall, P., Aina, T., Stone, D. A., Stott, P. A., Nozawa, T., Hilberts, A. G., Lohmann, D., & Allen, M. R. (2011). Anthropogenic greenhouse gas contribution to flood risk in England and Wales in autumn 2000. *Nature*, *470*(7334), 382–385.

Peterson, T. C., & Manton, M. J. (2008). Monitoring changes in climate extremes: A tale of international collaboration. *Bulletin of the American Meteorological Society*, *89*(9), 1266–1271.

Petrow, T., & Merz, B. (2009). Trends in flood magnitude, frequency and seasonality in Germany in the period 1951–2002. *Journal of Hydrology*, *371*(1-4), 129–141.

Pettitt, A. N. (1979). A non-parametric approach to the change-point problem. *Journal of the Royal Statistical Society: Series C (Applied Statistics)*, *28*(2), 126–135.

Rapp, J. (2000). *Konzeption, problematik und ergebnisse klimatologischer trendanalysen für Europa und Deutschland*. Deutscher Wetterdienst Offenbach am Main.

Renard, B., Lang, M., Bois, P., Dupeyrat, A., Mestre, O., Niel, H., Sauquet, E., Prudhomme, C., Parey, S., Paquet, E., et al. (2008). Regional methods for trend detection: Assessing field significance and regional consistency. *Water Resources Research*, *44*(8).

Renner, M., Brust, K., Schwärzel, K., Volk, M., & Bernhofer, C. (2014). Separating the effects of changes in land cover and climate: A hydro-meteorological analysis of the past 60 yr in Saxony, Germany. *Hydrology and Earth System Sciences*, *18*(1), 389–405.

Ribeiro, S., Caineta, J., & Costa, A. C. (2016). Review and discussion of homogenisation methods for climate data. *Physics and Chemistry of the Earth, Parts A/B/C*, *94*, 167–179.

Robinson, A., Lehmann, J., Barriopedro, D., Rahmstorf, S., & Coumou, D. (2021). Increasing heat and rainfall extremes now far outside the historical climate. *npj Climate and Atmospheric Science*, *4*(1), 1–4.

Rogger, M., Agnoletti, M., Alaoui, A., Bathurst, J., Bodner, G., Borga, M., Chaplot, V., Gallart, F., Glatzel, G., Hall, J., et al. (2017). Land use change impacts on floods at the catchment scale: Challenges and opportunities for future research. *Water Resources Research*, *53*(7), 5209–5219.

Ruiz-Villanueva, V., Stoffel, M., Wyżga, B., Kundzewicz, Z. W., Czajka, B., & Niedźwiedź, T. (2016). Decadal variability of floods in the northern foreland of the Tatra Mountains. *Regional Environmental Change*, *16*(3), 603–615.

Ruiz-Villanueva, V., Wyżga, B., Kundzewicz, Z. W., Niedźwiedź, T., Łupikasza, E., & Stoffel, M. (2016). Variability of flood frequency and magnitude during the late 20th and early 21st centuries in the northern foreland of the Tatra Mountains. *Flood Risk in the Upper Vistula Basin* (pp. 231–256). Springer.

Schmocker-Fackel, P., & Naef, F. (2010). Changes in flood frequencies in Switzerland since 1500. *Hydrology and Earth System Sciences*, *14*(8), 1581–1594.

Sheffield, J., Wood, E. F., & Roderick, M. L. (2012). Little change in global drought over the past 60 years. *Nature*, *491*(7424), 435–438.

Slonosky, V., Jones, P., & Davies, T. (2000). Variability of the surface atmospheric circulation over Europe, 1774–1995. *International Journal of Climatology: A Journal of the Royal Meteorological Society*, *20*(15), 1875–1897.

Smith, A., Tetzlaff, D., Kleine, L., Maneta, M., & Soulsby, C. (2021). Quantifying the effects of land use and model scale on water partitioning and water ages using tracer-aided ecohydrological models. *Hydrology and Earth System Sciences*, *25*(4), 2239–2259.

Squintu, A. A., van der Schrier, G., van den Besselaar, E., van der Linden, E., Putrasahan, D., Roberts, C., Roberts, M., Scoccimarro, E., Senan, R., & Klein Tank, A. (2021). Evaluation of trends in extreme temperatures simulated by HighResMIP models across Europe. *Climate Dynamics*, *56*(7), 2389–2412.

Šraj, M., Viglione, A., Parajka, J., & Blöschl, G. (2016). The influence of non-stationarity in extreme hydrological events on flood frequency estimation. *J. Hydrol. Hydromech*, *64*(4), 426–437.

Stähli, M., Seibert, J., Kirchner, J. W., von Freyberg, J., & van Meerveld, I. (2021). Hydrological trends and the evolution of catchment research in the Alptal valley, central Switzerland. *Hydrological Processes*, *35*(4), e14113.

Stam, M. (2002). Effects of land-use and precipitation changes on floodplain sedimentation in the nineteenth and twentieth centuries (Geul River, The Netherlands). *Flood and Megaflood Processes and Deposits: Recent and Ancient Examples*, 251–267.

Sun, W., Mu, X., Song, X., Wu, D., Cheng, A., & Qiu, B. (2016). Changes in extreme temperature and precipitation events in the Loess Plateau (China) during 1960–2013 under global warming. *Atmospheric Research*, *168*, 33–48.

Swennen, R., Van Keer, I., & De Vos, W. (1994). Heavy metal contamination in overbank sediments of the Geul river (East Belgium): Its relation to former Pb-Zn mining activities. *Environmental Geology*, *24*(1), 12–21.

Tabari, H., & Talaee, P. H. (2011). Temporal variability of precipitation over Iran: 1966–2005. *Journal of Hydrology*, *396*(3-4), 313–320.

Tian, J., Liu, J., Wang, J., Li, C., Nie, H., & Yu, F. (2017). Trend analysis of temperature and precipitation extremes in major grain producing area of China. *International Journal of Climatology*, *37*(2), 672–687.

Tomer, M. D., & Schilling, K. E. (2009). A simple approach to distinguish land-use and climate-change effects on watershed hydrology. *Journal of Hydrology*, *376*(1-2), 24–33.

Tramblay, Y., El Adlouni, S., & Servat, E. (2013). Trends and variability in extreme precipitation indices over maghreb countries. *Natural Hazards and Earth System Sciences*, *13*(12), 3235–3248.

Trenberth, K. E., Fasullo, J. T., & Shepherd, T. G. (2015). Attribution of climate extreme events. *Nature Climate Change*, *5*(8), 725–730.

Tu, M. (2006). *Assessment of the effects of climate variability and land use change on the hydrology of the Meuse river basin* (PhD dissertation). UNESCO-IHE Institute for Water Education, The Netherlands.

Uijlenhoet, R., De Wit, M., Warmerdam, P., & Torfs, P. (2001). *Statistical Analysis of Daily Discharge Data of the River Meuse and its Tributaries (1968-1998): Assessment of Drought Sensitivity* (tech. rep.). Sub-department Water Resources, Wageningen University, Wageningen, The Netherlands.

Vaes, G., Willems, P., & Berlamont, J. (2002). 100 years of Belgian rainfall: Are there trends? *Water Science and Technology*, *45*(2), 55–61.

van den Hurk, B., Siegmund, P., Klein Tank, A., Attema, J., Bakker, A., Beersma, J., Bessembinder, J., Boers, R., Brandsma, T., van den Brink, H., Drijfhout, S., Eskes, H., Haarsma, R., Hazeleger, W., Jilderda, R., Katsman, C., Lenderink, G., Loriaux, J., van Meijgaard, E., … van Zadelhoff, G.-J. (2014). *KNMI'14: Climate Change scenarios for the 21st Century – A Netherlands perspective*. Royal Netherlands Meteorological Institute, KNMI, De Bilt, The Netherlands.

van den Munckhof, G. (2020). *Forecasting river discharge using machine learning methods with application to the Geul and the Rur river* (Master's thesis). Delft University of Technology, The Netherlands.

Vandenberghe, J., De Moor, J., & Spanjaard, G. (2012). Natural change and human impact in a present-day fluvial catchment: The Geul River, Southern Netherlands. *Geomorphology*, *159*, 1–14.

van Dijk, Y. H. C. (2022). *Flooding problems in the catchment area of the River Geul: The impact of measures on the consequences of extreme flooding* (Master's thesis). Delft University of Technology, the Netherlands.

van Heeringen, K.-J., Asselman, N., Overeem, A., Beersma, J., & Philip, S. (2022). *Analyse overstroming Valkenburg. Watersysteemevaluatie Waterschap Limburg* (tech. rep.). Deltares, report 11207700-000-ZWS-0014, The Netherlands.

Vicente-Serrano, S. M., Domínguez-Castro, F., Murphy, C., Hannaford, J., Reig, F., Peña-Angulo, D., Tramblay, Y., Trigo, R. M., Mac Donald, N., Luna, M. Y., et al. (2021). Long-term variability and trends in meteorological droughts in Western Europe (1851–2018). *International Journal of Climatology*, *41*, E690–E717.

Villarini, G., Smith, J. A., Serinaldi, F., & Ntelekos, A. A. (2011). Analyses of seasonal and annual maximum daily discharge records for central Europe. *Journal of Hydrology*, *399*(3-4), 299–312.

Visser, H. (2005). *The significance of climate change in the Netherlands:An analysis of historical and future trends (1901-2020) in weather conditions, weather extremes and temperature-related impacts* (tech. rep.). National Institute for Public Health and Environment (RIVM) report 550002007 / 2005, The Netherlands.

Wang, X. L., Wen, Q. H., & Wu, Y. (2007). Penalized maximal t test for detecting undocumented mean change in climate data series. *Journal of Applied Meteorology and Climatology*, *46*(6), 916–931.

Wu, C., Huang, G., Yu, H., Chen, Z., & Ma, J. (2014). Spatial and temporal distributions of trends in climate extremes of the Feilaixia catchment in the upstream area of the Beijiang River Basin, South China. *International Journal of Climatology*, *34*(11), 3161–3178.

Yang, L., Yang, Y., Villarini, G., Li, X., Hu, H., Wang, L., Blöschl, G., & Tian, F. (2021). Climate more important for Chinese flood changes than reservoirs and land use. *Geophysical Research Letters*, *48*(11), e2021GL093061.

Zhang, X., Alexander, L., Hegerl, G. C., Jones, P., Tank, A. K., Peterson, T. C., Trewin, B., & Zwiers, F. W. (2011). Indices for monitoring changes in extremes based on daily temperature and precipitation data. *Wiley Interdisciplinary Reviews: Climate Change*, *2*(6), 851–870.

Zhou, C., van Nooijen, R., Kolechkina, A., & Hrachowitz, M. (2019). Comparative analysis of nonparametric change-point detectors commonly used in hydrology. *Hydrological Sciences Journal*, *64*(14), 1690–1710.

Zhou, C., van Nooijen, R., Kolechkina, A., & van de Giesen, N. (2020). Confidence curves for change points in hydrometeorological time series. *Journal of Hydrology*, *590*, 125503.

A

Trend analysis of rainfall time series

A.1. Long term variability

A.1.1. Winter

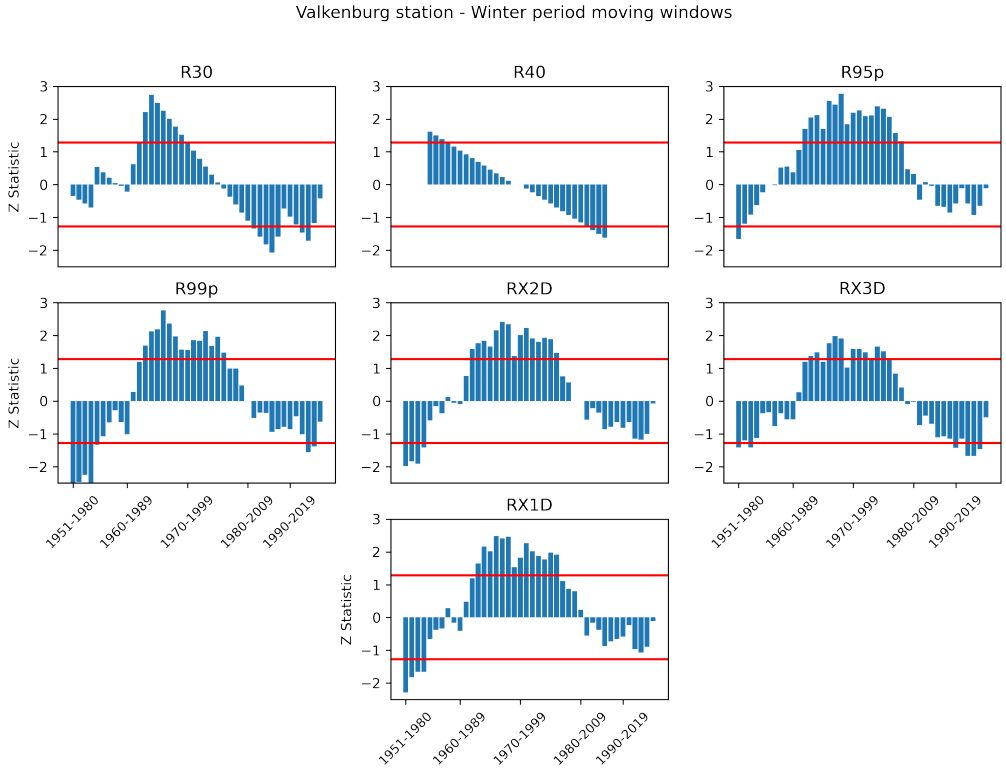

Figure A.1: Calculated extreme precipitation Z statistic for each moving period in winter for Valkenburg station.

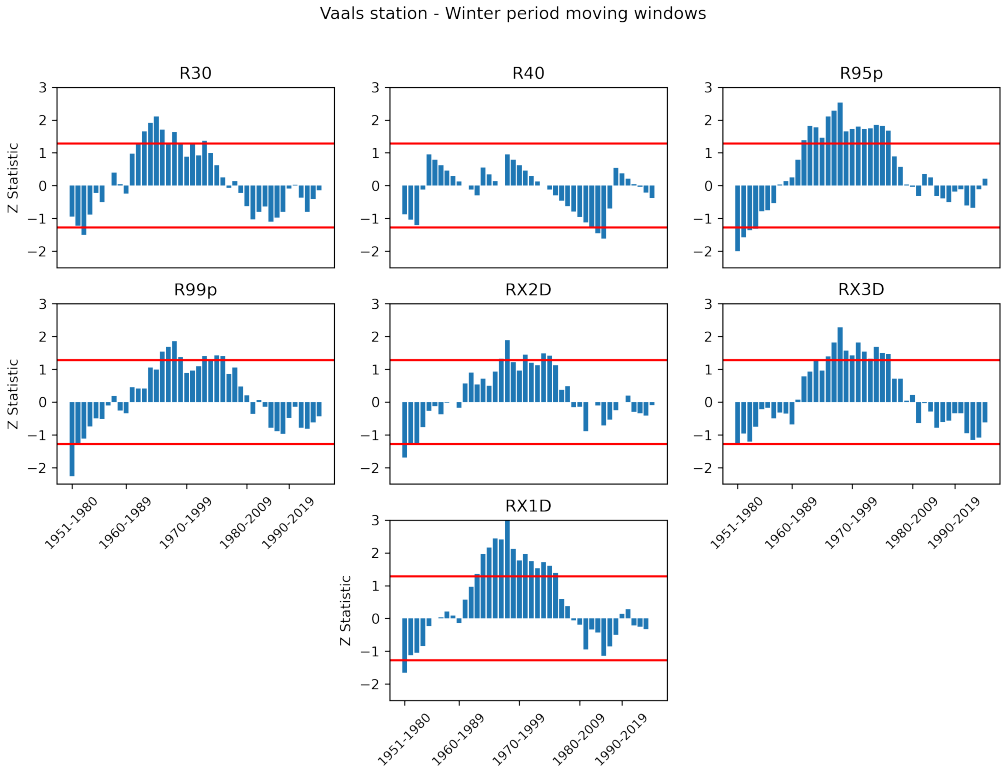

Figure A.2: Calculated extreme precipitation Z statistic for each moving period in winter for Vaals station.

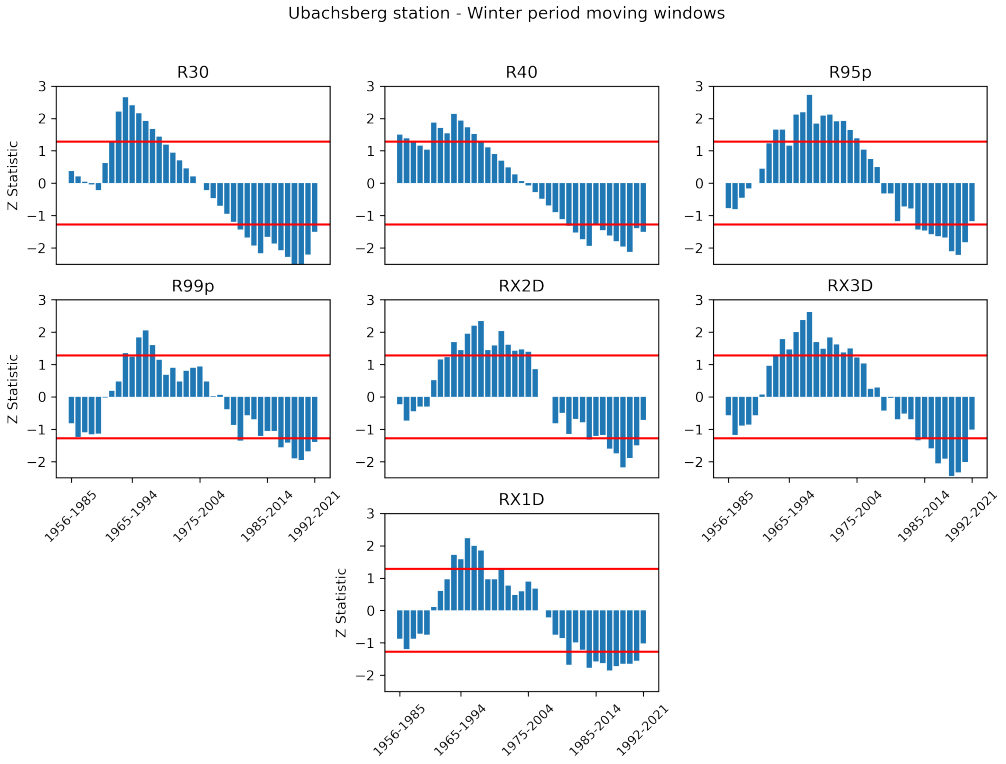

Figure A.3: Calculated extreme precipitation Z statistic for each moving period in winter for Ubachsberg station.

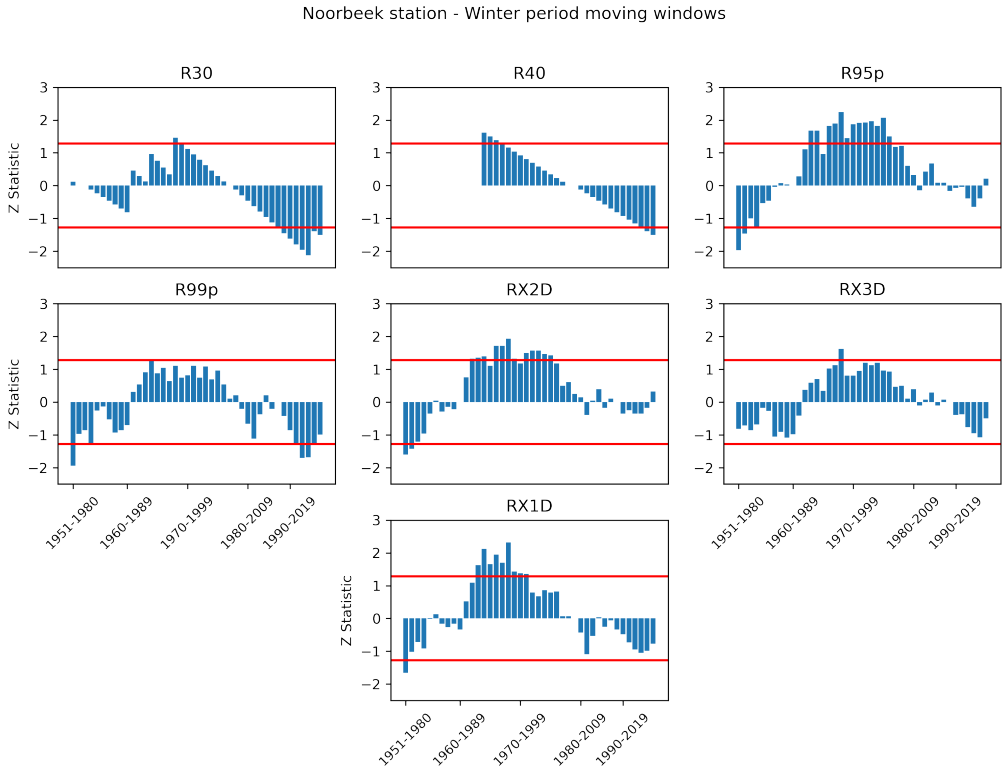

Figure A.4: Calculated extreme precipitation Z statistic for each moving period in winter for Noorbeek station.

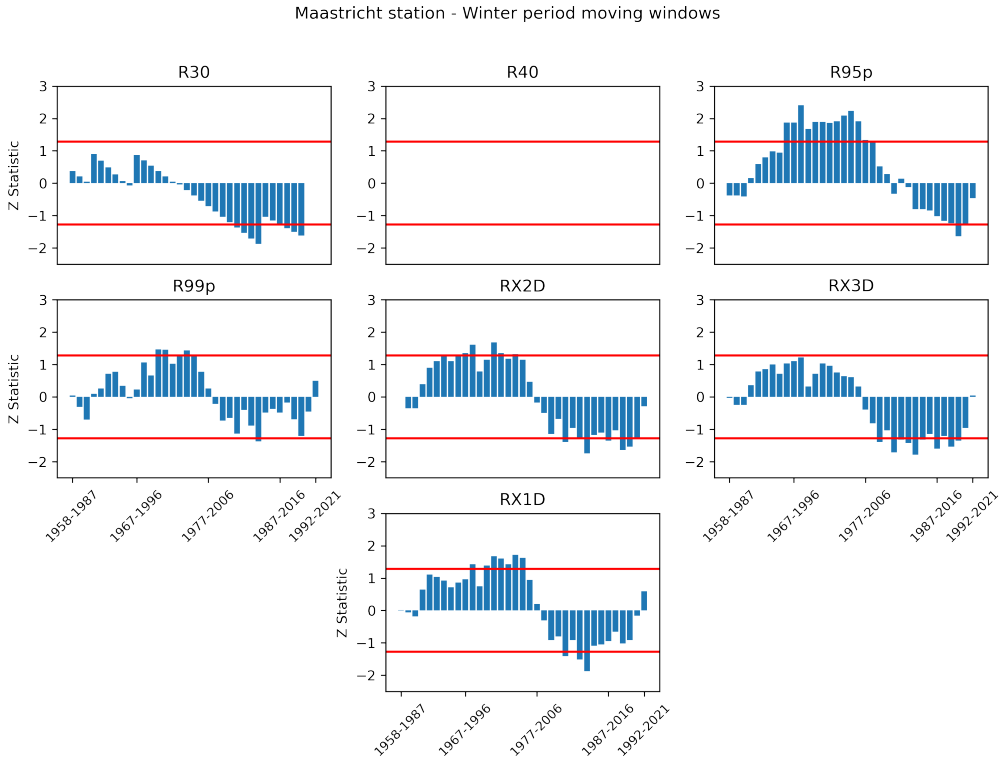

Figure A.5: Calculated extreme precipitation Z statistic for each moving period in winter for Maastricht station.

A.1.2. Spring

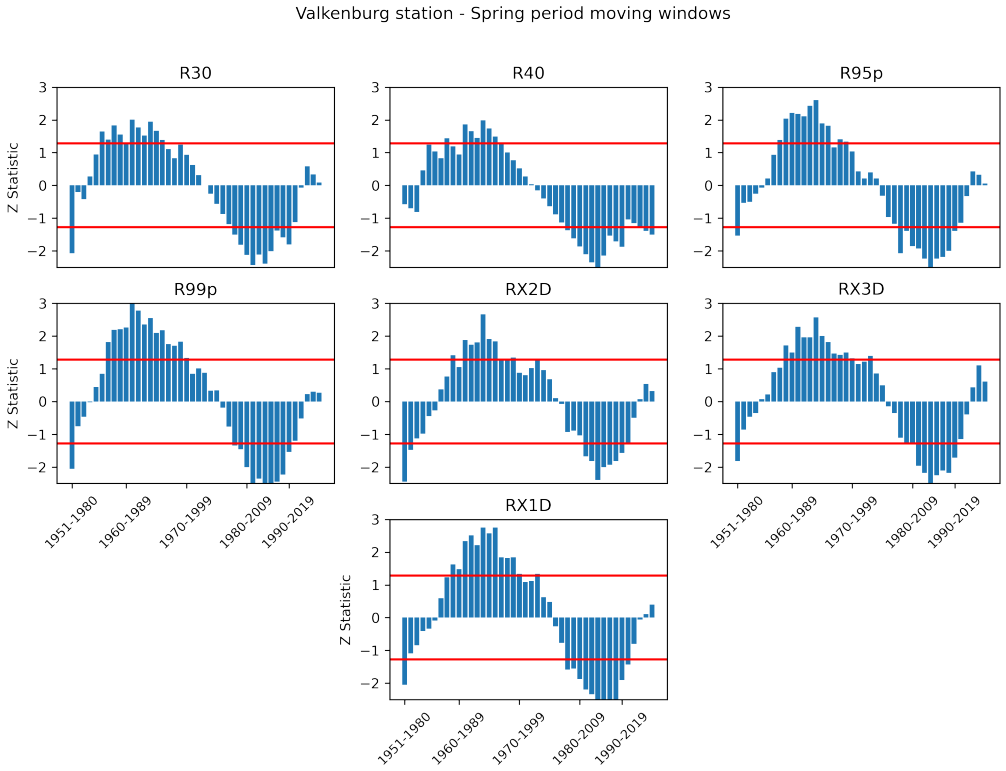

Figure A.6: Calculated extreme precipitation Z statistic for each moving period in spring for Valkenburg station.

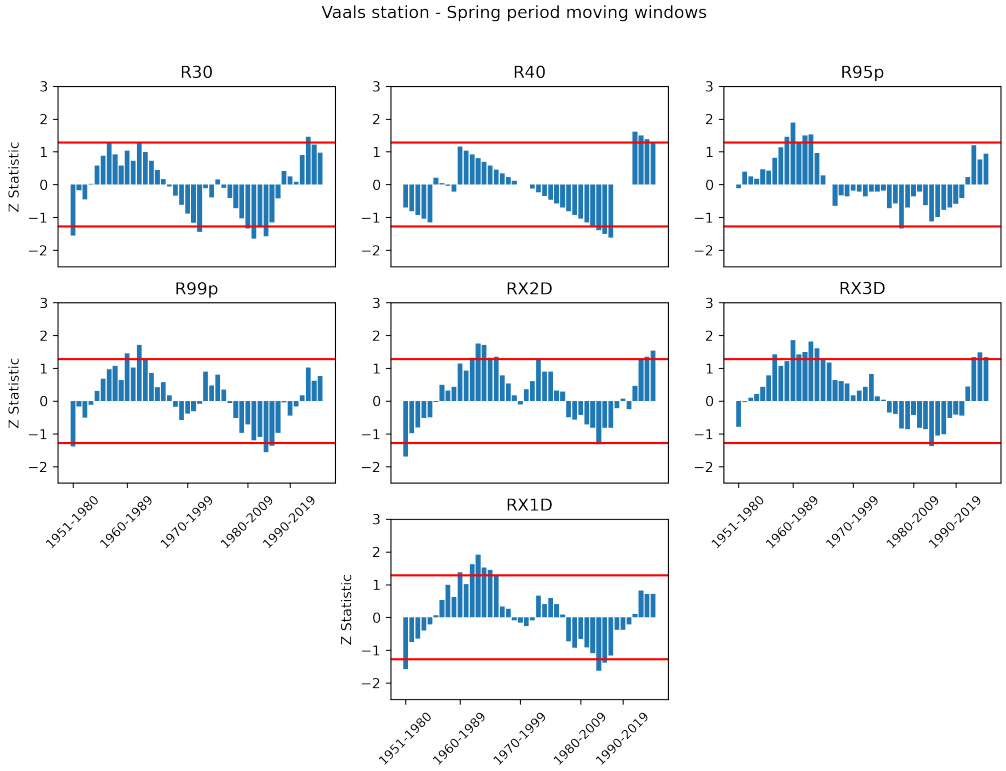

Figure A.7: Calculated extreme precipitation Z statistic for each moving period in spring for Vaals station.

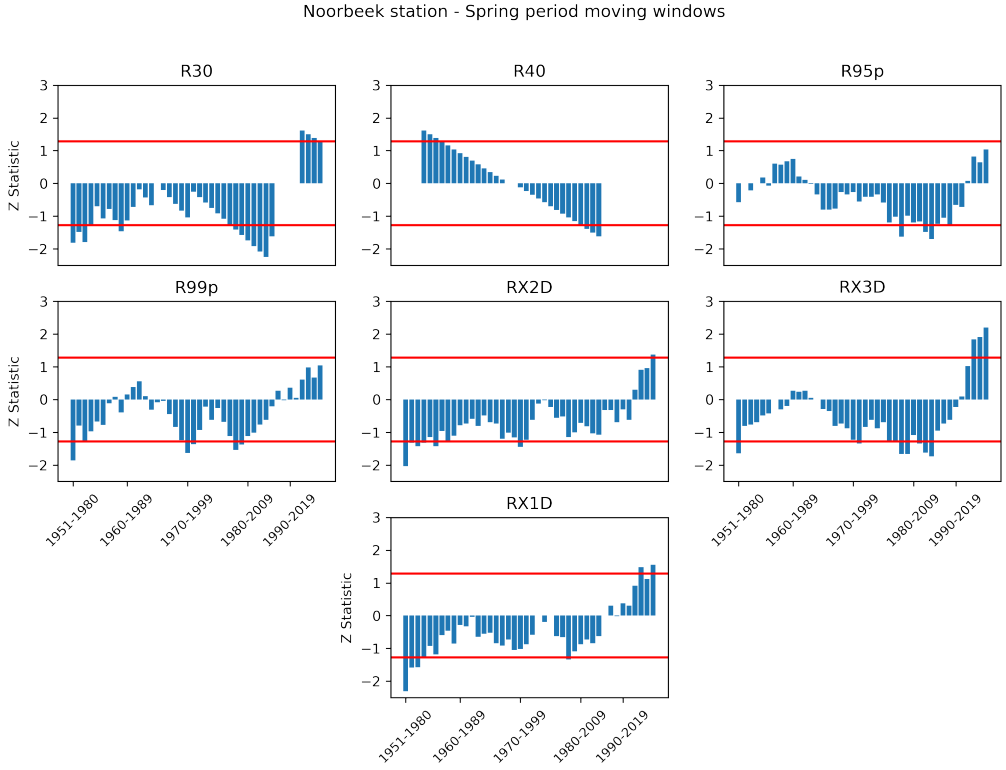

Figure A.8: Calculated extreme precipitation Z statistic for each moving period in spring for Noorbeek station.

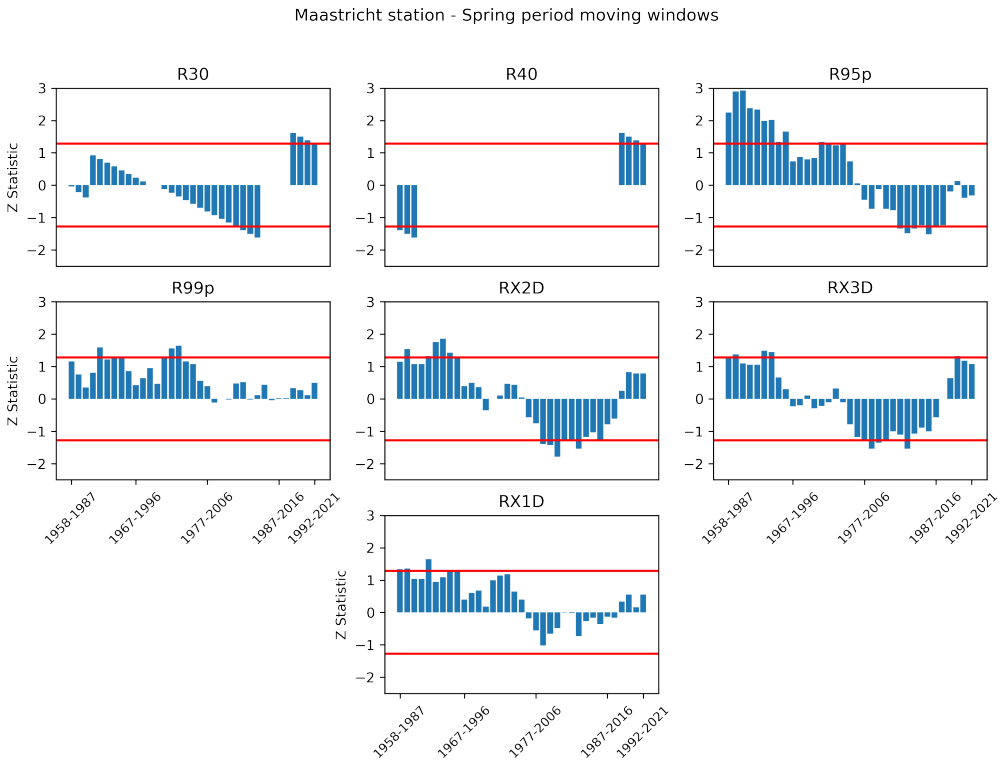

Figure A.9: Calculated extreme precipitation Z statistic for each moving period in spring for Maastricht station.

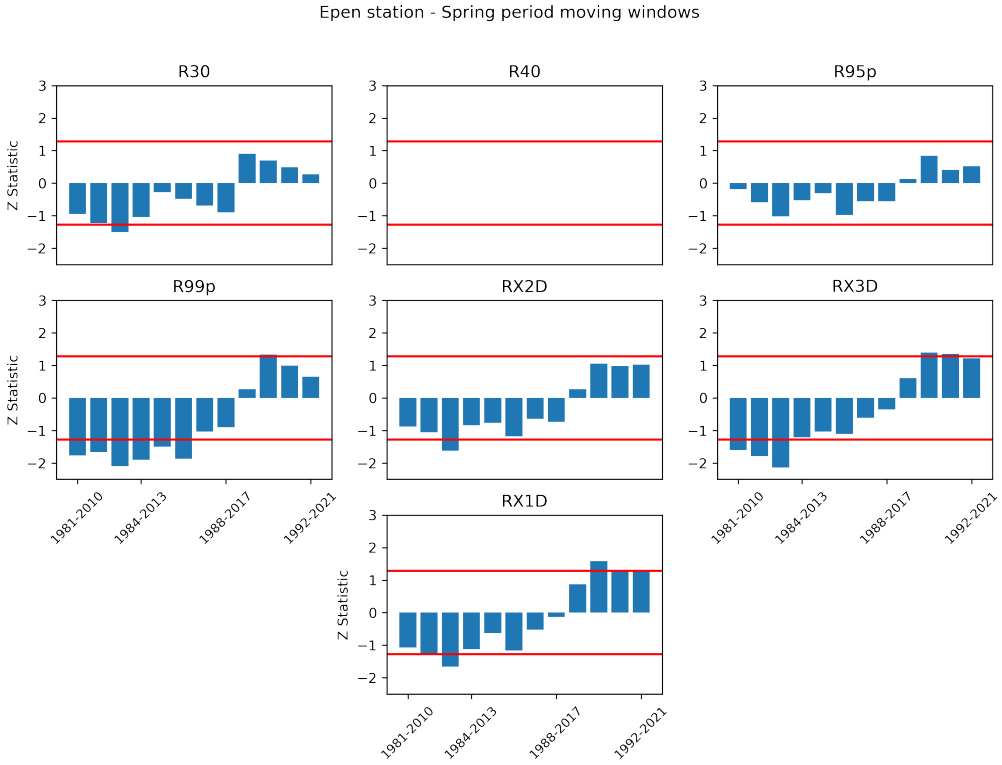

Figure A.10: Calculated extreme precipitation Z statistic for each moving period in spring for Epen station.

A.1.3. Summer

Table A.1: Z-statistic values before (Zbef) and after (Zafter) 1980. Bolds show significant values at the 20% level, * Significant at the 10% level, ** Significant at the 5% level

	RX1D		R95p		R99p		R30		R40		RX2D		RX3D		Rtot	
Station	Zbef	Zafter	Zbef	Zafter	Zbef	Zafter	Zbef	Zafter	Zbef	Zafter	Zbef	Zafter	Zbef	Zafter	Zbef	Zafter
Valkenburg	-1.25	1.7*	-1.18	**1.38**	**-1.60**	**1.53**	-0.70	1.81*	-0.33	**1.28**	-1.18	1.66*	-1.78*	**1.28**	-1.23	0.52
Vaals	-0.61	2.93**	-1.07	**1.51**	-0.88	1.98**	0.59	2.44**	**-1.40**	3.06**	-1.91*	1.97**	-2.23**	**1.38**	-1.90*	0.71
Noorbeek	-0.88	0.77	-1.78*	0.52	-1.08	0.51	-1.33	0.62	**-1.55**	**1.40**	-1.72*	0.65	-1.22	**1.52**	**-1.63**	0.34
Ubachsberg	0.47	1.86*	0.67	**1.47**	-0.05	**1.57**	0.36	2.02**	1.22	2.44**	0.57	1.87*	0.02	**1.50**	-0.57	0.74
Maastricht	-0.51	2.25**	-1.01	**1.50**	-0.08	2.50**	0.91	**1.44**	-0.28	0.18	-0.14	1.74*	-0.90	1.67*	-1.12	1.08
Epen	-	**1.60**	-	0.98	-	1.77*	-	2.11**	-	0.75	-	0.82	-	0.68	-	0.68

Table A.2: Sen's slope estimator calculated only for statistically significant trends highlighted in Table A.1

	RX1D		R95p		R99p		RX2D		RX3D		Rtot	
Station	βbef	βafter	βbef	βafter	βbef	βafter	βbef	βafter	βbef	βafter	βbef	βafter
Valkenburg	-	0.29	-	1.55	-1.10	0.95	-	0.34	-0.65	0.24	-	-
Vaals	-	0.46	-	0.70	-	0.90	-0.75	0.36	-0.93	0.25	-2.90	-
Noorbeek	-	-	-2.01	-	-	-	-0.50	-	-	0.39	-2.75	-
Ubachsberg	-	0.34	-	0.96	-	0.97	-	0.36	-	0.36	-	-
Maastricht	-	0.37	-	1.23	-	1.17	-	0.30	-	0.30	-	-
Epen	-	0.25	-	-	-	0.83	-	-	-	-	-	-

A.2. Precipitation trend stabilities

Figures A.11 - A.15 present the stability of statistically significant trends in the precipitation indices, as explained in Section 3.1.2.

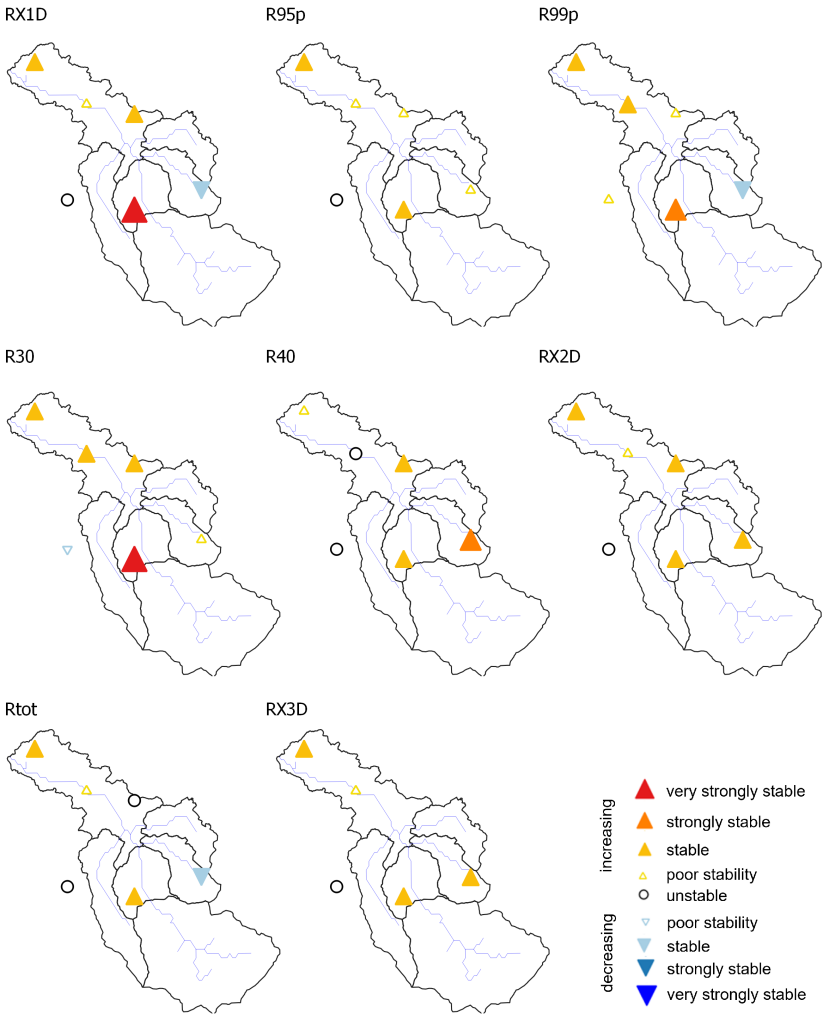

Figure A.11: Stability of statistically significant trends in precipitation indices - summer.

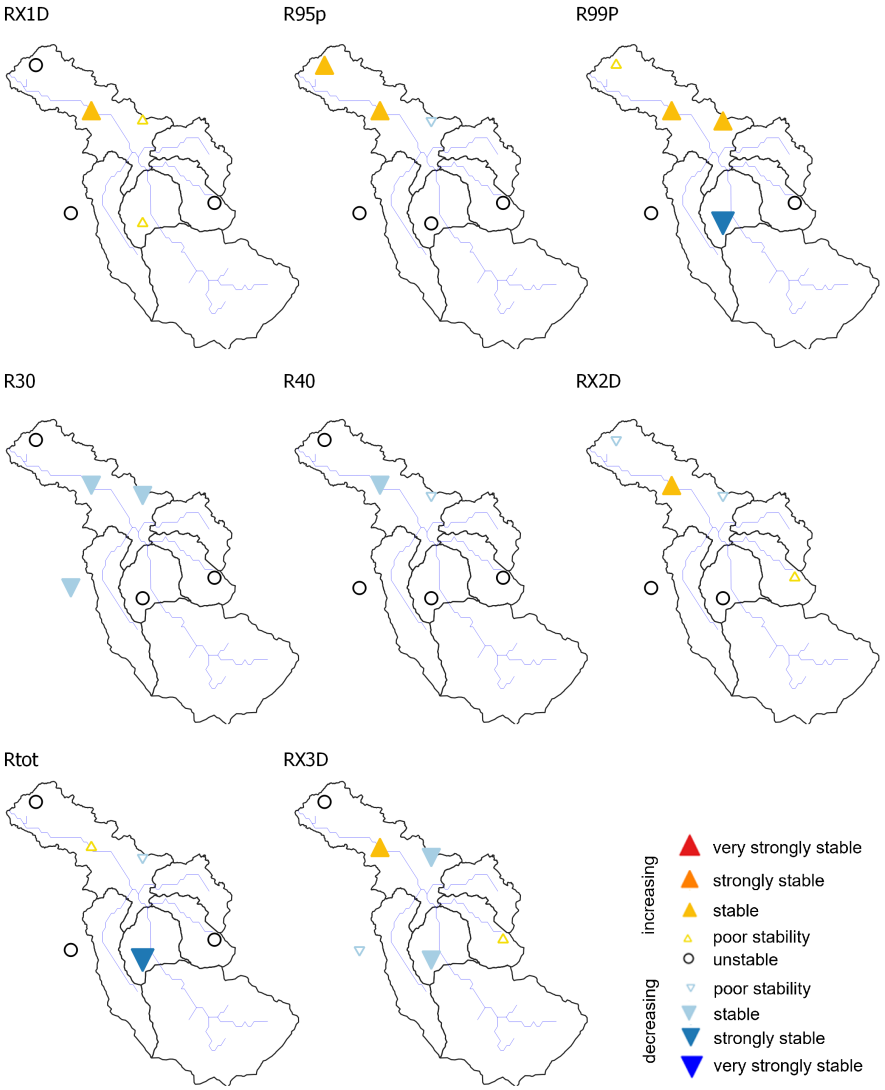

Figure A.12: Stability of statistically significant trends in precipitation indices - spring.

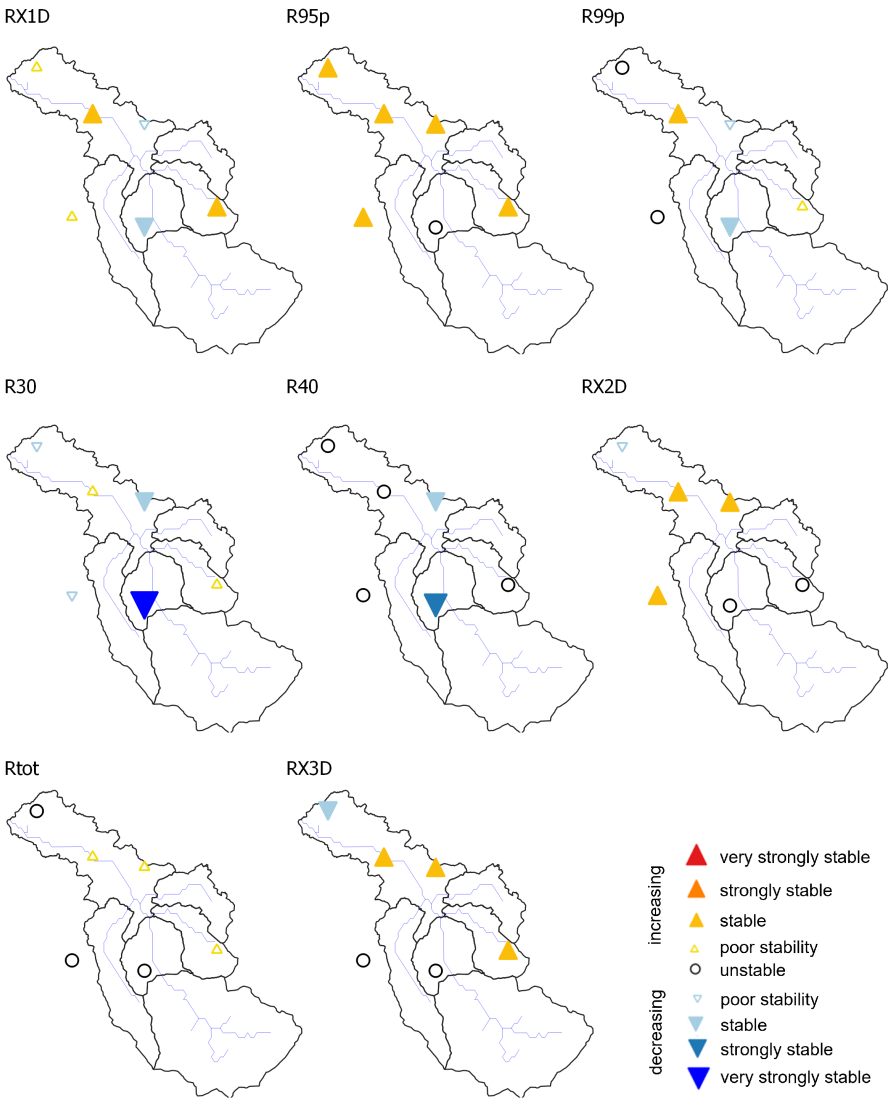

Figure A.13: Stability of statistically significant trends in precipitation indices - winter.

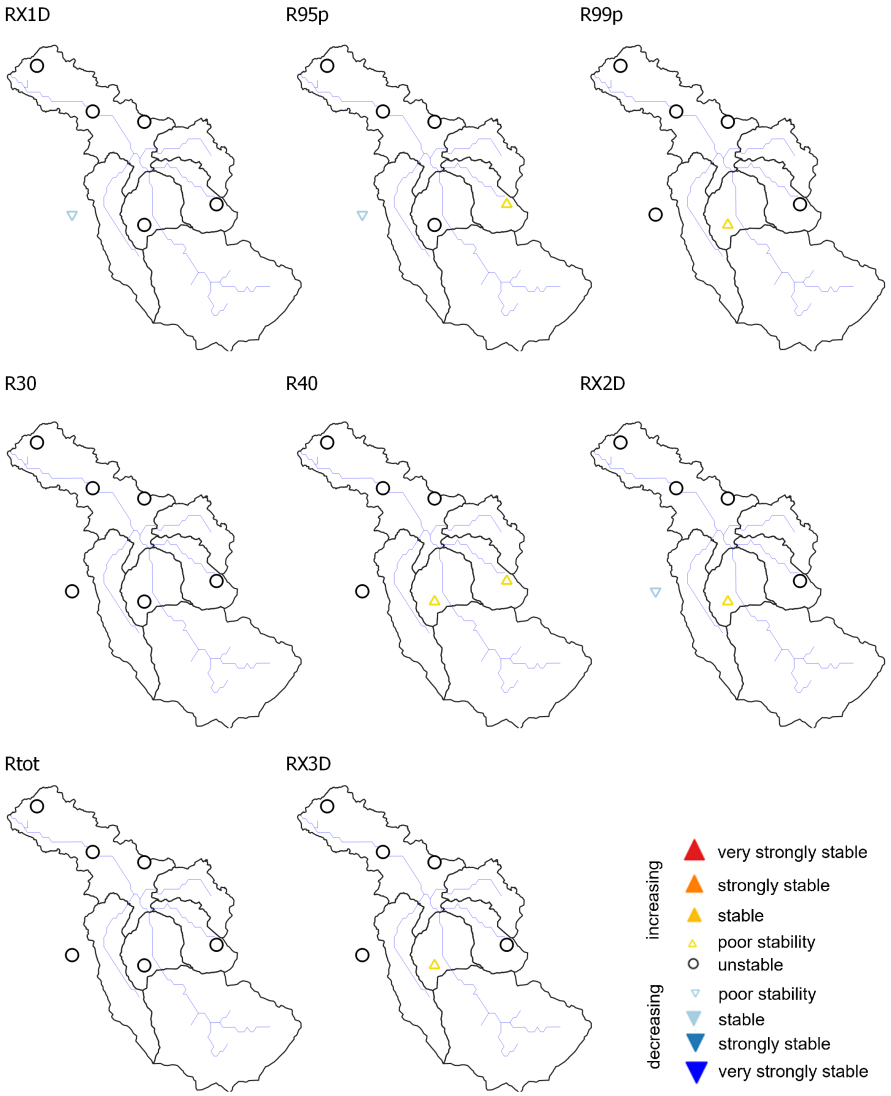

Figure A.14: Stability of statistically significant trends in precipitation indices - autumn.

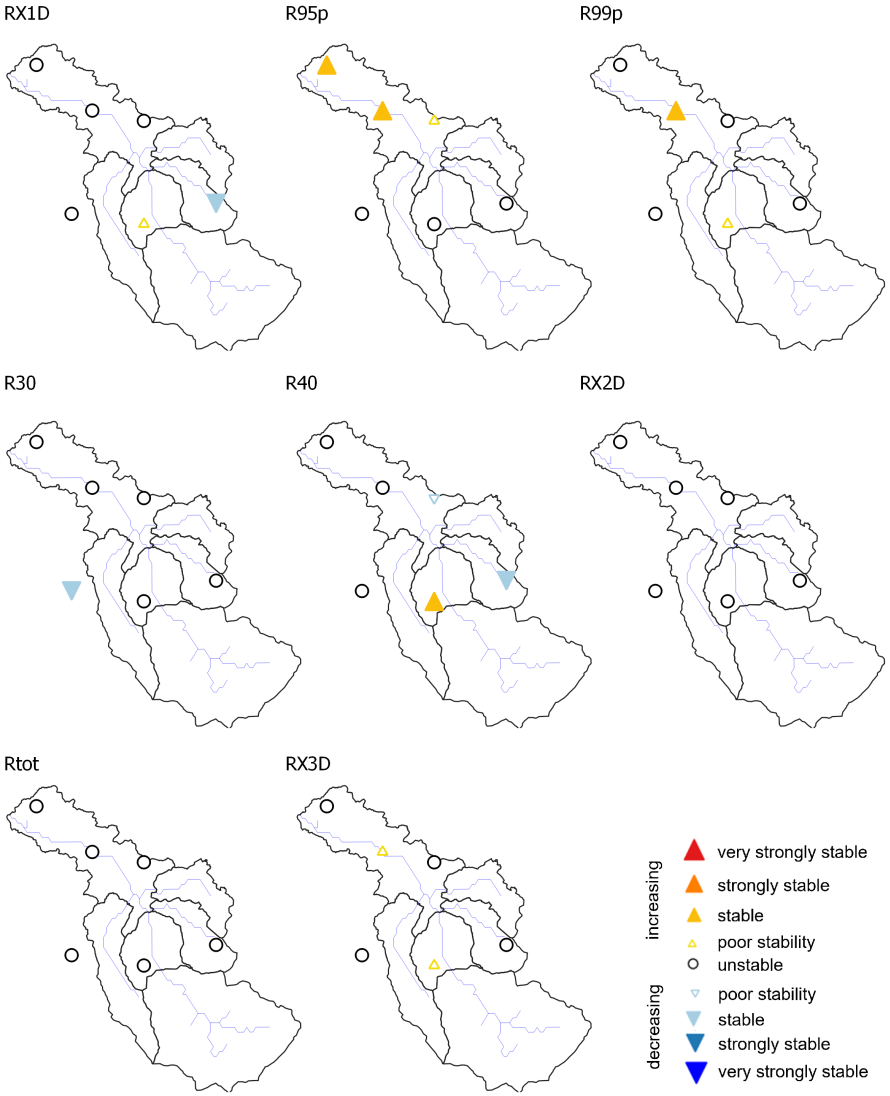

Figure A.15: Stability of statistically significant trends in precipitation indices - full year.

B

Land use changes

Figures B.1 and B.2 illustrate the area change of each class (gray bars) and its percentage increase or decrease based on the area in 1990 (not the percentage change of the total area that occupies in the catchment). The changes of each land cover class from 1990 to 2018 are reported in Table B.1.

B.1. Whole catchment

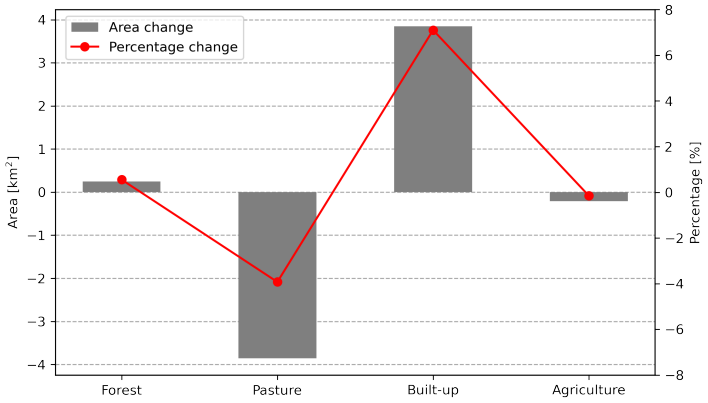

Figure B.1: Area and percent land cover changes between 1990 and 2018 for the whole catchment.

Table B.1: Cross-tabulation of land use changes from 1990 to 2018 (values per class in km^2)

	Built-up	Pasture	Agriculture	Forest	Sum	Loss
Built-up	52.40	0.74	0.99	0.04	54.17	1.77
Pasture	2.63	92.18	3.24	0.26	98.31	6.13
Agriculture	2.53	1.13	135.56	1.03	140.25	4.69
Forest	0.46	0.40	0.22	43.91	44.99	1.08
Sum	58.02	94.45	140.01	45.24	-	-
Gain	5.62	2.27	4.45	1.33	-	-

B.2. Subcatchments

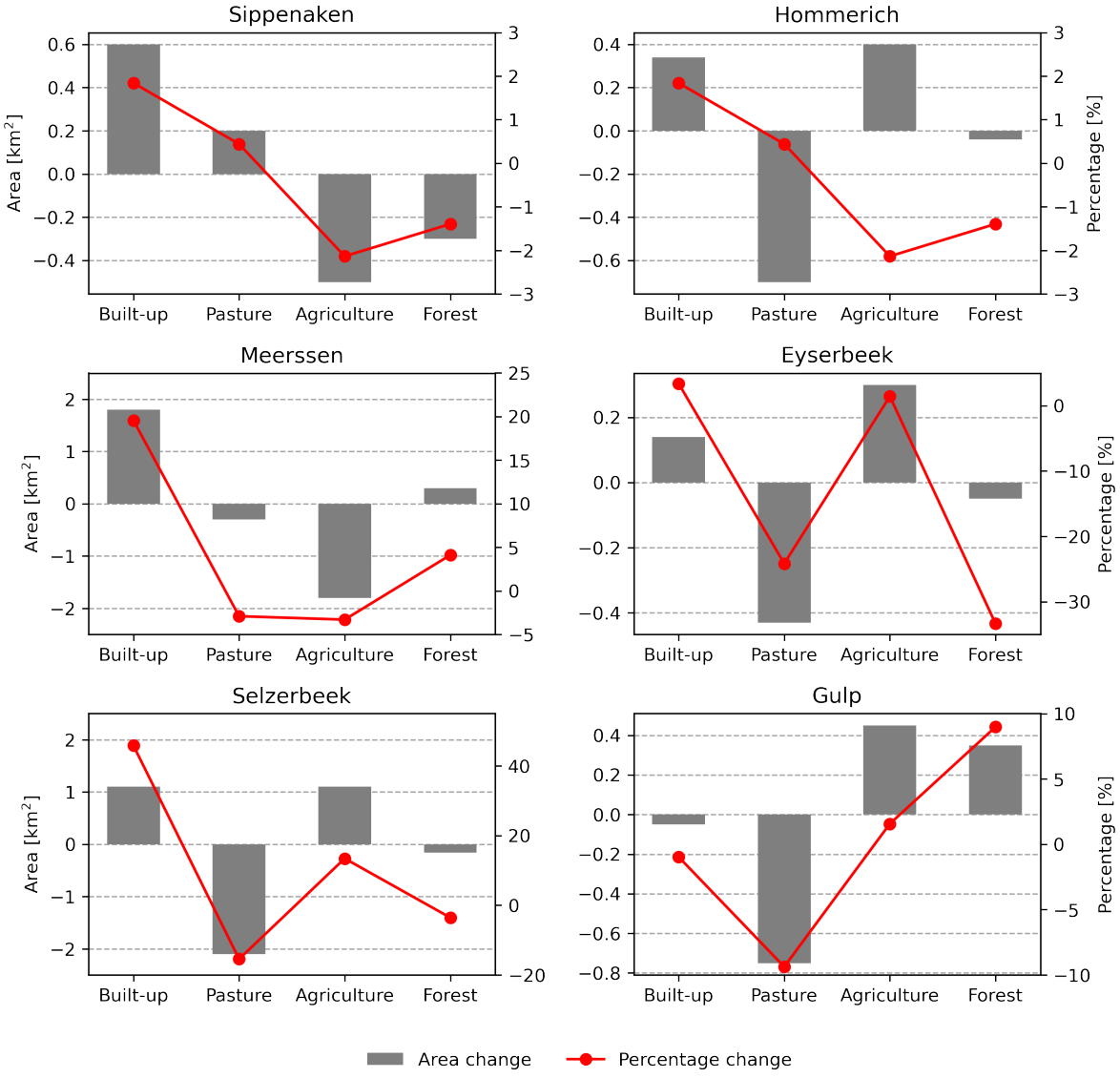

Figure B.2: Area and percent land cover changes between 1990 and 2018 for each subcatchment.